Investigating the extension of service life of box-beam bridge girders

And it's impact on circularity

Harikrishnan Sushin

TU Delft
Delft University of Technology

INVESTIGATING THE EXTENSION OF SERVICE LIFE OF BOX-BEAM BRIDGE GIRDERS

AND ITS IMPACT ON CIRCULARITY

by

Harikrishnan SUSHIN

Student number: 5077214

Committee members:

Dr. ir. Y. Yang,	Technische Universiteit Delft (Chair)
Dr. ir. H.W.M van der Ham,	Technische Universiteit Delft
Dr. W. Cao,	Technische Universiteit Delft

An electronic version of this dissertation is available at
http://repository.tudelft.nl/.

Cover image retrieved from: Alexander, M., Beushausen, H. (2019). Durability, service life prediction, and modelling for reinforced concrete structures – review and critique. Cement And Concrete Research, 122, 17-29

ACKNOWLEDGEMENTS

Before we begin, there's simply too many people I would like to thank. My journey here at TU Delft has been one full of lessons. Some of which I learnt from, and some which I still need to learn from. This place has brought some new and wonderful people into my life and for that I am ever grateful. Below is just one attempt to try and express the support gifted to me by some wonderful people.

My parents, without whom I would not be here were always a constant support and I know all their love and support is something I will never be able to repay. My sister who had a habit of knowing when I needed a long and distracting conversation.
My committee without whom this would not be possible, from their constructive feedback to their guidance throughout the thesis has been invaluable. I would like to thank Dr. Yuguang Yang, first of all for agreeing to be the chair of the committee, and for his support and ideas which helped shape the thesis. Dr. Herbert van der Ham, who helped shape the initial parts of the thesis especially the more practical side of bridge design. I would also like to thank Dr. Wenjun Cao who was a wealth of information regarding the topics of circular construction, a new topic for me.

My friends new and old, here in the Netherlands and back home in India who have always been a great source of comfort. Whether it was a much needed distraction from the hard work of a thesis, or a discussion and exchange of ideas to get back into the groove of working. Words will never express enough my gratitude towards them.

Harikrishnan Sushin
January 2022

CONTENTS

List of Figures

NOMENCLATURE

γ_c	Density of concrete
γ_G	Load factors for permanent loads
γ_P	Load factors for prestressing
γ_Q	Load factors for variable loads
ψ	Combination factors
ADP	Abiotic Depletion Potential
BCI	Bridge Circularity Indicator
$C(x,t)$	Chloride content at depth x (in mm)
C_i	Initial chloride content
C_s	Surface chloride content
$CB'23$	Circular Bouwen 2023
CE	Circular Economy
CI	Circularity Indicators
$D(t)$	Time dependant diffusion coefficient
D_o	Diffusion coefficient determined through RCM tests
DfA	Design for Adaptability
DfD	Design for Deconstruction
$DfReu$	Design for Reuse
EC	Eurocode
EOL	End of Life
erf	Error function
Ext	Extensibility
$f_{ctm,fl}$	Tensile strength of concrete in flexure
FE	Finite Element

$FLM1$	Fatigue Load Model 1
H	Heightenability
IFD	Industrial Flexible Demountable
K_{tot}	Environmental factor
LCA	Life Cycle Analysis
$LM1$	Load Model 1
M_i	Mass of component 'i'
MCI	Material Circularity Indicator
MU	Model Uncertainty
P_f	Probability of failure
RCM	Rapid Chloride Migration
SCM	Supplementary Cementitious Materials
SLD	Service Life Design
SLS	Serviceability Limit State
SOP	Surplus Ore Potential
St	Strengthenability
t	Time (days)
t_0	Reference period (28 days)
T_i	Transportability of component 'i'
TS	Tandem System
UDL	Uniformly Distributed Load
ULS	Ultimate Limit State

SUMMARY

The increasing demands of a growing population are a strain on already limited resources, and this is a major reason for concern. There is a need to shift towards practices that are more environmentally friendly, and the construction industry is no exception. This thesis focuses on a durability study to improve the service life of the concrete beam, against the ingress of chlorides. The main research goal for this study was chosen to be potential recommendation(s) that could be made to improve the service life and whether this positively affected the circularity of box-beam girders.

The methodology followed first a literature review into the areas concerning circularity and sustainability. Literature study also revealed existing indicators and how circularity was assessed. The principle of life span extension was seen to be one that could be applied to a box beam to improve durability. The main focus however was to incorporate this during design phase. The choice was made to focus on the durability issue related to ingress of chlorides, since this was deemed to be the most common environment bridges in the Netherlands were designed for. The next step was to design a standard beam using the Eurocodes. This beam provided the basic model on which the potential design recommendations could be applied directly. The impact of the design recommendations could be quantified using the standard beam as a reference point.

The codes were studied to understand how service life was guaranteed. The exposure classes in EN1992-1-1 dealt with the different types of environment that the concrete was subjected to during its service life. Hence the next step was to investigate how the service life could be improved beyond the limits of the current standards to better protect against corrosion due to ingress of chloride ions. The DuraCrete model was identified to be a good match for the goal of improving durability. Due to the limitations of the model in terms of lack of samples and variability of parameters over time, a model uncertainty (MU) parameter was used to try and reduce the uncertainty and was calibrated according to obtained chloride profiles. The model was used to decide an appropriate cover, following which the effect of a cover increase on the circular aspects of the beam was studied. By using the Monte Carlo simulation, the probability of the critical chloride content being exceeded at a particular depth was checked. The results of the Monte Carlo simulation for a cover value of 78 mm showed that there was a 92 % probability that the critical chloride content would not be exceeded. Finally it was checked whether achieving better durability and design life made the box beams more circular.

Circularity was considered in two ways, future adaptability in terms of adapting to changing space requirements/function and the technical issue of disassembly of the beam from the bridge. An impact analysis was conducted to study the adaptability to changing function, where a scenario of increase in traffic was considered and the performance of the beam was evaluated in terms of its capacity to adapt to these changing loads. The key aspects affecting disassembly were identified and a scoring system was developed by

weighing these key aspects of the box-beam designed (with and without cover increase).

The main conclusions of the thesis were that a cover increase would be a suitable way to improve durability against ingress of chlorides. Subsequently this allows for overdesign which allows the beam to adapt better to future scenarios of traffic load increase. This fictitious future scenario involved an increment of the tandem system loads in Load Model 1 by a factor of 2. For the future scenario considered, the SLS and ULS requirements of the beam were met. The cover increase also improves the recyclability of the steel embedded in the concrete. By accounting for corrosion due to ingress of chlorides potential for multiple service lives is also improved. Further value creation can be achieved by improving the disassemblability of the box-beam. To improve the future scope of demountability, key aspects affecting this property were identified. The weighing of these key aspects against each other allowed for a scoring system to be determined, highlighting future areas for improvement.

1

INTRODUCTION

This chapter will give a broad outline of the contents in this thesis. Section 1.1 deals with the motivation behind the research topic. Section 1.2 describes the scope and the objective behind the research. Section 1.3 discusses the objectives to be achieved in the form of main and sub-research questions, while section 1.4 describes the methodology followed to answer the research questions. An overview of the structure of the thesis is shown in section 1.5.

1

1.1. MOTIVATION AND BACKGROUND

1.1.1. NEED FOR A CIRCULAR ECONOMY

The demands of a growing population place a large strain on already limited resources forcing the need for a more sustainable and circular economy (CE). "A circular economy describes an economic system that is based on technological advances and new business models which replace the 'end-of-life' concept with reducing, alternatively reusing, recycling, and recovering materials and energy in production/distribution and consumption processes in order to keep products at their highest possible value, thus operating at the micro-level (products, companies, consumers), meso-level (eco-industrial parks), and macro-level (city, region, nation, and beyond), with the aim to accomplish sustainable development, which implies creating environmental quality, economic prosperity, and social equity, to the benefit of current and future generations."[1]
The Dutch government aims at a completely circular economy by the year 2050[2]. The construction industry as part of the economy provides a lot of opportunities to incorporate circularity since it primarily follows a linear life cycle (figure 1.1). The construction industry is a drain on resources and is responsible for 50 % of raw material used, 40 % of total energy consumption and 30 % of total water consumption in the Netherlands. Besides, it also contributes approximately 40 % towards waste accumulation and also contributes heavily towards CO_2 emissions[3]. Therefore, a transition to an economy where demolition can be substituted with deconstruction and land filling with reuse (or recycling) is required. Substitution with these two alternatives would reduce the strain on natural resources as well as lead to less waste accumulation. This in turn reduces the extent of negative impacts on the environment in the form of excessive resource usage and harmful emissions. Within a circular economy there will be no (or considerably less) waste through the reuse of materials (at an asset as well as component level). If reuse is not possible, recycle as much as possible from the product (end-of-life phase) and this becomes the raw material, either in the manufacturing process or in the assembly process of the same or another product (figure 1.2).

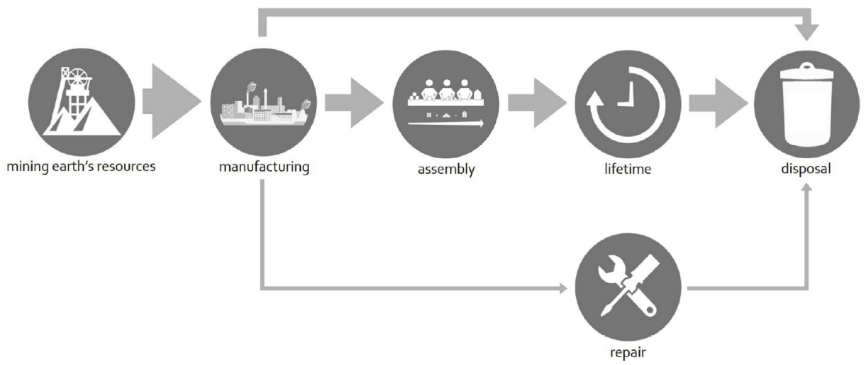

Figure 1.1: Material flow in a linear economy [1]

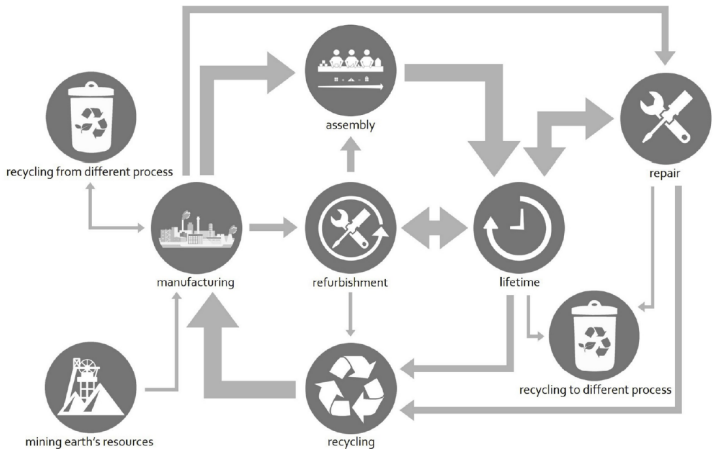

Figure 1.2: Material flow in a circular economy [1]

1.1.2. TRANSITIONING TO A CIRCULAR ECONOMY

There are various plans put in place by the government, to transition from linear to circular economy. One such plan is to reduce the consumption of raw materials by 50 percent by 2030 and ultimately be waste free by 2050 [2]. These involve making more efficient use of raw materials such that only what is needed is used, making use of resources that are inexhaustible (renewable), and in turn also reduce the dependency on fossil fuels, and develop newer methods of production and design of more circular products. The last strategy of designing more circular is one of the reasons behind the topic chosen in this thesis. The design of more circular products provides an interesting opportunity, especially in the construction industry since most products today were never designed with circularity (or even sustainability) in mind until now. There is a growing popularity for sustainable products and the construction industry should be no different. The construction industry in the Netherlands in most cases do use the strategies of recycling of concrete from buildings into recycled aggregates used as foundation material for roads and other civil engineering works but this type of reuse is quickly becoming saturated [4]. This is also a form of down-cycling where a loss in value of the concrete is seen i.e. it is being reused but not in the same way as before where it provided more value as structural concrete. Other forms of reuse to promote the CE in the construction industry need to be investigated to replace this form of down-cycling of concrete.

Hence the reuse at the product level is looked into, where individual beams/girders or columns could be reused to perform the same function elsewhere. Research has been done in the fields of circular economy and construction but until quite recently most of it concerned buildings and the circular design of buildings [5, 6, 7]. Since bridges also contribute to the construction industry, one of the goals in this thesis is to explore the topic of circular bridge construction in the form of reuse of bridge components.

The idea behind the study is to attempt to validate the benefits of life span extension from the point of view of multiple life cycles and better recyclability potential. Another benefit of life span extension is the reduction in energy needed for the production of

new components and a subsequent reduction in greenhouse gas emissions (produced through concrete production). The CE focuses on certain design principles to transition quickly from a linear one. One such design principle is the lifespan extension of products for the purpose of value retention [8]. This design principle is investigated further to see how it can be applied to circular bridge construction from a design stage. Circularity is a way of thinking rather than a process with a fixed set of rules. For the purpose of narrowing the scope and providing more clarity, it becomes important to limit our definition of the term 'circularity' or 'circular construction'. Briefly, circularity can be achieved by making use of the 3R's policy, namely reduce, recycle, and reuse. The reuse strategy within circularity is investigated since it involves keeping products at a higher value level as compared to recycling.

1.2. OBJECTIVE AND SCOPE

Numerous bridges in the Netherlands are approaching their end-of-service life, some of which will require immediate attention. Currently the strategy is to increase the service life through repair/maintenance or additional strengthening measures to keep these bridges functioning. However, this is not a permanent solution as it does not extend the service life indefinitely. This provides an opportunity for the government as well as various other sectors within the construction industry to incorporate circularity (circular designs) into the bridge construction process when designing new bridges for the future. By doing this, the same process of building new bridges and having to having to carry out extensive repair operations can be avoided. This line of thinking could lead to the development of design principles (or strategies) to be followed in the future to realise circular bridge construction. One strategy could be the extension of life from the design stage onward to improve the service life.
To narrow the scope down to a realistic level, this thesis will focus on prefabricated box-beam girders applied in the construction of single span bridges without any skew owing to the simplicity of such a system when compared to continuous multi-span bridges. Of the different types of precast bridges, this thesis further investigates precast box-beam bridges since these beams can offer spans upto 50 meters and more. Box beams provide several advantages such as:

1. Better torsional stiffness
2. Better transverse redistribution of loads
3. No additional deck need be cast (only asphalt)

This thesis will focus on circularity of box-beam bridge girders by trying to enhance their reusability through an increase in service life of these girders by making them more durable. The extent of increase of service life is limited to 200 years, since this was the upper limit seen from literature review [9, 10]. The objective thus becomes to check if a long lifespan can be achieved and whether it contributes positively or negatively to the overall circularity of the beam. Methodologies such as Design for Deconstruction (DfD), and its subsection Design for Reuse (DfReu) will be investigated [1]. DfD is a design

[1] These methodologies are discussed in the sub-section 2.2.1

methodology applied during the initial planning stage of structures and can be achieved through use of smart materials or easy to detach connections [11]. DfReu, is a subset of DfD since it involves the disassembly and subsequent reuse [12]. Along with this, the codes and standards used for the design of concrete structures (including bridges) may not always allow for circular designs to be incorporated. One factor to be kept in mind is that the Eurocodes make no mention of the terms reuse and 200 year service life. All the official documents and guidelines used for design take into account a maximum design service life of 100 years [13]. Hence, this will need to be kept in mind when proceeding through this document as the design of a standard box-beam girder will be carried out with a reference period of 100 years. The scope is not about a demountable design, rather a design recommendation that might help add value to the design principle of life extension of components or materials.

1.3. RESEARCH QUESTIONS

For the purpose of achieving the objectives mentioned within the scope of this thesis (section 1.2) a main research question along with several sub-research questions are framed. Through answering these sub-questions the objective and scope are more thoroughly addressed. The main research question for this thesis can be stated as:

How can prefabricated box beam girders be designed for the future (design service life of 200 years) keeping in mind the circular plans for the economy?

The sub-research question will thus become:

1. Where and how do the current practices deviate from those involved in circular practices regarding a box-beam girder?

   Chapter 3 is about the design of a standard bridge box-beam, designed using the Eurocodes. After which, the limitations/barriers to circularity (and reusability) were put forward.

2. What are the main factor(s) that affect the service life of concrete and what design recommendations can be made to increase the service life?

   A detailed literature review (chapter 2) about deterioration of concrete over time and the most common reasons for deterioration reveal what a bridge beam must be designed for. How this was designed for is answered in chapter 4.

3. How do these design recommendations affect the adaptability and demountability of the beam?

   This is answered through a literature review (chapter 2) and an impact analysis (chapter 5) to understand better the adaptability to change in load. The circularity of the beam is explored in chapter 6 by discussing how it can be detached from the bridge.

1

1.4. METHODOLOGY

The main issue explored in this thesis is the circular performance of a box-beam, more specifically the reusability in multiple life cycles. In order to facilitate multiple life cycles, long service is required and this thesis explores the increment of service life during the design phase rather than as an end-of-life practice. Hence, the deterrents to a long service life were identified and the objective was to come up with design recommendations to improve this service life. The next step was to apply these recommendations and evaluate the performance of the beam to understand the feasibility of such a recommendation. Understanding the extra investment that would be required from an initial design stage to increase service life to facilitate multiple life cycles.

A detailed literature review into the topics of service life design, circular economy, circularity indicators was the main form of data collection. Research papers and articles from the year 2000 and onward were considered for the literature review. These papers were experimental [14, 10], theoretical [15], and sometimes even qualitative [16] in nature. The publications and articles were selected based on their relevance to the topics mentioned at the beginning of the paragraph. Documents published by the government of the Netherlands were also considered in the literature study to understand how the Dutch government was planning on proceeding with the topic of circularity in the economy [2, 3, 4].

Once the information from the literature was studied, the first step was to design a standard box beam using the Eurocodes. SCIA Engineer 21.0.0030 was used to run a linear analysis on a bridge deck to obtain the critical cross-section forces used to design the reinforcement and prestressing steel. Once the beam was designed, it acted as a prototype on which to test the design recommendation. Understanding how service life was guaranteed through the Eurocodes was also important since one aim was service life improvement. The service life improvement had to come from a design recommendation that could be applied in the design phase. The impact of the design recommendation on circularity was studied further by using existing indicators as inspiration [5, 6, 7, 17]. This resulted in a scoring system to understand the key aspects regarding detaching the box beam from the viaduct on a global level.

For the improvement of service life against chloride-induced corrosion, the DuraCrete model was used since it conforms quite well to Dutch codes and practices. It allows for increased service life through cover increase which could be applied in the design phase. The improvement in the DuraCrete model was done using a Monte Carlo simulation since this was an accurate forecasting method especially when random variables were involved [18].

1.5. THESIS STRUCTURE

Chapter 2 will consist of the literature review conducted in order to investigate existing work regarding circularity, circular construction, durability, and corrosion. Chapter 3 will give the initial steps of this thesis. This involves the use of a finite element software (SCIA Engineer 21.0.0030) and the relevant codes (Eurocodes) to design a prefabricated box-beam girder for 100 years. Chapter 4 will go into detail over what design recommendation(s) were chosen, while chapter 5 will discuss the effects of these design rec-

ommendation(s). The design recommendations will be applied to the beam designed in chapter 3. Chapter 6 will cover the effect of these recommendation(s) on the circularity of the beam. Finally, chapter 7 will conclude overall whether the main and sub-research questions were answered.

2

Literature Review

This thesis proposes to investigate the extension of service life of box-beam bridge girders and whether this could improve the circular performance of the beam. Hence some of the main topics reviewed are:

The principles of circular economy, circularity, its introduction in the construction industry through design methodologies is discussed in section 2.1 and 2.2. Understanding its application in the building industry could help identify areas where it could be applied to bridges and viaducts. This is done in section 2.3. This could help to identify possible indicators or key aspects affecting reusability for future research as well.

Section 2.4 discusses the main challenges when trying to increase the service life, the mechanism of deterioration, and possible strategies to overcome these deterioration mechanisms.

Section 2.5 provides a summary of the main takeaways from the literature study.

2.1. CIRCULARITY AND SUSTAINABILITY

There is a pressing need for the implementation of circular practices in all facets of the economy. This is necessary for two reasons, the achieving of sustainable practices and the differentiation between economic progress and resource depletion [19]. Sustainability in a nutshell can be described as the efficient management of our resources without compromising these resources for future generations. A detailed explanation of circularity is given in the following section (see section 2.2). Sometimes it can be quite confusing to differentiate between the two since every industry will have its own definition of the same concept, but there do exist quite a few differences. A key concept to be understood before proceeding is that CE (Circular Economy) is the means by which sustainability becomes a reality. Circular practices are changes made to the traditional way (processes) of doing things such that they become more sustainable. Sustainability is only limited by the technological advancements (in theory) but also depend largely on the reception by the public.

Currently, the most popular tools relating to circularity are MCI (Material Circularity Indicator) and LCA (Life Cycle Analysis) [19]. However there are shortcomings with these existing tools since the LCA which is the most popular, does not really evaluate circularity. It follows the life cycle of a product from cradle-to-grave and evaluates the environmental effects until the EOL (End OF Life) of the product is reached. However it does this keeping the model of the linear economy in mind (see section 1.1.1). From literature, it was seen that when circularity indicators were developed (for a particular industry), there was always contrasting results between CI (Circularity Indicators) and the LCA analysis [19]. Simply put, it means that the most circular option need not be the most environment friendly. Hence the LCA analysis could be thought of (additionally) as a tool to keep CI's in check. The MCI does a better job, in that it does indicate whether a product is more circular or not but on a material level. A good example to clarify this is the work done by Lonca et al. where MCI's were used to determine the circularity of tires through life extension but were not completely good for the environment or health of people in the long run [20].

2.2. CIRCULAR ECONOMY

This section of the Literature Review will deal with circularity and the circular economy. A Circular Economy can be achieved through replacing traditional end-of-life practices and business models with strategies of reuse, recycling, and reducing. The circular aspects becomes clear when the material loops (energy loops) are closed (see figure 1.2). However, over time there have been various additions to these 3R's such that a 9R strategy can be envisioned for a construction supply chain. These additions (see figure 2.1) include **R**efuse, **R**ethink, **R**epair, **R**efurbish, **R**emanufacture, **R**epurpose, and **R**ecovery. Of these 9R's Recovery (R9) and Recycling (R8) deal with the outer stages of the supply chain.

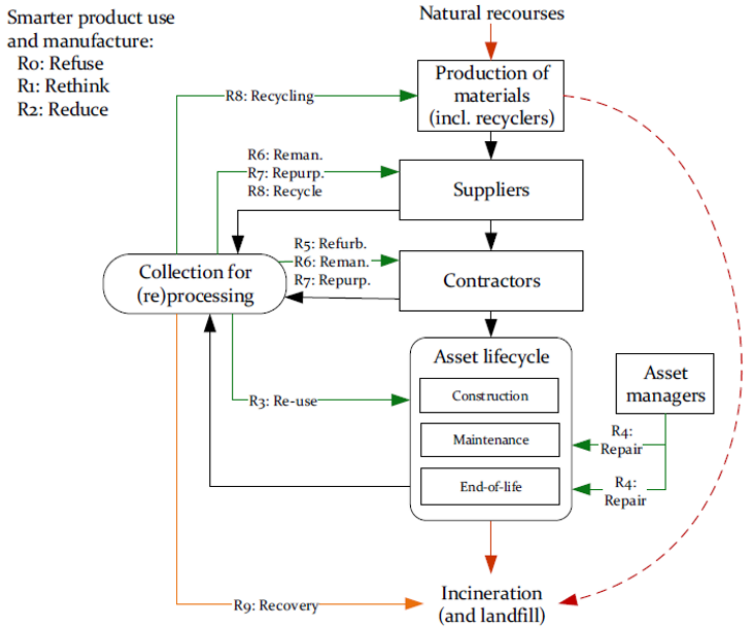

Figure 2.1: Material flow in a circular economy [17]

For a circular economy to become a reality, the aim must be to extend the useful life of the structure through repair and refurbishing (R4 and R5). This ensures that the value of the product (structure) remains at the highest possible level. Another area of interest is Reuse (R3) where once end of life is reached the asset components are collected for reprocessing and then put back into the construction supply chain to be reused. This would be the R strategy that gives maximum gain, since no repair, re-manufacturing, or refurbishment is involved (hence saving costs) and the reuse as a component would keep it at a high value level as well.
Failing that, adaptive reuse must be the goal, wherein certain components within the structure (beams for example) can be reused. Adaptive reuse maintains the value of the component, which is still higher than if it were stripped down to its base components and then reused (down-cycling). By not making use of the residual life cycle there is a wastage of embedded resources which is still quite exploitable [21].
The reasons behind the growing importance of adaptive reuse can thus be stated as follows:

1. A vast portion of the earths existing resources are already embedded within the built environment

2. The price of extraction is becoming higher

3. The negative effects on the environment due to these extraction activities is also quite high

Adaptive reuse could be a way to circumvent most (if not all) the above mentioned negatives. This is where the methodology of Design for Disassembly (DfD) comes into play. For adaptive reuse to take place, the components of a structure must be detachable or disassembled. The reality of the situation might not allow for complete disassembly, rather a partial one. During the planning phase of the project, the disassembly of the various components must be considered, where the disassembly could be through selective disassembly, selective demolition or through installation of a temporary replacement [21].

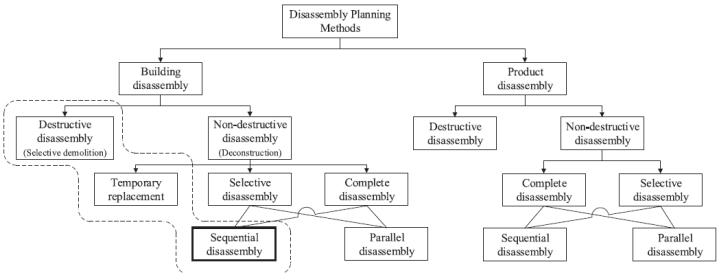

Figure 2.2: Disassembly sequence for buildings and products. Source: [21]

The construction industry is a heavy contributor to the waste in landfills and harmful emissions through concrete and steel production [3]. This thesis aims to investigate the effects of reuse and increased lifespan of concrete members to see whether it has a positive or negative effect on circularity. There are already various methodologies where circularity is concerned. These include Design for Disassembly (or Deconstruction), Design for Reuse (DfReu), Design for Adaptability (DfA) and these methodologies need to be implemented during the early stages of planning of any project for there to be any effect. Another area of focus of this thesis is how the prefabricated box-beam girders can be reused. What must be done (from a design point of view) for the extension of lifespan (which hopefully makes it more reusable) so that the above mentioned methodologies can become effective.

2.2.1. DESIGN FOR DISASSEMBLY (DFD)

Design for Disassembly is a design methodology to be implemented during the planning stage of any structure to enable demountability or disassemblability and can be achieved through the use of smart materials or smart designs [22]. Currently, smart designs are the way to move forward owing to the increased knowledge and experience in this department. The main principle behind this methodology is to use temporary connections between different components of a structure along with more mechanical connections rather than chemical connections between components. Although the aim of this thesis is reuse of prefabricated girders, due to which Design for Reuse (DfReu) is governing, DfD will come into effect in the long run where recovery is concerned.
As seen in the figure below 2.3, there are many factors that affect DfD. Akinade et al concluded that there are 43 critical success factors for DfD to succeed in the construction industry [11].

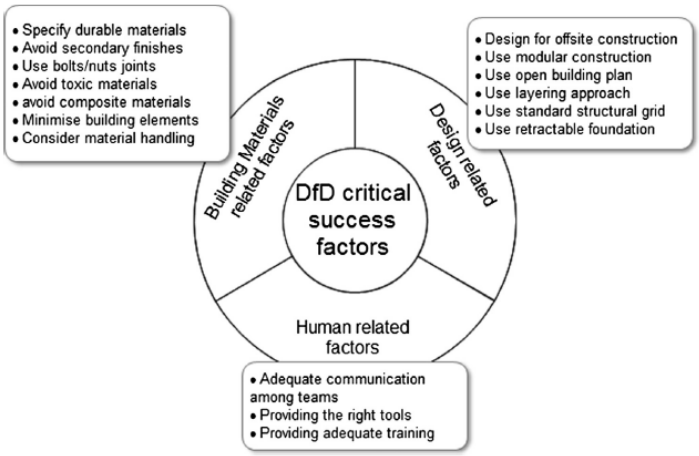

Figure 2.3: Critical success factors [11]

If one brings attention to the building and material related factors, it becomes clear that specification of durable materials is a critical success factor. The design related factors call for the need to design for offsite construction and the use of modular elements. These factors quite closely resemble the factors that were needed for successful application of Design for Reuse (DfReu) methodology. This will be discussed in detail in the next subsection. One cannot stress enough how important some of these factors are for the progress of DfD and DfReu within the construction industry and the economy as a whole. Human related factors especially play a crucial role in the success of DfD since there are many parties involved within the supply chain of construction. The role of each involved party needs to be made clear where circularity is concerned. There have been a number of cases where human beings tend to follow a 'first is best' policy due to which they refuse to change from the traditional way of doing things and ultimately it will always be people (society as a whole) who decide what is good and bad. Hence it becomes even more important for stringent legislative policies to be put in place that allow for the smooth transition from traditional (linear) to circular practices. Akinade et al. [11] conducted research into the critical success factors for avoiding waste ending up in landfills and it was seen that 'Stringent legislation and policy' was weighed above factors such as 'Deconstruction design process and competencies' and 'Design for material recovery'.

DESIGN FOR REUSE

The Design for Reuse (DfReu) methodology is a subset of DfD since deconstruction serves as a means to disassemble the asset into its respective components which can then be reused or recycled. The purpose of DfReu is to try and use the embedded energy as much as possible by keeping the product at a high level of value [12]. It is not always possible to directly reuse products or components directly after disassembly owing to constraints such as differing spatial requirements and structural integrity. Simply put there will always be difficulty to find a match for reuse of a component unless predetermined. From the point of view of the circular economy, reuse can be achieved by designing more

durable products so that they last longer. Products that require less maintenance and have ease of access such that it can be kept clean over a long period of time are also important factors for improving the reusability of a component.

LIFE EXTENSION

The principle of life extension is another important feature of the CE where savings can be seen in the form of less material and resources being needed by avoiding the need for a new product. The objective is to extend the useful life and keep structures/assets contributing at their maximum value level. This is one of the circular design principles used by Rijkswaterstaat to achieve value retention. This is discussed further in sub-section 2.2.3.

2.2.2. INDUSTRIAL FLEXIBLE DEMOUNTABLE (IFD) CONSTRUCTION

Another source of literature namely the NTA 8085:2021 IFD construction of fixed bridges and viaducts [23] provides information to promote the disassembly of bridge components in a realistic manner. It provides technical information for the design and construction of bridges and viaducts with the option of eventual disassembly. This can be brought about through the standardization of connections between different bridge interfaces. It ultimately falls into the category of circular practices and makes use of many of the same principles such as modularity and standardization of elements. The main principles of IFD however are:

1. Use of standard and prefabricated elements (**I**ndustrial)
2. Adaptable construction (**F**lexible)
3. Disassembled and reusable (**D**isassembled)

Modularity and standardization go quite well together since it is easy to standardize repeatable elements. IFD construction aims to make use of this fact to facilitate simple, flexible, and even cost saving designs for a fixed bridge. The NTA 8085:2021 gives details about the bridge superstructure, substructure and transition joints in new construction as well as in renovation of existing structures. From the point of view of this thesis, only new construction information was looked at instead of how this standard could have been applied to existing bridges. Of particular interest were the design recommendations for single span (statically determinate) structures and the corresponding application of IFD principles. Some of the characteristics of bridges to which IFD construction can be applied are:

1. straight beams between 5 - 45 metres in length
2. statically determinate beams
3. crossing angle of 90 degrees
4. constant cross-section over entire length
5. road width between 6m and 30m

6. concealed slope (using the wear layer)

Much of the requirements meet current prefabrication rules as well, for example the rule where the elements are cast off-site and only assembly takes place on site. The parts used for construction are hoist able and transportable is another feature that resembles current practice involving precast elements. The NTA 8085:2021 also requires the use of material passports for all elements to facilitate future identification and then reuse.
The manual also provides information regarding the disassemblability of connections for the superstructure. These include the railings, barriers etc. and was another step in the right direction towards full disassembly (followed by reuse) of bridge components. Not much information is provided regarding the transverse post-tension connection between beams (box-beams) and how to overcome the monolithic connections in place when following traditional practice. There is a lot of potential seen here and new more circular designs can enhance IFD design practices. New and innovative design strategies will always be developed with increasing development of technology, however not all of this is put into practice leading to a gap between research and practice. An example of this is seen in the development of service life models over time but still a lag in what is codified (in the Eurocodes or other official documents) [24]. This will be described in more detail in section 2.4 where the durability of concrete structures and service life are discussed. Before addressing the gap in research and literature it becomes important to know to what extent circularity is already being put into practice and the impact of these practices.

2.2.3. CIRCULAR PRINCIPLES AND RIJKSWATERSTAAT

There are a few notable projects set up by the government for the transition towards a more circular economy. The most notable of which is the Platform CB'23-Core method for measuring circularity in the construction sector which aims to come up with a new way of thinking to successfully measure circularity by the year 2023 [25]. Additionally, the Dutch government (Rijkswaterstaat) along with Witteveen + Bos engineering firm have come up with certain 'circular' design principles as seen in the figure 2.4 [17]. These design principles describe the line of thinking behind achieving a circular structure. As seen in figure 2.4, after prevention, the principle of value retention can be achieved through the expansion of lifespan of the existing object. This case refers to already existing structures/structural members, but possibly could also be extended to new components/members where extended lifespan (greater than the norm) becomes a prerequisite before the start of construction. Literature concerning circularity and its implementation [11, 12] highlight the importance of incorporating this in the planning stage. This extension of lifespan (see figure 2.4, refers mainly to additional strengthening measures to keep the structure in use. Although this purpose is achieved, it is not a permanent one and will require replacement in the future. The application of life extension can also be a premature action taken such that the principle of applying circular principles in design phase is also achieved. This would hopefully delay the strengthening measures required and also take into account future deterioration. The next step in the circular design scheme (figure 2.4) mention the actions to achieve value creation through 'designing for multiple life cycles', designing future proof', and 'designing for minimum maintenance'.

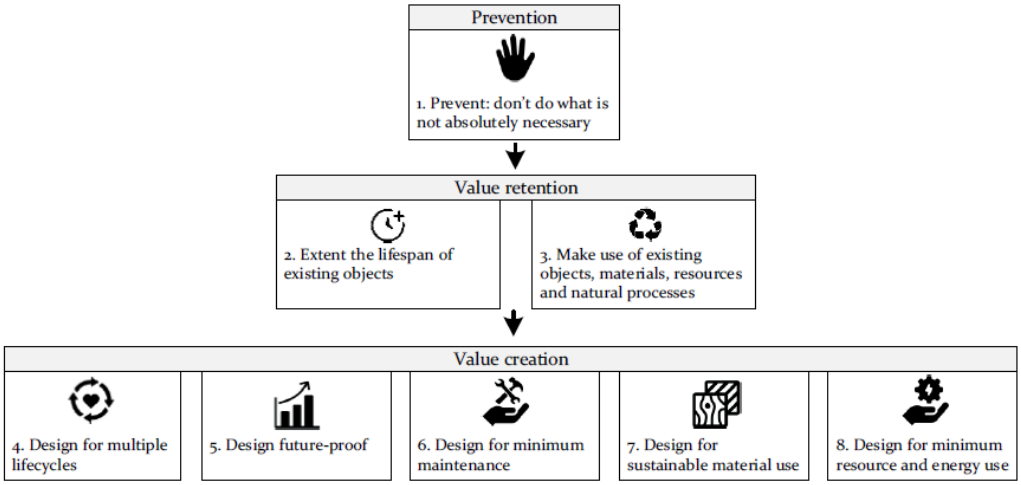

Figure 2.4: Circular design principles [17]

There are already several plans in place to achieve circularity within the economy put in place by the government. But the aim for full circularity in the economy by 2050 is an ambitious goal and requires a lot of research especially if the construction industry has to meet this goal. Although the Platform CB'23 has been setup there have been other circularity measurement tools over the years [26, 17, 27, 5]. Most of the indicators were developed for buildings rather than for other civil engineering structures (bridges, tunnels etc.), excluding the work done by Coenen T. which was specifically for bridges and viaducts [17]. Platform CB'23 aims to assimilate all the existing information regarding circularity in the building industry and try to present a core method such that an easier understanding of 'what constitutes circularity' for structures is facilitated [25]. The future adaptive capacity of structures (or components) as mentioned in this guide refer to two types of adaptability, 1) spatio-functional adaptive capacity, and 2) technically adaptive capacity. The former refers to the adaptability of the structure for changing functions and space requirements and the latter about the detachable connections. An example of spatio-functional adaptive capacity could be the broadening of a bridge.

2.3. CIRCULARITY INDICATORS

Literature concerning circularity has been growing over the past decade, especially as it is fast becoming a necessity rather than just an additional perk. The most notable reference seems to be the work done by Ellen MacArthur Foundation launched in 2010, in the hopes to accelerate the transition towards an economy that is more circular. The work done by this foundation along with their partners was indeed a step in the right direction as it served as the base for further research and development [26]. Circularity as a concept is rather vague and does not have concrete steps that can be taken for it to be applied in any industry especially the construction industry. The Ellen MacArthur founda-

tion did develop certain ways in which circularity could be measured (for an asset) [26]. These indicators developed by the Ellen MacArthur foundation along with their partners focus on circularity on a material level, taking into account the amount of virgin materials used, the amount of recycled and reused materials used. This would not be the best way to measure circularity for this thesis since the beam here is being designed for the future making use of all virgin materials. Work done by Durmisevic E. [5] also provides information regarding the transformation capacity of structures (exclusively buildings), where it was highlighted that buildings could be separated into layers depending on the service life of different components. However, a better degree of independence between these layers would lead to better economic and sustainable development. A differentiation is also made between use life cycle and technical life cycles, where the former is governed by changing spatial requirements and the later by durability. Verberene J. [7] proposes building circularity indicators to introduce the topic of circular economy in the built environment to an extent where it can be used to differentiate construction/design options. It is a consistent theme in most literature [7, 5, 28], where Brand's Shearing Layers are used as a basis upon which the circularity of an asset is looked at. The type of connections also play a major role in deciding reuse (which ultimately decides circularity) as discussed by Berlo S. [16]. From the point of view of reusability, disassemblability has the highest priority [7] since this facilitates replacement and reuse. The separation of functions of the different sub-systems or components in an asset ultimately also play a role in disassembly [5]. The literature discussed thus far relate to circularity of buildings. The following paragraph describes the only circularity indicator (to the best of the authors knowledge) found from literature to measure and score the circularity of bridges and viaducts and is therefore explored in detail. Understanding the indicator would help conclude whether it could be adapted for use on a component level.

Coenen T.B.J. has taken efforts to document the circularity and circularity indicators for bridges and viaducts [17]. Therefore this was first looked into to study how circularity could be measured on as asset level, and whether it could be adapted to a component level directly. Coenen T.B.J. discusses the use of four main sub-indicators that should encapsulate circularity (at least broadly) in a contextual manner for a bridge. The reasons behind a bridge being built will always be the same, i.e. to get from one point to another, spanning either a road, railway, or a water body. The secondary purpose of a bridge in some cases is to be aesthetically pleasing and to compliment the surrounding infrastructure of an area. The variables here stem from the wishes of the owner, the design service life of the bridge, the dynamicity of the area, the (changing) functional requirements of the bridge, robustness (decided by owner) etc. Hence it becomes clear that these indicators cannot have fixed values and will change with the bridge in question. A possible solution to this could have been a standardization of bridges but this can be a called a restriction on architectural freedom. Hence it becomes even more important to be able to weigh these indicators in the right way to assess the circularity of a bridge. The four indicators proposed by Coenen T.B.J. are:

1. Design Input
2. Resource availability
3. Reusability

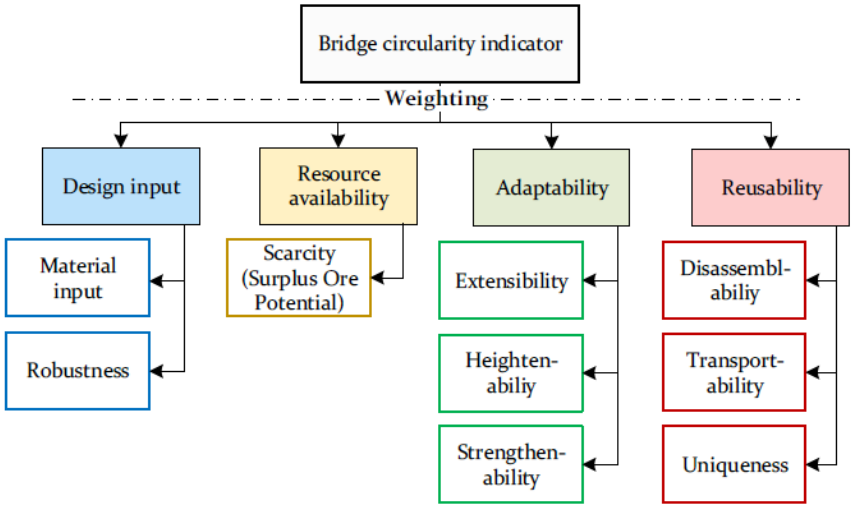

Figure 2.5: Bridge Circularity Indicator [17]

4. Adaptability

2.3.1. BRIDGE CONTEXT

If the scores for these indicators are given by the framework user, a certain amount of personal bias will exist. To avoid this, in addition to the indicators, a bridge context was also defined. The context here refers to three variables namely (i)Spanned area, (ii) Dynamacity of the area, (iii) Design life of the structure. This bridge context allows the framework user to weigh the indicators in an appropriate manner.

TYPE OF SPANNED AREA

The type of spanned area and its relation to the indicators is described here. Depending on the type of spanned area, each indicator will have a certain value as seen in figure 2.6.

Type of spanned area	*Design input/robustness*	*Adaptability*	*Reusability*
Roads	0,6	0,8	0,8
Railroad	0,8	0,4	0,6
Land	0,8	0,6	0,4
Water <10 m	0,6	0,8	0,8
Water >10 m, <30 m	0,8	0,6	0,6
Water >30 m	1,0	0,6	0,6

Figure 2.6: Relation between spanned area and indicators. Source: [17]

DYNAMACITY OF THE AREA

How likely an area is to change can never be predicted, only estimated and dynamacity here refers to how the surrounding area might change with time. The range of dynamacity is from 1-5, where 1 means least dynamic and 5 is most dynamic. The relation between dynamacity and the indicators is seen in figure 2.7.

Dynamicity	*Design input/robustness*	*Adaptability*	*Reusability*
1	1,0	0,2	0,2
2	0,8	0,6	0,2
3	0,6	0,8	0,4
4	0,4	1,0	0,6
5	0,2	1,0	0,8

Figure 2.7: Relation between dynamacity and indicators [17]

DESIGN LIFETIME

The third and final variable described by the framework is the design lifetime of the structure and is by the owner. The study done by Coenen [17] made use of expert opinions to decide the relation between the importance of the indicator (0-1) and the expected lifetime of the structure.

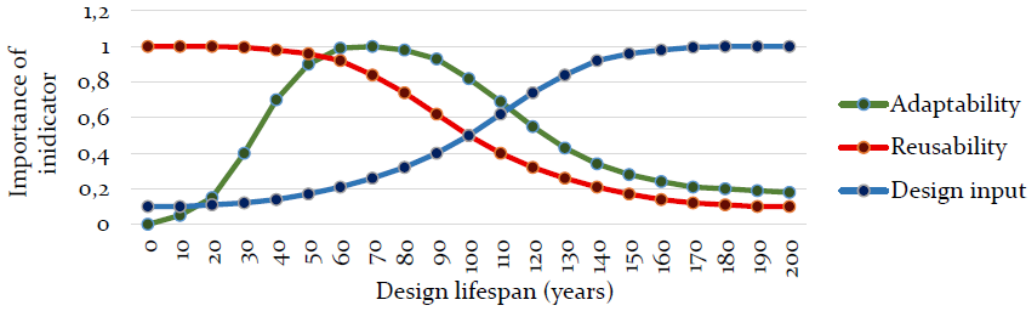

Figure 2.8: Relation between design lifetime and indicators[17]

The personal bias that cannot be accounted for (coming from the framework user) will always exist but in the end has to be weighed and this reduces to some extent the effect of bias. The user of the framework is allowed to have a bias by scoring an indicator however they like but only a certain predetermined weight of that indicator is taken into account. For example, the user can decide what the dynamacity of the potential bridge site is but then figures 2.6,2.7, and 2.8 are used to decide weight of the scores of the indicator. For example, a particular scenario involving a road bridge, designed for 80 years and the dynamacity of 3 can be considered to better explain the use of the tables. When referring to the three figures mentioned, each indicator (DI, Adaptability, Reusability) will have three weight values, the average of which is used to determine the final contribution to the circularity score.

2.3.2. DESIGN INPUT

The design input indicator is two-fold since it indicates the amount of recycled and reused material used in the bridge and also takes into account the robustness of the bridge.

MATERIAL INPUT

A Material Input indicator was introduced to calculate the fraction of linear flow.The LF (Linear Fraction) [17] indicates the fraction of materials coming from recycled or reused sources (F_{Rec} and F_{Reu} respectively). The possibility that a renewable virgin raw material was used is also taken into account through the term $F_{ren,v}$ (fraction of renewable raw materials).

$$LF = 1 - (k * F_{Rec} + F_{Reu}) - F_{ren,v} \tag{2.1}$$

where, k is a reducing factor to weigh the importance of recycling and reusing (0.8 recommended). It was chosen to weigh recycling less than reusing since reusing leads to more value retention.
The Material Input (MI) is then finally calculated using the formula shown below. The recyclability of a material is

$$MI = \frac{(LF + (1 - recyclable))}{2} \tag{2.2}$$

ROBUSTNESS

This aspect decides the resilience and design life of the asset. Robustness can be defined as the structures ability to withstand external loads. With increasing robustness comes an increase in lifespan of the structure (bridge). The ultimate goal is to prove to the client that the design robustness is more (or equal) to the wishes of the client. Flexibility and adaptability might be reduced if robustness is too high, which is the trade-off the client will have to make. As seen in other sources of literature [5], the technical life of a product or component is not nearly as important as the use life cycle. Hence very high robustness is only useful when the bridge needs to remain in place for a long time. Robustness as calculated by Coenen [17] is shown in equation 2.3.

$$Robustness = \frac{Design\ Robustness}{Minimum\ Robustness} \tag{2.3}$$

The design robustness and minimum robustness both have the same units. However in order to avoid having a DI score of 0, this formula is corrected by introducing a constant 'a' to calculate a term called the 'Corrected Robustness (CR)'. The formula for this is seen in equation 2.4.

$$CR = \frac{a}{Robustness} \tag{2.4}$$

In the above formula Robustness refers to the Design Robustness that the designer can offer (which obviously has to be higher that the baseline Robustness that the client wants). This correction to the robustness was seen in the work done by EMF and their partners as well [26].

The Design Input is calculated using all the above mentioned terms, and has a value between 0 and 1. Where 0 means a non-conformance with circularity and 1 being a good agreement with circularity.

$$DI = 1 - MI \times CR \tag{2.5}$$

2.3.3. ADAPTABILITY

The adaptability of a bridge can be summarised as follows: the ability of a bridge to accommodate the evolving demands of its context, thus maximising its value throughout its service life [17]. Within the framework developed by Coenen Tom B.J. [17], the adaptability of a bridge can further be split into sub-indicators to measure whether the crossing can be broadened, the underpass can be broadened, strengthening the bridge, and increasing the clearance of the underpass. This indicator has three sub-indicators namely Heightenability, Strengthenability, and Extensibility.

The Heightenability sub-indicator is confirmed through the answering of a single question, and must be supported with proof by design. 'Can the overhead clearance of the viaduct be increased without creating waste?' If the answer is 'Yes' the Heightenability has a weight of 1.

The Strengthenability sub-indicator is also given a score in the same manner, through the answering of 3 questions.

1. Can the elements to be strengthened be accessed?
2. Are the reinforcing measures applicable to the geometry of the structure?
3. Do the reinforcing measures result in a decrease in functionality of other system elements?

The Extensibility indicator is split into two parts, extensibility of the crossing road (upper) and extensibility of the crossed road (lower). For the crossed road (lower) if two lanes can be added (one on each side if a two lane road) then a weight of 1 is given, if only one lane can be added a weight of 0.5 and, if no roads can be added a score of 0.
The extensibility of the upper road is decided in the same manner but waste generation and functionality are also taken into account. The designer has to prove whether, 1) a lane on both sides of the bridge is possible without waste creation from the existing structure, or 2)waste creation of a maximum of 5 % (mass of existing structure). The third option was the the possibility of two lanes (on either side) with a lower functionality, without needing an additional sub-structure. If addition of two lanes is not possible, the fourth, fifth and sixth option deal with the addition of a single lane with the same additional criteria of waste creation and functionality. The last option is that the lane is not extensible. The weights for all these statements were decided together with RWS experts [17].
Once these sub-indicators are decided, the final Adaptability score can be calculated, the formula for which is seen in equation 2.6.

$$Adaptability = \frac{2Ex + 2St + He}{5} \tag{2.6}$$

Where Ex = Extensibility, St = Strengthenability, and He = Heightenability.

2.3.4. REUSABILITY

The definition of reusability here refers to, the ability to reuse the entire asset (bridge) or components (parts of the bridge) at a new location as part of another bridge. Reusability can be thought of from two perspectives, asset level (bridge) or component level (beams, piers, abutments etc.). A bridge that is disassemblable, its components transportable, and having a standard design would score a high reusability score.

DISASSEMBLABILITY

For a bridge to be reusable it has to be demountable (disassemblable) first and foremost. This appears to be the most important requirement for anything (component) to be reusable. As per the literature [5], it was seen that with the changing times, a long technical life is becoming a burden. Let us take the example within this thesis, if the bridge was only needed for a short amount of time (20 years) and then reached its end of life (in terms of function) but has been designed for 100 years, the only possible course of action would be to demolish it. This scenario can be avoided if the components of the bridge could be made disassemblable and that gives the owner (or government) the option to reuse these components in another project. The advantages here are plain to see, the demolition could be avoided, leading to lesser amount of waste that would end up in a landfill. Second, the components (beams, abutments, piers) still have a lot of embodied energy that can be exploited if it is reused elsewhere. There was no one formulation for the Demountability indicator and it is decided by an external calculation method, where the methodology proposed by Durmisevic [5], or Beurskens, P. R. [29] can be used as a guide.

TRANSPORTABILITY

Another important sub-indicator is the 'transportability' indicator. A score of 0 in this sub-indicator means the reusability of the girder is not possible. The future scenarios of use of the girder are almost impossible to predict unless predetermined, therefore, only the available modes of transport were investigated to score this sub-indicator. There are three modes of transport available, these are road, rail and over water (if the bridge was constructed close to or over a water body). After this one needs to look into the restrictions for each mode of transport as there will be certain restrictions placed by the transport authorities regarding the tonnage (weight) that can be moved over road. If the bridge components (girders for example) exceed this weight, then other modes of transport will need to be arranged, which might further increase the cost of reuse and this will have to be calculated in the life cycle cost of the beam. The valuation decided by Coenen can be seen in figure 2.9.
The valuation applies to each component that makes up the asset (bridge) individually, and is used in equation L.9 to obtain the total transportability of the asset.

$$T = \frac{\sum(M_j \times T_j)}{\sum M_j} \tag{2.7}$$

Where,

$$M_j = mass\ of\ component\ j$$
$$T_j = transportability\ of\ component\ j$$

Transport infrastructure	Valuation	Transport infrastructure	Valuation
Water, rail, 1-lane road	1,0	Water, 2,3-lane road	0,7
Water, 1-lane road	0,9	Rail, 2,3-lane road	0,7
Rail, 1-lane road	0,9	2,3-lane road	0,6
1-lane road	0,8	Water	0,4
Water, rail, 2,3-lane road	0,8	Rail	0,3

Figure 2.9: Valuation of transportability as per Coenen [17]

UNIQUENESS

Another sub-indicator of interest is the uniqueness of the components to be reused. The use of standardized components will make the (eventual) reuse of said components that much easier. A component with a very unique design will be difficult to use for other projects and hence would get a lower reusability score. One potential solution could have been a fixed standardization but that would lead to arguments regarding restriction on architectural freedom. A middle ground could be achieved wherein rough dimensions could be agreed upon for certain spans. Doing this could ensure to a certain extent that a beam could be reused for another project with a similar span.

2.3.5. RESOURCE AVAILABILITY

This indicator is somewhat difficult to measure since it is quite an open environment if we consider everything (all the supply chains involved) and not just the availability (scarcity) of raw materials. For the time being the SOP (Surplus Ore Potential) indicator is being used since it also accounts for feasibility of extraction of materials from the earth when compared to ADP (Abiotic Depletion Potential). The weight of this indicator towards the circularity score is taken as 70 percent of the Design Input indicator since these two indicators deal with materials (recommended by the work done by Coenen [17]).

$$S_{total} = \frac{\sum_{i=1}^{n} SOP_i \times M_i \times 10}{M_{total}} \tag{2.8}$$

Where

$$S_{total} = Asset\ scarcity$$

$$SOP_i = Surplus\ Ore\ Indicator\ of\ material\ 'i'$$

$$M_i = Mass\ of\ material\ 'i'$$

$$M_{total} = Total\ mass\ of\ asset$$

The SOP of different material can be found in literature and the formula shown in equation L.6 can be used to calculate the score for this particular indicator.
The four indicators described above form the basis on which circularity was calculated for a bridge as per Coenen [17]. Not much literature was found where circularity of bridges in particular were measured. The CB'23 group make it clear that having a large number of circularity measuring methods is not always an advantage if these methods are not comparable with each other [25]. One limitation that was seen was the open ended nature of the demountability indicator where no fixed method was proposed.

This section provided an overview of an existing bridge circularity indicator developed and its sub-indicators for an asset. The adaptation of this indicator (and sub-indicators) to a component (beam) is explored is chapter 6.

2.4. INCREASE IN SERVICE LIFE

As seen in figure 2.4, the principle of life extension is one of the options used by the government to keep structures in use once end-of-life is reached. However, it was concluded from the previous sections 2.2 and sub-section 2.2.1 (also see figure 2.3) that circular methodologies need to be incorporated from the design phase onward. On of the critical success factors were also seen to be 'specification of durable materials'. Hence this section explores the how durable materials can be used to try and incorporate life span extension from the initial stage of design. The use of more durable materials would also facilitate multiple life cycles since the material/component can be used for longer.
From literature [30, 14, 9], it becomes clear that one of the main deterioration mechanisms that reduces the service life of concrete structures is corrosion. It affects the long-term mechanical properties of reinforcing and prestressing steel as well reducing the capacity of concrete elements. Hence, overcoming this barrier through design recommendations was the next step. There are ways to increase the resistance against corrosion especially through a decrease in water cement ratio [31]. This is a mix-design recommendation and not a design recommendation due to which further literature in this area was not pursued. The current guidelines mention that 100 years of service life can be achieved by following the prescribed deemed-to-satisfy approach [24]. The Eurocodes (EN 1992-1-1 and EN 206) however place certain restrictions in the form of minimum requirements (cement content, water/binder ratio, strength class, etc.)[32, 33]. Therefore, the best way to improve durability further was through the use of extra cover [34].

FATIGUE AND TRAFFIC LOADS

When designing for 200 years other aspects such as fatigue strength and possible increase in traffic loads will also be important factors to consider. A longer service life of bridge components will lead to more number of cycles of stress ranges. The magnitude of this stress range would be subject to change as well depending on the change in traffic loading over the long service life. The damage that might occur due to fatigue cannot be ignored in the long run. The effect of special vehicles also needs to be considered to model traffic loading [35]. An increase in freight traffic is also expected by the European Commission [36], however permissible limits set by the government will also play a role in the expected increase. Within this thesis the immediate problem was identified to be corrosion since it could start to affect the structure as soon as 10 years into use. Hence, the next step was to understand the mechanism through which corrosion occurred.

2.4.1. CORROSION

It has to be said that concrete that has a high level of design, workmanship and finish should, in theory at least have sufficient durability against corrosion. Owing to its high alkalinity, the steel embedded in concrete is passivated and therefore safe from corrosion. Passivation of steel (reinforcement) is the formation of a thin oxide film on the

surface of the steel bar hindering corrosion. This passive protective layer is in fact the initial corrosion product but protects the steel from further corrosion. From literature [30], it is seen that there are two main reasons for corrosion. Chloride induced corrosion and corrosion due to carbonation. The effect of corrosion on a beam with reinforcement are two-fold. First, the formation of corrosion products (which have a higher volume) can cause cracks in the concrete matrix. The formation of these cracks can lead to more impurities (corrosive agents) to reach the steel further increasing the rate of corrosion. If left unchecked, this process will lead to loss of steel cross-section further weakening the capacity of the beam.

MECHANISM

Corrosion is an electrochemical process that requires several chemical reactions to bring about. Three main components of a corrosion cell are anode, cathode, and electrolyte. The anode and the cathode can be on the same steel bar (micro-cell) or on different steel bars separated by a finite distance (macro-cell). These different cells (micro and macro) exist due to the uneven distribution of chlorides on the surface of the concrete. A common example of a source of chloride is the de-icing salts used on roads and bridges. Other sources include admixtures, mix-water, sea water, and even aggregates. Due to all these sources of chlorides, the distribution of chlorides in and over concrete is uneven. This uneven distribution of chloride ions lead to 'positive' and 'negative' areas, and this sets up the galvanic corrosion cells within the concrete matrix.
Corrosion can also be introduced through carbonation reactions taking place within the concrete matrix. Carbon dioxide can penetrate the concrete and mix with the pore water to form carbonic acid and reduce the pH of concrete. When the alkalinity becomes low enough the steel becomes de-passivized, and corrosion starts to take place. The corrosion products formed tend to take up a larger volume (3-6 times) than that of steel and this induces stress in the concrete resulting in spalling and cracking of concrete. However, carbonation induced corrosion seems to be less likely to take place if the proper steps are taken to prevent chloride induced corrosion initiation. According to EN 1992 exposure classes for concrete, environments containing chlorides are more aggressive that those containing carbonates. For both, carbonation as well as chloride induced corrosion, sufficient concrete cover is an effective way to prevent corrosion initiation. The reader is advised here that, there is a marked difference in both carbonation induced and chloride induced corrosion and how they affect structural concrete. The use of the current edition of the eurocodes makes it out to be that a higher cover is required when dealing with XD environments than with environments with an exposure class of XC. XD simply means those environments where chloride ions can make its way on to the surface of the structure through means other than sea water/marine environments. A choice was made within this thesis to focus on chloride induced corrosion as it eventually leads to a loss of steel cross-section and could potentially lead to structural failure.

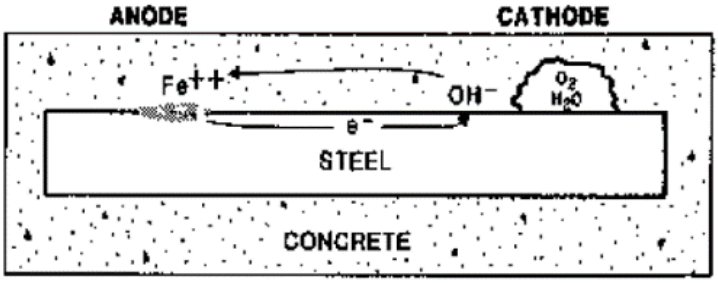

Figure 2.10: Corrosion cell [37]

Formation of corrosion cell

Two reactions, one at the anode (oxidation) and at the cathode (reduction) take place and are called half-cell reactions. Loss of electrons at the anode (oxidation) converting Fe to Fe^{2+}. At the cathode (same or different steel bar where the metal is not consumed), oxygen in water accepts these electrons to become OH^- ions. This is the cathodic (reduction reaction). The flow of electron is made possible due to the concrete (which acts as an electrolyte). Concrete being exposed to several wet-dry cycles has enough conductivity to serve as an electrolyte.

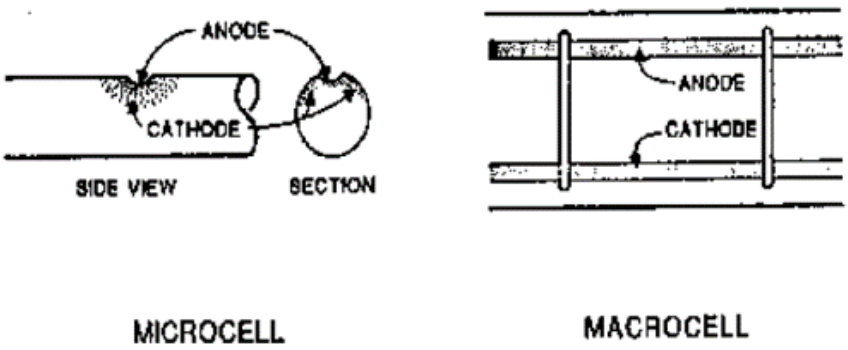

Figure 2.11: Corrosion microcell (same bar), macrocell (separated by a finite distance) [37]

Concrete is highly alkaline in nature (12-13 pH), due to the presence $Ca(OH)_2$, KOH, NaOH. The steel bar in concrete is protected by an oxide film (passivated steel), which is the initial corrosion product. The Fe^{2+} ions react with the OH^- ions to form $Fe(OH)_2$ (Ferrous hydroxide). Ferrous hydroxide is not very soluble and in the presence of water is oxidized to form Fe_2O_3 to form the passive oxide layer. In order for corrosion to take place the steel bar needs to be depassivated, through the action of water, aggressive ions (Cl^-) and oxygen (all acting simultaneously) as seen in figure 2.12.

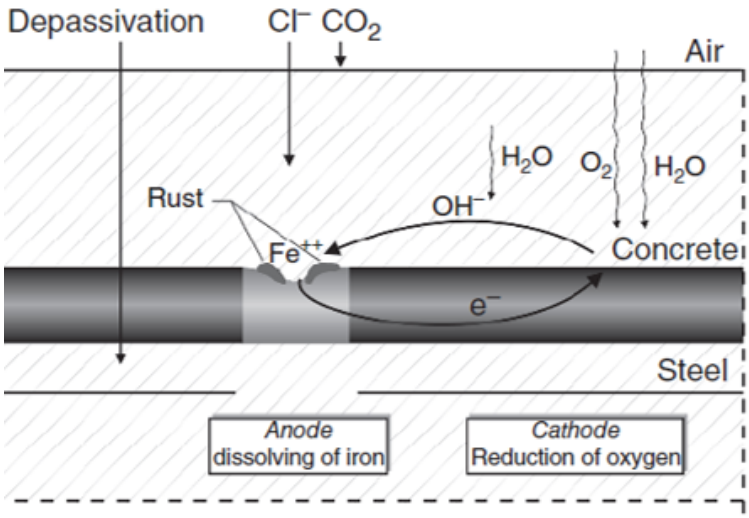

Figure 2.12: Depassivation of steel [37]

Depassivation of steel The depassivation of steel is not completely understood, but several theories do exist, namely the oxide film theory (Chloride ions break down the oxide film), the adsorption theory (Chloride ions are adsorbed into the surface of the steel and attack directly) and the transitory complex theory (Cl acts as a catalyst). Thus, we can conclude that for corrosion to take place several preconditions need to be met :

1. Difference in potential between anode and cathode
2. Anode and cathode must be connected electrolytically as well as electrically
3. Dissolution of iron should take place (depassivation)
4. Continuous supply of oxygen at the cathode

Slowest of the above mentioned points decide the corrosion rate. Various literature suggest that chloride induced corrosion progresses in much the same way in all concrete structures [38, 37].

1. Chloride contamination and corrosion initiation
2. Cracking – when the tensile stresses produced exceed the capacity of concrete
3. Delamination – occurs when the cracks are parallel to the road, usually at rebar level
4. Spalling – when the inclined cracks reach the surface, freeze-thaw cycles, and traffic cause bits of concrete to fall (spall) off (which further accelerates the corrosion process)

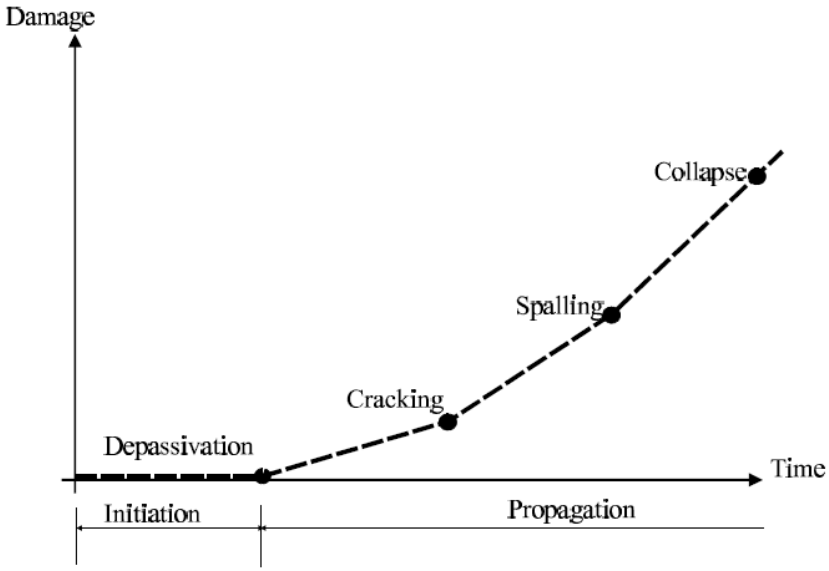

Figure 2.13: Progression of chloride ingress. Source: [38]

Further literature review where the durability of concrete was concerned [38, 31] showed that there were several ways to improve the performance of concrete against corrosion.

2.4.2. PREVENTIVE MEASURES

The mechanism of corrosion described in the previous section occurs because of ingress of ions into the concrete matrix and reaches the steel reinforcement. Holland et. al.[31] discuss various factors affecting the rate of chloride ingress and thereby the long term performance of concrete structures. The water/binder ratio affects the transport of ions since it influences the pore structure of cement paste. This directly influences the diffusion coefficient and diffusion is considered as the main form of transport of ions when the long term performance of concrete structures is investigated [31, 9]. Hence lowering the water/binder ratio is one way to reduce the transport of ions (chlorides). Use of supplementary cementitious materials (SCM's) also influences the rate of transport of ions [31] but is not within the scope of this thesis.

Within this thesis the initiation of corrosion is assumed as the end of service life. Thus once depassivation occurs the end of service life is reached (figure 2.13). The cracking, spalling, and collapse is not considered within the service life of the structure making the approach more conservative. The accumulation of chlorides up to a limit known as critical chloride level causes the depassivation of steel. There is still much debate over the value of critical chloride content (taken as percentage of cement mass). The value of this ranges from 0.4-0.6 percent of the cement mass [14] [9]. The build up or accumulation of chlorides on the surface if the reinforcement is not a fast process and can take many decades if the workmanship and quality of materials is high. From literature it becomes clear that increasing the cover could in fact delay the accumulation of chlorides

to a critical level [30] [14][37][9].

The fib Bulletin 76 [34] also states that an increase in concrete cover could be a possible way to increase the durability, after following the guidelines specified in the Eurocodes [32, 33]. An increase in cover would prolong the time taken for depassivation to occur, further prolonging the service life of the structure. Therefore, concrete cover was investigated further since this was one of the ways through which service life could be increased, and along with this increased durability comes an improvement in the reusability potential (more durable for use in the next life cycle), since the steel within the concrete is better protected. The extent to which cover must be increased is explored in the following section.

2.4.3. SEMI-PROBABILISTIC DURACRETE MODEL

There exist a few service life design models and the study by Šomodíková et. al. [39] discusses the various approaches through which limit state verification can be done regarding durability of structures. However, none of the service life design models make any mention of long service life or 200 years of service life. The DuraCrete model does mention this and proposes to achieve this through application of sufficient concrete cover[9]. The DuraCrete model is a semi-probabilistic model that was developed in the early 1990's in Europe funded by the EU, in order to improve the prediction of service life models. The aim of this particular model was to improve the durability of concrete structures through an increase in concrete cover. The sustainability issue was also explored by trying to make concrete perform better (for longer), and hence reduce the production (short-term) of concrete in the future [9]. DuraCrete reports for concrete performance against corrosion, both through ingress of chlorides (chloride induced corrosion) and through carbonation have been published. DuraCrete model for chloride ingress is investigated further in this thesis due to the severe nature of the consequences of chloride induced corrosion. The semi-probabilistic nature comes from two parts, the deterministically obtained cover (which had a probability of failure of 50 %) and a probabilistic calculation to determine how much extra cover is required to reduce this probability to a permissible limit of below 10 % [10]. Some of the values of the parameters will also change depending on the needs of the owner, design service life etc. The author of this thesis knows that there are various probabilistic models that perhaps could map the variables accurately. That option is not a practical one especially when considering this is just a simply supported 45 meter bridge structure. The designers, contractors and owners of each new project cannot spend time and money making new models or modifying existing probabilistic models to fit the requirements of the structure being designed/built. Hence a more simple approach is needed especially for common structures (example: box-beam bridge). This is where the deemed-to-satisfy approach is the most attractive. It is relatively simple to use and makes the decision making process a little faster. It is the approach where a particular requirement (100 years design service life) only needs a condition or conditions to be satisfied (certain amount of concrete cover). Some terms and definitions need to be made clear so that confusion can be avoided later. As per the DuraCrete background report [10], the terms, design lifespan, durability,chloride initiated rebar corrosion, surface chloride content, initial chloride content, concrete cover, D_{RCM} value, semi-probabilistic calculations need to be under-

stood/defined to remove ambiguity regarding these terms since they will be used quite a lot throughout the document.
Design lifespan: The amount of time that the structure was planned to be in use for. Not to be confused with **lifespan** which means the amount of time the structure meets performance requirements.

Durability: The ability of the structure to withstand internal and external influencing factors.

Chloride initiated rebar corrosion: The corrosion caused due to the presence of a certain amount of chloride ions on the surface of prestressing or reinforcing steel.

Surface chloride content: The concentration of chloride ions on the surface of the concrete expressed as percentage of cement mass (or concrete).

Initial chloride content: The concentration of chloride ions inside the cement expressed as percentage of cement mass (or concrete).

Concrete cover: The shortest distance from the surface of the concrete to the reinforcement surface.

D_{RCM} **value**: The mean value of the chloride migration coefficient obtained through Rapid Chloride Migration (RCM) tests.

Semi-probabilistic calculations: Method in which calculations are done in a simplified manner, where variations are taken into account through the use of fixed factors or a fixed margin that was selected based on probabilistic calculations.
The main assumption within this model was that the ingress of chlorides into the surface of concrete follows Fick's second law of diffusion, and the solution to Fick's second law provides for the concentration (in percentage) of chlorides at a particular point within the concrete matrix.

DURACRETE CHLORIDE TRANSPORT MODEL

As mentioned in the previous paragraph the DuraCrete model makes use of Fick's second law of diffusion [10].

$$\frac{\delta C}{\delta t} = D\frac{\delta^2 C}{\delta t^2} \tag{2.9}$$

Under certain boundary conditions such as a constant diffusion coefficient and constant surface area the solution to the above partial differential equation becomes:

$$\frac{C(x,t)}{C_s} = 1 - erf\frac{x}{2\sqrt{Dt}} \tag{2.10}$$

This solution was used to fit intrusion profiles and get the diffusion coefficient and surface chloride values (C_s). Large collection of samples from structures in the field (>10 years of age) suggested that the diffusion coefficient was decreasing with time, and was therefore time dependant. Although this goes against the boundary condition used to solve Fick's 2nd law, it is another important assumption of the DuraCrete model. This allowed for long term prediction in the short term. The explanation for this was the continued hydration of cement which led to the capillary pores to become finer coupled

with the dehydration of concrete thereby reducing the diffusion of chloride ions. The following empirical- relationship describes the decrease of diffusion coefficient with time:

$$D(t) = D_0(\frac{t_0}{t})^n \tag{2.11}$$

where D_0 is the diffusion coefficient at reference time ($t_0 = 28\ days$), and n is the ageing coefficient. Over time, the European research team DuraCrete came up with a penetration equation which involved the use of different parameters calibrated through laboratory tests and field trails, and is shown below:

$$C(x,t) = C_s - (C_s - C_i)erf\frac{x}{2\sqrt{K_{tot}D(t)t}} \tag{2.12}$$

where
$C(x,t)$ = the chloride content at a particular depth x (in mm)
C_S = the surface chloride content
C_i = initial chloride content of the concrete
erf = the error function, a mathematical function that solves Fick's 2nd Law under certain preconditions
$D(t)$ = time dependant diffusion coefficient
K_{tot} = coefficient to take into account post-treatment and environmental influences
t = time

Equation 2.12 describes the ingress of chloride ions into the concrete matrix, over a period of time 't' (specified by the user). The model was originally meant to be used for making decisions regarding concrete cover to have adequate protection against corrosion (due to chloride ingress) for a specified period of time. The different parameters in equation 2.12 need to be a constant value in order to obtain a critical chloride content at a distance 'x' from the surface of concrete.
The values of these parameters have been obtained through field testing and fitting these values through back calculating the obtained chloride profiles to calculate the ageing coefficient n[10, 40]. The value for the diffusion coefficient after 28 days D_0 similarly has been calculated by performing Rapid Chloride Migration tests on a number of samples and matching diffusion coefficients with water:binder ratios of the tested concrete. K_{tot} is the product of two factors k_e and k_c, where k_e is the coefficient for the environment (depending on cement type) and k_c is the post treatment coefficient depending on where (on land or submerged) and for how many days the concrete was cured for.
The use of the DuraCrete model in other countries showed a slight deviation in expected performance of the model. The use of the DuraCrete model on the Krk bridge in Croatia showed that some of the parameter values have been slightly overestimated [15].

2.5. KEY POINTS

This chapter covers literature concerning sustainability and the CE (section 2.1 and 2.2), DfD (see section 2.2.1), its subset design methodology namely DfReu. Various other indicators developed and proposed have also been discussed along with their salient points. It was seen from literature that DfD is considered to be the way in which circular designs

can be achieved. Different indicators provide information over various features such as the type of connection, number of connections, number of functions etc., all of which contribute to the overall circularity in different ways. This is discussed in section 2.3.
It was seen that the government intends to move into a CE as quickly as possible through design principles of value retention and subsequently value creation. For achieving value retention, the goal is to extend service life, and value creation through planning for multiple life cycles and designing future proof. Hence in order to achieve value retention through life extension, the durability and service life design of concrete was investigated further. The durability of concrete, it was seen was most affected through corrosion, and within the different types of corrosion, chloride ingress was deemed to be the more governing mechanism (discussed in section 2.4.1. As per Eurocode 2, section 4, the hierarchy of aggressive environments places corrosion due to chloride ingress above that of corrosion due to carbonation. Hence the service life design for corrosion due to chloride ingress was studied next.
The service life design (SLD) as per current codes and guidelines was studied along with other SLD models that could prove useful in extension of life. Literature provides us with the DuraCrete model which conforms well with the Dutch codes and hence a detailed literature review over the DuraCrete model and its application was done (see section 2.4.3). It was also seen from this section of the literature review that some deviations were seen when the DuraCrete model was applied in other countries, especially regarding the ageing coefficient (n) and the surface chloride content (Cs).

The findings from literature lead to the following steps being taken to tackle the issue of life extension and improved demountability:

1. In order to facilitate comparison and study the codes a basic box beam will be designed. This can be found in chapter 3.

2. The circular design principle of 'life extension' was being used as an end-of-life practice, but circular strategies need to be applied from design stage onward. This is explored through an increase in durability since service life in the Eurocodes is guaranteed this way. This DuraCrete model from literature (section 2.4.3) is implemented in chapter 4.

3. The important features regarding reusability were identified from literature (2.2 and 2.3) but needed to be adapted for box-beams and is discussed further in chapter 5 and 6.

4. By adapting them for box-beams the areas for future improvement become clearer.

3

DESIGN OF A BOX BEAM BRIDGE ACCORDING TO STANDARD PRACTICE

-

This chapter will discuss the design of a standard box-beam, designed for a simply supported span. The first section (section 3.1) will discuss the standard viaduct chosen for which the box-beam was designed along with the need for the design of a standard box-beam.

The subsequent section (section 3.2 will give information regarding the Finite Element software that was used to model the bridge deck and obtain the governing forces at the critical cross-sections. Section 3.3 discuss the loads and load combinations along with the codes and standards from which they were obtained.

Further, section 3.4 shows the results of the analysis done on SCIA Engineer 21.0.0030 (student version) and the major outputs used to design the beam at critical cross-sections. Section 3.5 deals with the detailing of the reinforcement in the box-beam. Lastly, section 3.6 concludes the design of the standard box beam.

3.1. STANDARD BOX-BEAM

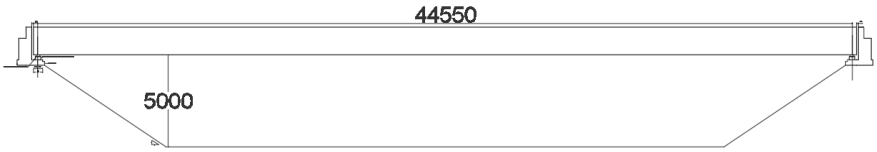

Figure 3.1: A simple sketch showcasing the bridge profile

As mentioned within the scope, the aim of this thesis was to investigate how box-beam girders could be designed to have a service life of 200 years. Therefore, it becomes important to know for what type of bridge the box-beam within this thesis is designed for. The bridge that is used to facilitate the design of the box-beam is henceforth referred to as a standard viaduct.

The NTA 8085:2021 [23], is a technical document discussed in section 2.2.2 of chapter 2. Following from the guidelines mentioned within the technical agreement the span of the standard viaduct for this thesis is chosen. It was mentioned that the NTA 8085 applies only to straight bridges within a span range of 5-45 meters. Keeping the upper limit in mind, the choice is made to investigate the possibility of designing a single span, simply supported bridge with a span of 45 meters. The reason behind this choice (single span) was that two-span bridges can be built in two ways, as two simply supported spans or as a continuous two-span bridge which would require a complex monolithic connection to ensure continuity of the spans. This second option reduces the possibility of removal of girders, owing to the monolithic connection at the intermediate pier. Designing for one long span negates the need for an intermediate pier (and the extra bearings required).

Designing the bridge as a single, simply supported span improves the possibilities for disassembly, which in turn increase the chances for reuse of the girder. The bridge for which the box-beam is designed has no skew (i.e crossing angle of 90 degrees). The width of the bridge deck was chosen to be 12 meters such that two lanes, one in each direction was possible.

Bridge properties	Value
Span [m]	45
Width of deck [m]	12
Lane width [m]	3.5
Number of lanes	2
Crossing angle [°]	90°

Table 3.1: Properties of the standard viaduct

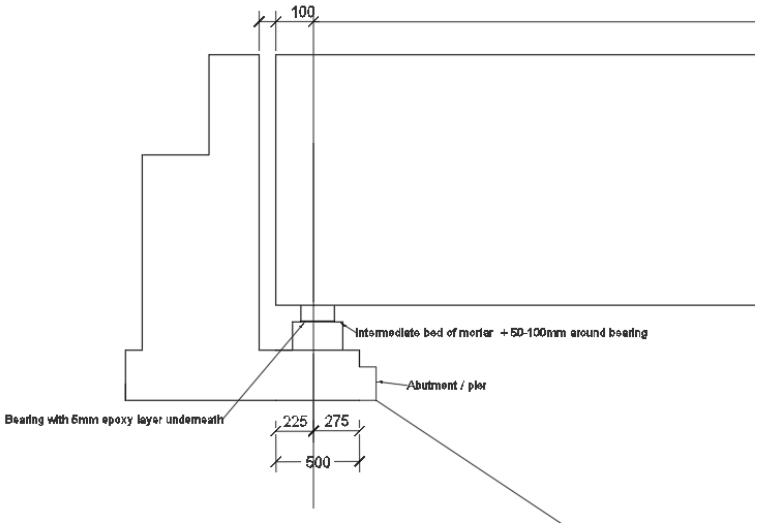

Figure 3.2: A simple sketch showcasing the bridge profile

The standard viaduct will dictate the type of box-beam designed, i.e. straight or curved, amount of skew, traffic loads occurring on it etc. The need for this design was to have a reference point to which all future changes (in design) can be compared. It also provides an opportunity to understand how the current codes and guidelines work, and where it deviates from practices that could be considered as circular.

3.1.1. GEOMETRY OF STANDARD BOX-BEAM

The scope of this thesis, is limited to the design of a box-beam girder due to which dimensions of the other components of the bridge (abutments, wing-walls, piers etc.) were not investigated. The beam was designed for a standard viaduct as described in section 3.1. In order to assist with the initial dimensions of the box-beam girder, the catalogue published by Consolis Spanbeton [41] was used. Using the graph in figure 3.3a, the choice of SKK 1500 profile (see figure 3.3b) was made as it agrees well with a span of 45 meters). The adjacent box-beams were designed to be simply-supported over 45 meters.

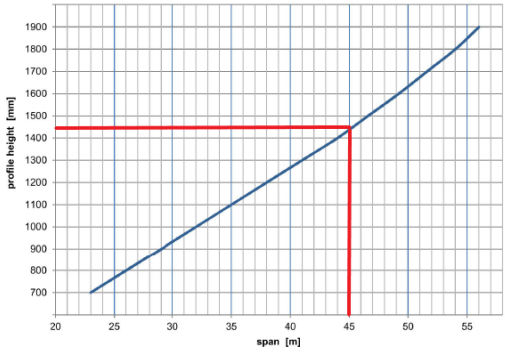

(a) Cross-section estimation using span length [41]

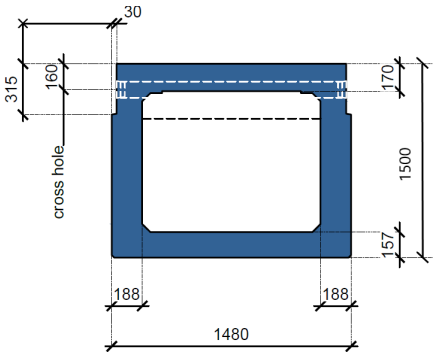

(b) Dimension of SKK1500 in mm [41]

Figure 3.3: Cross-section estimation and dimensions of SKK1500 in mm

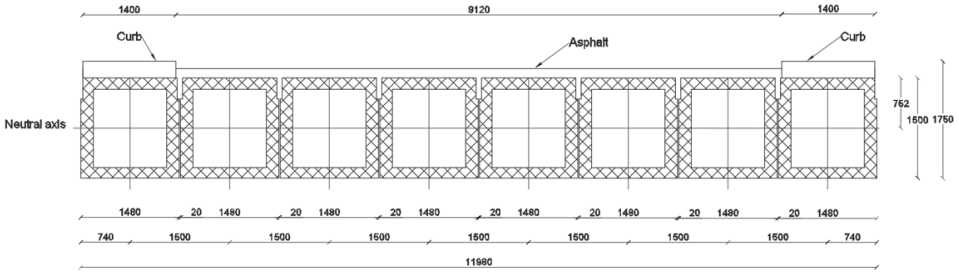

Figure 3.4: Cross section of the bridge

The kerbs are situated on top of the deck and are considered as dead loads acting on the bridge. The width of the kerbs were chosen as 1.4 m as per the standard details of Rijkswaterstaat (RTD 1010), with a height of 0.25 m (figure 3.4.
The beam shown in figure 3.3b, is referred to as a standard beam (or SKK1500) for the remainder of this report. The subsequent sections will deal with the finite element model after which the outputs at the critical cross-sections will be used to decide the final detailing of the reinforcement in the box-beam.

3.2. FINITE ELEMENT MODEL

The Finite Element (FE) Software SCIA Engineer 21.0.0030 (student version) was used to model the bridge deck. Orthotropy parameters were assigned to model a plate, such that it behaved similar to the box-beams placed adjacent to one another. The structure type was chosen as 'Road Bridge', so that the right load types could be assigned within SCIA Engineer.

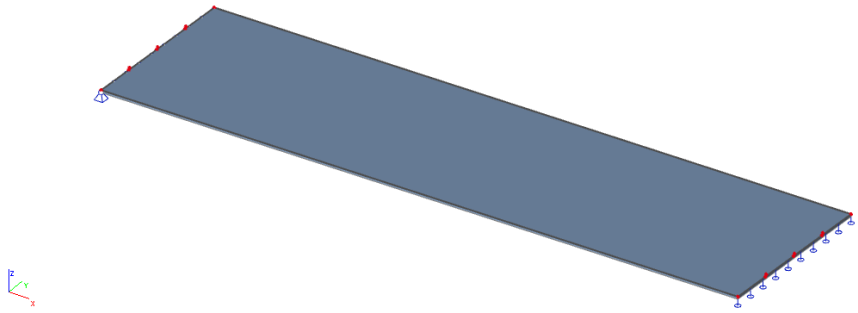

Figure 3.5: Plate model of bridge deck

As seen in figure 3.5, the bridge deck (plate) was modelled as a simply supported structure, hinged on the left and a roller on the right. In reality, one would need to model spring stiffness in X, Y, and Z directions to take into account the effect of the supports, substructure, and subsoil. For the simple analysis of the beam in this thesis, the choice was made to model the supports as line supports, and by doing this neglect any support settlements in order to simplify calculations. The author is aware that for the design of a bridge in practice, the support settlements would have to be modelled through a number of supports with variable stiffness. The plate has a width of 12 meters in the Y direction accounting for the total width of all the adjacent box-beams that form the deck, a span of 45 meters (in the X direction) and a thickness of 1500 millimeters (similar to that of a single box-beam). A physical orthotropy was used to model the bridge deck to avoid creating complicated elements to recreate the box-beams as well as the cast-insitu concrete and is explained in the next section.

3.2.1. ORTHOTROPY

To avoid the tedious work that came with modelling each box-beam separately, the choice to use physical orthotropy was made. The traditional construction procedure of box-beam bridges makes use of cast-insitu concrete between the joints of the box-beams and this leads to a different stiffness in the transverse direction. The presence of the webs act as stiffeners further changing the stiffness in the longitudinal direction and due to this isotropic properties could not be applied to the plate.
One disadvantage was that the edge beams had to be ignored as it could not be modelled using orthotropy since it was not a repeatable cross-section. Orthotropy requires repeatable cross-sections to be applicable and the edge beam (normally chosen for aes-

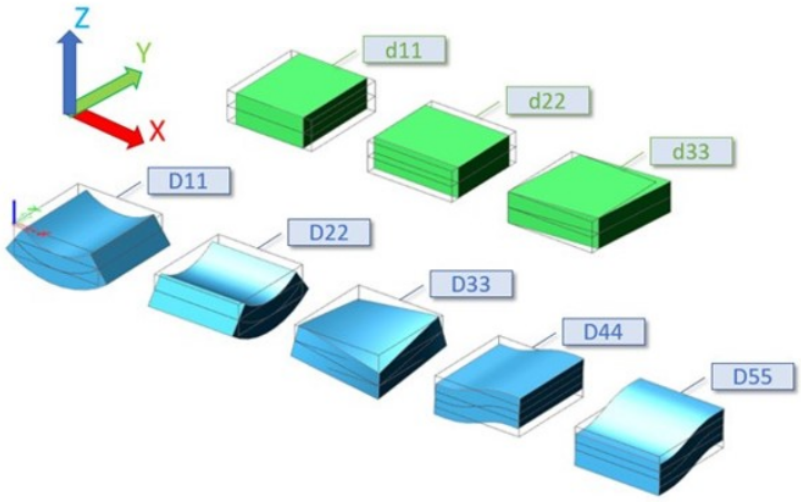

Figure 3.6: Orthotropy parameters to be defined in SCIA Engineer[42]

thetic purposes) made the cross-section non-repeatable. With this choice, one needs to determine the different stiffness parameters for bending, shear, and torsion in different directions. There are 10 orthotropy parameters that had to be defined in order for the plate to mimic the bridge deck in terms of stiffness.
By defining the properties as seen in figure 3.6, one can ensure that the plate shown in figure 3.5 will behave like a adjacent box-beam girders. As was mentioned the edge beams were not modelled but assumed as normal box-beam girders (figure 3.3b). The calculation of the the orthotropic parameters can be found in Appendix H. The work done by Hogendoorn G. [43] and Boersma J. W. [28] were used to calculate the orthotropy parameters. The different parameters calculated for the cross-section (figure 3.3b) are:

1. D11: Flexural stiffness in X direction (longitudinal)
2. D22: Flexural stiffness in Y direction transverse)
3. D12: Transverse contraction stiffness (takes Poisson's ratio into account)
4. D33: Torsional stiffness
5. D44: Shear flexural stiffness in X direction
6. D55: Shear flexural stiffness in Y direction
7. d11: Normal membrane stiffness in the 'x' direction (stretching)
8. d22: Normal membrane stiffness in the 'y' direction
9. d12: Mixed stiffness of 'd11' and 'd22' (transversal contraction)
10. d33: Shear membrane stiffness

D11 [MNm]	7.9E+03
D22 [MNm]	7.85E+01
D12 [MNm]	1.57E+01

Table 3.2: Bending stiffness in longitudinal and transverse directions

D33 [MN/m]	1.1E+03
κ_{xy} [MNm]	4.33E+03
κ_{yx} [MNm]	7.13E+01

Table 3.3: Torsional stiffness of orthotropic plate

The torsional stiffness parameter depends on κ in X and Y directions, where κ represents the torsional rigidities in both directions. In the case of an orthotropic plate the torsional rigidities in both directions are not equal as was the case in an isotropic plate. In the longitudinal direction the box-beam (made of C60/75 concrete) contribute to the torsional stiffness, whereas in the transverse direction only the cast insitu part contributes to the torsional stiffness (cast-insitu concrete C30/37).
The D44 and D55 parameters representing the shear flexural stiffness in X and Y directions respectively are shown in table 3.4.

D44 [MN/m]	5.105E+03
D55 [MN/m]	3.59E+03

Table 3.4: Shear flexural stiffness of orthotropic plate in X and Y directions respectively

The last few parameters that were defined dealt with the axial stiffness properties of the orthotropic plate (table 3.5).

d11 [MN/m]	2.77E+04
d22 [MN/m]	1.08E+04
d12 [MN/m]	2.15E+03
d33 [MN/m]	7.43 E+03

Table 3.5: Normal and shear membrane stiffness in X and Y directions

3.3. LOADS AND LOAD COMBINATIONS

In order to design the box-beam it was important to understand the loads acting on the bridge, and subsequently the relevant load combinations for Ultimate Limit State (ULS) and Serviceability Limit State (SLS). Further, these loads and load combination were applied on the Finite Element Model mentioned in section 3.2. The loads and their combinations were obtained using the relevant Eurocodes as listed.

1. EN 1990 - Basis of Structural Design [44] - Load combinations (ULS and SLS), load factors (γ), combination factors (ψ)
2. EN 1991-1-1: Eurocode 1: Actions on structures-Part 1-1 General actions- Densities, self weight, imposed loading for buildings [45] - densities of the different materials used to calculate dead loads
3. EN 1991-2 - Traffic loads on bridges [46] - Traffic loads (Load Model 1), crowd loading (Load Model 4), horizontal loads (braking and acceleration)

ADDITIONAL CODES USED

1. EN 1992-1-1 - Design of concrete structures-General rules and rules for buildings [32] - checks to verify bending, shear, torsion and detailing of reinforcement
2. EN1992-2- Design of concrete bridges - additional rules not mentioned in EN 1992-1-1 and fatigue verification
3. ROK 1.4 Bijlage document Deel A [47] - Additional rules after following the Eurocodes

3.3.1. LOAD CALCULATION

The different types of loads that can act on a bridge structure need to be determined before the relevant combinations can be made. The basic load combinations (for both Ultimate and Serviceability Limit States) consist of permanent loads (self weight and dead loads), prestressing, and live loads. The different types of live loads that can act on a bridge are:

1. Traffic loads
2. Horizontal loads (braking and acceleration)
3. Pedestrian and cyclist loads
4. Wind loading
5. Thermal loading

Since the scope of this thesis is limited to the design of a box beam girder, only those loads which were relevant, i.e. loads which affected the beam were considered to make the necessary load combinations (ULS and SLS) were considered and later modelled. The loads considered are shown in table 3.6

- Resting load
- Vertical loads according to LM1 and LM4 (EN 1991-2 article 4.3 [46])
- Vertical loads according to FLM1 (EN 1991-2 article 4.6 [46])
- Vertical loads due to accidents on bridge deck (EN 1991-2 article 4.7.3 [46])

Some loads were determined manually using the relevant Eurocode. These were:

- Shrinkage and creep
- Prestressing
- Braking and acceleration loads
- Temperature loading
- Collision of the superstructure (Accidental loads)

Load type	Example
Permanent loads	Self weight, shrinkage/creep, dead loads
Traffic loads	LM1, braking/acceleration loads
Pedestrian and cyclist loads	Area loads
Other live loads	Temperature loads

Table 3.6: Type of loads acting on the bridge

LOAD CASES

For the determination of the loads a reference period of 100 years is chosen as this is the maximum lifespan considered by the Eurocodes. The load cases are described in the sub-sections that follow.

PERMANENT LOADS

Self Weight

SCIA Engineer automatically takes into account the self weight of the structure modelled, but would have led to wrong results since orthotropy was used. This is because SCIA takes the entire self weight of the plate which does not contain hollow sections (as seen in the SKK 1500) leading to a higher self weight. Hence, to solve this the density of the plate (concrete) was given as $0 kN/m^3$ instead of $25 kN/m^3$. The self weight of the beams was obtained from the catalogue published by Consolis Spanbeton [41] and modelled as physical loads on the deck (plate). The corresponding area loads are shown in table 3.7. The weight of the wet concrete in the longitudinal joints between the box beams was not considered.

Dead loads

This load case contained all the dead loads acting on the deck (asphalt, safety barrier, kerbs, and parapet). Table 3.8 show the densities of the different materials used in the construction process and table 3.9 gives an overview of the dead loads and their values.

Concrete girder	Weight [kN/m]	Corresponding area load [kN/m^2]
Massive part	55.1	37.2
Hollow part	28.1	18.98

Table 3.7: Self weight of the girders

Material	Density [kN/m^3]
Prefabricated concrete	25
Cast insitu concrete	25
Steel	78.5
Asphalt	23

Table 3.8: Material densities. Source: [45]

Shrinkage/creep

The permanent load arising due to shrinkage and creep were calculated and found to be 0.3 per mille. The formulas found in EN 1992-1-1 (2004) Annex B [32] were used for the calculation of the creep coefficient and ultimately the strain arising from creep.

TRAFFIC LOADS

The division of the deck into notional lanes (see figure 3.7) was done as per EN 1991-2 (Traffic loads on bridges) [46]. This allowed for the application of the Tandem System (TS) loads (axles of the vehicles) and the respective uniformly distributed loads (UDL's) per lane, as specified by Load Model 1 (LM1). The width of each notional lane is 3 meters. With a carriageway width of 9.2 meters (excluding the kerb width), 3 notional lanes were possible. Two lane orientations were considered, (1) where lane 1 starts from the left edge (1.4 m from left edge), and (2) where lane 1 is in the center of the deck with the remaining lanes on either side. Where the first orientation was used, the respective combinations is referenced to as 'edge' and when the latter was used, it was referenced to as 'center' (figure 3.7).

Vertical traffic load

EN 1991-2 (article 4.3) was used to determine the vertical traffic loads acting on the bridge deck. This traffic load model consists of UDL's and double axle concentrated (tandem system : TS) loads (see figure 3.8). The UDL has value per meter square and acts over the entire lane and the concentrated loads are a pair of tandem axles (or double tandem axles). Only one pair of tandem axles act per lane, and depending on the lane number, the value of the UDL and axle load changes. The α factors were selected based on expected traffic[46]. Train loads were used to move the double tandem axles over each lane separately (with a step size of 5 meters) while the respective UDL was applied on each lane. Table 3.10 gives and overview of the values of Load Model 1 and figure 3.8 provides a visual representation of the same.

Dead load	Load	Description
Kerb	6.25 kN/m^2	Kerb height multiplied with density (concrete)
Asphalt	3.22 kN/m^2	Asphalt height multiplied with density (asphalt)
Safety barrier	0.6 kN/m	1.4 m from edge of deck (both edges)
Pedestrian parapet	1.0 kN/m	Line load on edge of bridge deck (both sides)

Table 3.9: Dead loads acting on bridge deck

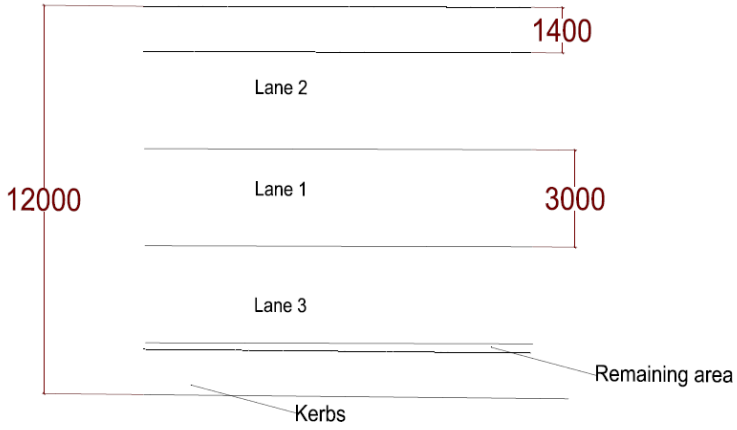

Figure 3.7: Top view of deck (Center lane arrangement)

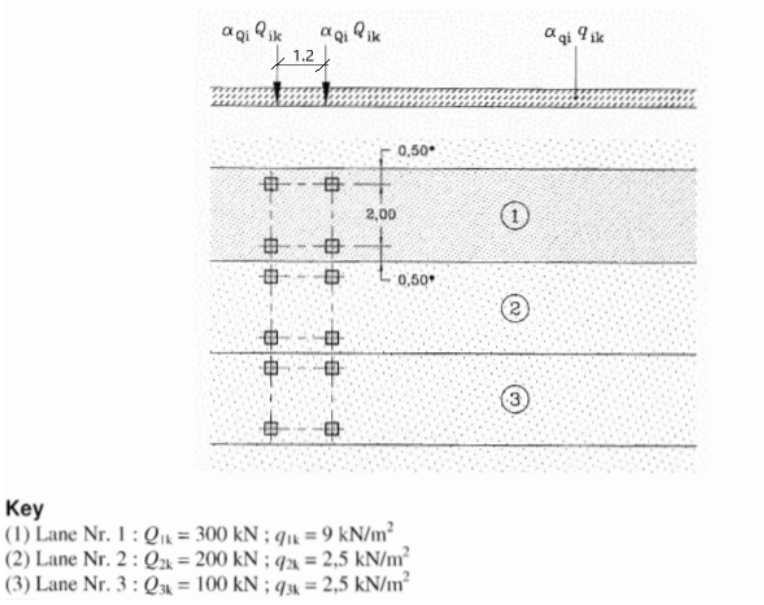

Figure 3.8: Load Model 1, distances in meters [46]

Lane	TS [kN]	$\alpha_{Q,i}$	UDL [kN/m^2]	$\alpha_{q,i}$
Lane 1	300	1	9	1.15
Lane 2	200	1	2.5	1.4
Lane 3	100	1	2.5	1.4
Remaining	-	-	2.5	1

Table 3.10: Load Model 1 overview

Horizontal traffic load

EN 1991-2 (article 4.4) was used to determine the horizontal traffic loads acting on the bridge deck arising from braking and acceleration (same magnitude but opposite in direction). TS loads were divided by the area of the axles to get the corresponding area loads. Equation 3.1 was used to calculate the horizontal load for braking and acceleration seen in table 3.11.

$$Q_{Ik} = 0.6\alpha_{Q1}2Q_{Ik} + 0.1\alpha_{q,1}q_{1k}w_1L \tag{3.1}$$

TS (Lane 1)	$0.6\alpha_{Q1}(2Q_{Ik}/(4*0.4*0.4)$	562.5 kN/m^2
UDL (Lane 1)	$0.1*\alpha_{q,1}*q_{1k}$	1.04 kN/m^2

Table 3.11: Horizontal load

Pedestrian and cyclist loads

To realistically depict the actions of pedestrians and cyclists on the bridge deck, LM4 according to EN 1991-2 [46] was applied over the kerbs of the bridge deck (1.4 meters from the edge of deck), along the entire span of the bridge. As per EN 1991-2, this load model consists of uniformly distributed load of $5kN/m^2$.

Thermal loads

The thermal loads were determined were adapted from the work done by Boersma J.W. [28], and were modelled as:

- Yearly temperature rise : $\delta T_{N,exp}$ = +23.2K
- Yearly temperature drop : $\delta T_{N,con}$ = -29.5K
- Daily temperature rise of $T_{M,heat,top}$ = +10.1 K on top of the deck and $T_{M,heat,bot}$ = -2.7K at the bottom of the deck
- Daily temperature drop was assumed to be $T_{M,cool,top}$ = -4.5K on top and $T_{M,cool,bot}$ = +1.2 K

Load		Value	Unit
Self weight	Massive	37.2	kN/m^2
	Hollow	18.98	kN/m^2
Dead load	Kerb	6.25	kN/m^2
	Asphalt	3.22	kN/m^2
	Parapet	1.0	kN/m
	Safety Barrier	0.6	kN/m
Vertical traffic-LM1 (TS)	Lane 1	300	kN
	Lane 2	200	kN
	Lane 3	100	kN
	Remaining area	-	-
Vertical traffic-UDL	Lane 1	10.35	kN/m^2
	Lane 2	3.5	kN/m^2
	Lane 3	3.5	kN/m^2
	Remaining area	2.5	kN/m^2
Horizontal load	TS	562.5	kN/m^2
	UDL	1.04	kN/m^2
Pedestrian load	Acting over the kerbs on both sides	5	kN/m^2
Thermal loads	Yearly rise	+23.3	K
	Yearly drop	-29.5	K
	Daily rise (top and bottom)	10.1 , -2.7	K
	Daily drop (top and bottom)	-4.5, 1.2	K

Table 3.12: Overview of loads acting on bridge deck

3.3.2. LOAD COMBINATIONS

The load combinations for Ultimate and Serviceability Limit States were determined using Annex A2 of EC 0 [13]. In order for the combinations to be made, the relevant load factors and combination factors needed to be determined as well. A list of the coefficients used for the combinations can be found in Appendix F.

LOAD FACTORS

The load factors differ for Ultimate and Serviceability Limit States. Article A2.3 along with Table A2.4 (A), Table A2.4 (B) [13], provide the load factors (γ) for Ultimate Limit State combinations. In addition to this The load factors for Serviceability Limit States were obtained from Table A2.6 [13].

COMBINATIONS FACTORS

In addition to the load factors, relevant combination factors are also required. This is obtained from Table 19 of NEN-EN 1990+A1+A1/C2:2019/NB:2019 [44].

3.4. ANALYSIS AND OUTPUTS

Once the deck plate was modelled and the relevant load cases and combinations were created, a linear analysis was carried out. It is possible to verify the resulting bending

moments and shear forces by a hand calculation and can be found in appendix **??**. For the extraction of bending moments and shear forces a section over the whole deck is drawn at critical points (mid span and support). This section allowed to understand where the peak in output was, following which an average value over a section (1.48m in width) was used for design of reinforcement and prestressing.

3.4.1. OUTPUTS FOR BENDING

BENDING AT ULTIMATE LIMIT STATE

As seen from figures 3.9 and 3.10, the maximum bending moment per meter was seen at the centre of the deck, following the theory of simply supported beams. A section was drawn over the total width of the deck to know which girder was loaded the most(figure 3.10). No peaks were visible from the output over the whole section (figure 3.9). Hence two beams were checked, an edge beam and the middle beam by drawing the respective sections of 1.48 meters. For the governing load combination the edge beam was seen to be loaded the most in bending (figure 3.11). The bending moment per beam (kNm) was obtained by multiplying the output by the width of a box-beam (1.48m) as seen in table 3.13.

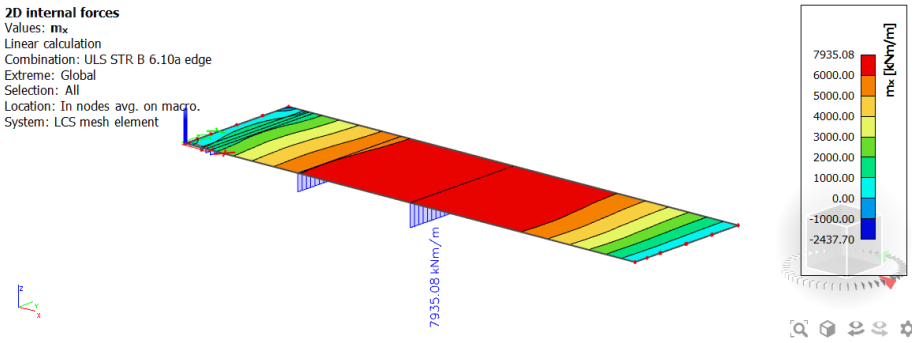

Figure 3.9: Maximum bending moment from governing ULS combination, isometric view

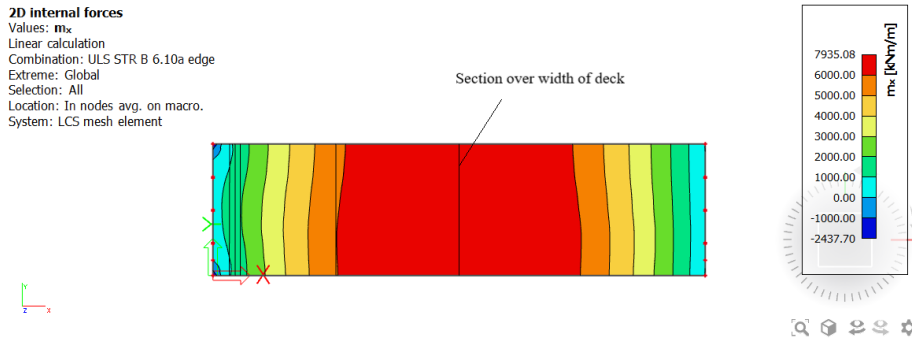

Figure 3.10: Maximum bending moment from governing ULS combination, top view

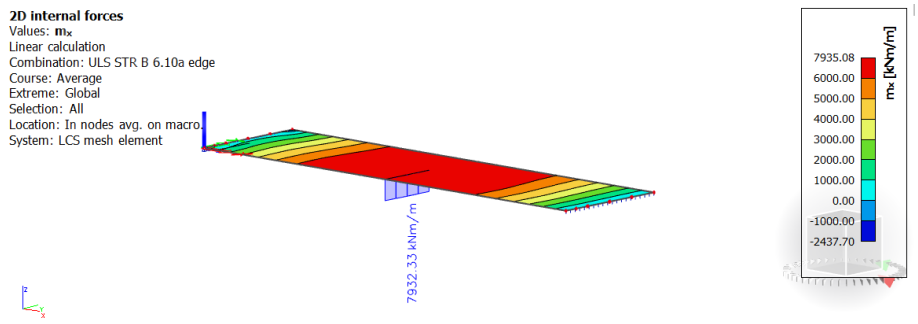

Figure 3.11: Maximum bending seen for 3rd beam from edge - section output

Bending output (ULS) in kNm/beam	
Contour plot	7935.08 * 1.48 = 11743.9
Section value (edge)	7932.33 * 1.48 = 11739.8 [1]

Table 3.13: Bending moment values at ULS

BENDING AT SERVICEABILITY LIMIT STATE

Similar to the procedure followed to determine the bending moment at ULS, the figures 3.12 and 3.14 show the contour plot and the section output for the governing SLS combination. Further, the SLS bending moments are calculated as shown in table 3.14 and this output value was used to design the required prestressing steel.

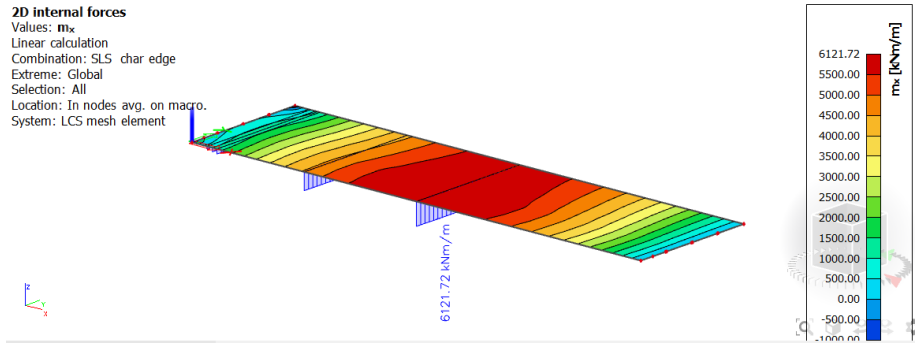

Figure 3.12: Maximum bending moment arising from governing SLS combination

[1] The moment due to prestressing needs to be subtracted from this to obtain the final M_{Ed}

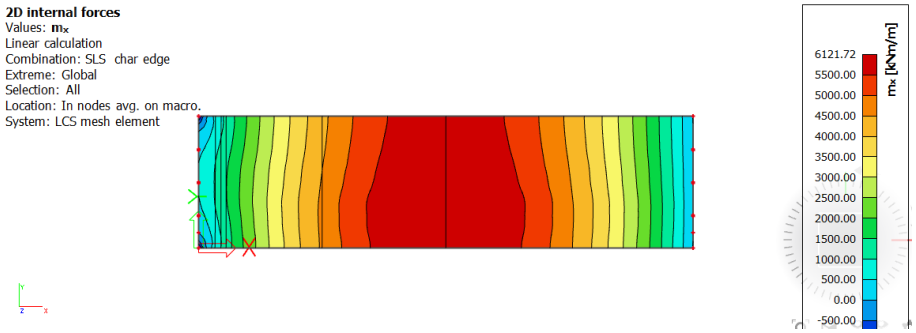

Figure 3.13: Maximum bending moment arising from governing SLS combination

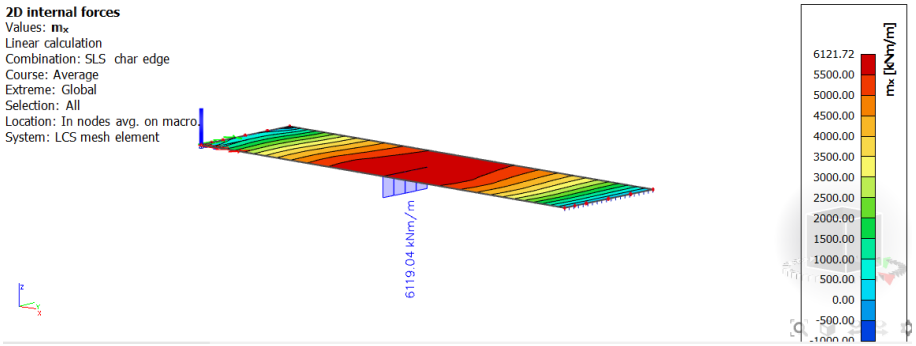

Figure 3.14: Maximum bending (SLS) - section output

Bending output (SLS) in kNm/beam	
Contour plot	6121.72 * 1.48 = 9060.1
Section value	6080.89 * 1.48 = 9056.1 [2]

Table 3.14: Bending moment values at SLS

[2] Moment value used to design the required prestressing

3.4.2. OUTPUTS FOR SHEAR

The shear forces used for design also follow from theory of simply supported beams, where shear was maximum near the supports. The figures 3.15 and 3.16 show the contour plots of the governing ULS combination. From figure 3.16, the peak (in the transverse direction) was seen at the edge. Figure 3.17 shows the value of shear force at a section 'd' (height of beam) from the support for an edge beam. Figure 3.18 shows the value of shear force at a section (width = 1.48m) at $1/4^{th}$ span for an edge beam. This value of shear force was used to design stirrups for the the span from 11.25 (quarter span) - 22.5 (mid span). The design of stirrups for the remaining span (22.5m - 45m) mirrors the design for (0 - 22.5m). The values used for stirrup design can be seen in table 3.15.

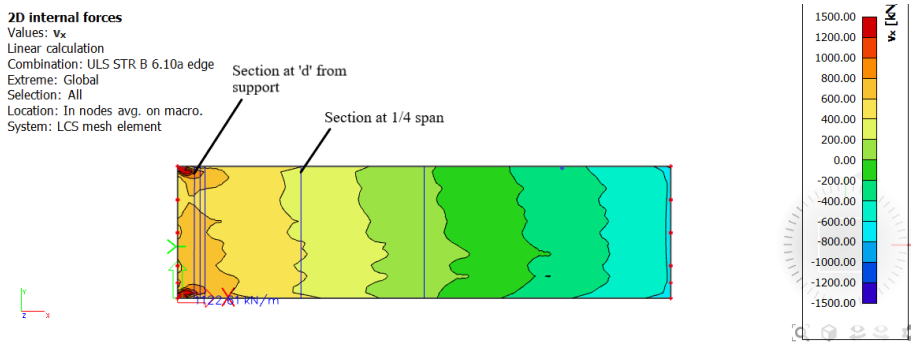

Figure 3.15: Maximum shear at cross-section 'd' from support - top view

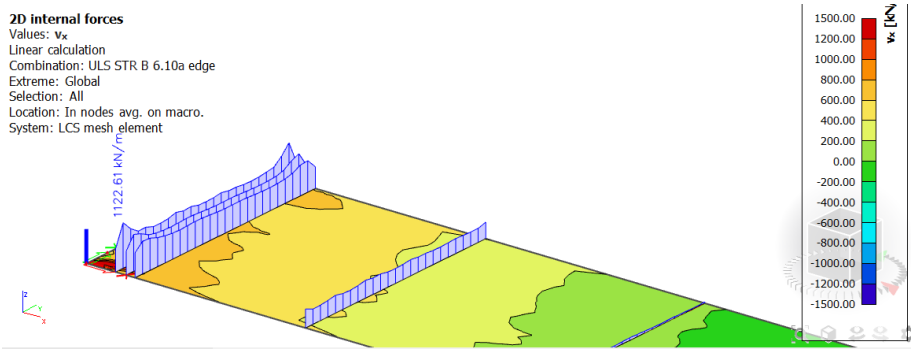

Figure 3.16: Maximum shear at cross-section 'd' from support, isometric view

Shear output (ULS) in kN/beam	
Contour plot	1500 * 1.48 = 2220
Section value ('d' from support)	888.13 * 1.48 = 1314.43
Section value (1/4 span)	396.69 * 1.48 = 587.1

Table 3.15: Shear force values at ULS

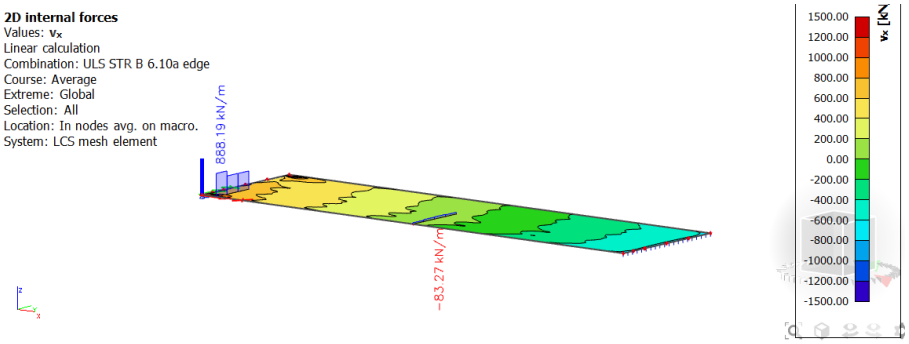

Figure 3.17: Maximum shear - section output

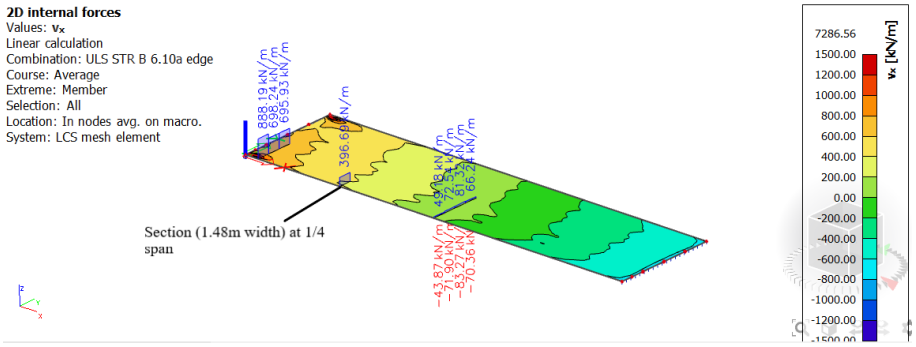

Figure 3.18: Maximum shear - section output at 1/4th span

3.5. DESIGN STARTING POINTS

This thesis is about the reusability of the box-beam girder, therefore only those loads affecting the box-beam girder were calculated and modelled. It is understood by the author that in a full-scale bridge design there would be other loads and load combinations that would need to be checked as well. The following assumptions were made as starting point to help with design of the beam:

1. Statically determinate structure (simply supported span): With this assumption the critical cross-sections are known to be near mid-span for bending and near supports for shear.

2. crossing angle 90 degrees (perpendicular): Allows for straight prestressing tendons at constant eccentricity

3. C60/75 precast concrete for the box-beam and C35/45 cast in-situ joints (between the girders)

4. Exposure class: XD3: Common starting point for most bridge designs unless specified otherwise [41]

5. Consequence Class 3 (CC3): When the structure has to be designed for a 100 years this consequence class applies and the load factors used in the combinations are also decided with this[44].

6. 100 year design service life: Standard reference period for bridge structures [13]

7. Vehicular loads applied - LM1 and crowd and pedestrian loading - LM4

8. No cracking in SLS: With this assumption the prestressing is decided and no further SLS checks need to be carried out.

9. The prestressing and reinforcing steel have been placed in such a way that both are at the same effective depth from top fibre

Concrete	Cement class
Prefab	C60/75
Cast insitu	C30/37

Table 3.16: Concrete used and the respective strength class

Steel type	Y1860S7
Characteristic diameter $[mm]$	15.7
Cross-sectional area $[mm^2]$	194
Maximum prestressing force [kN] after tensioning $\sigma_{po} = 0.75 f_{pk} = 1395 MPa$	270

Table 3.17: Prestressing steel properties

3.5.1. PRESTRESSING

The prestressing was decided using assumption number 8 in section 3.5. The design for prestress was done by ensuring that no tensile stresses occurred at the extreme fibres at mid-span. The first stage (t = 0) where only self weight and prestressing act on the beam, and tensile stresses at the top fibre were checked. The second governing stage was the use phase (t = ∞), where self weight, live loads and prestressing act on the beam, tensile stresses at the bottom fibre were checked. An assumption of 20 % losses to the initial prestressing force were assumed to obtain the working prestress.

It was seen that 52 prestressing strands were required to balance the bending moment coming from the governing SLS combination such that no tensile stresses occurred, and hence no cracking was ensured as well. The strands were arranged such that their centre of gravity coincide with the middle of the bottom flange as seen in figure 3.19. Table 3.18 shows an overview of the prestressing steel used for one girder.

Number of strands (n)	52
Area of a strand [mm^2]	150
Total area (A_p) [mm^2]	7800
Eccentricity [mm]	670
σ_{pm0} [MPa]	1395
$P_{m,\infty}$ [kN]	8704.8
$M_{P,\infty}$ [kNm]	5832.2

Table 3.18: Prestressing details

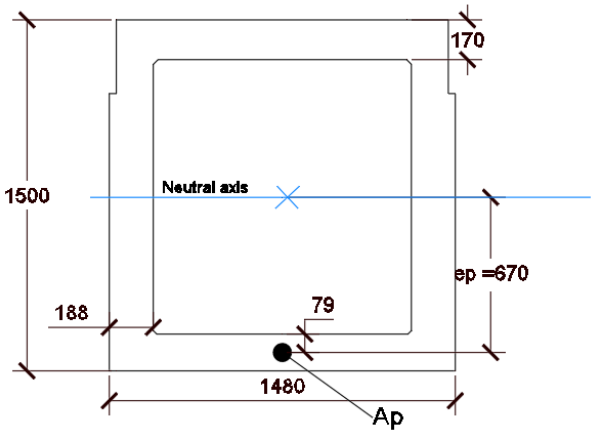

Figure 3.19: Prestressing with eccentricity = 0.67m from neutral axis

The calculation of this is seen in appendix A.

3.5.2. BENDING AT ULS

Using the result from section 3.4.1, the unity check for bending moment at ULS is carried out. As seen from table 3.19, horizontal equilibrium is maintained ($\sum H = 0$) and as a result moment equilibrium about neutral axis is also maintained ($\sum M = 0$).

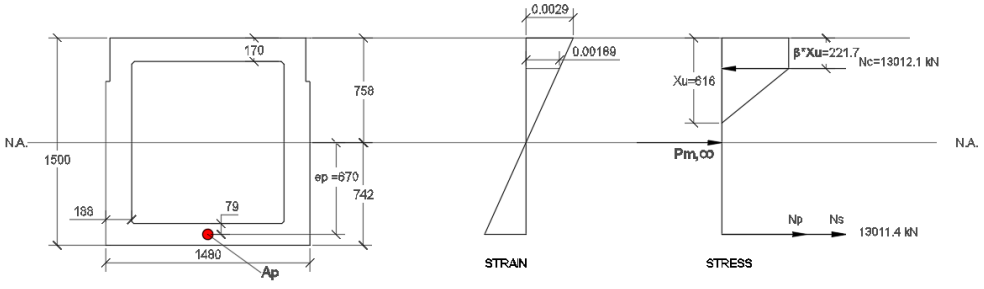

Figure 3.20: Stress and strain in the cross section

Property	Value
Compression zone height Xu [mm]	616
Concrete compressive force [kN]	13012.1
Total tensile force [kN]	13011.4
$M_{Ed,SCIA}$ [kNm]	11739
M_P [kNm]	5832.22
M_{Ed} [kNm]	5907.6
M_{Rd} [kNm]	11158.6
Unity check	0.56 < 1

Table 3.19: Unity check for Bending at ULS

The calculation of the results shown in table 3.19 is shown in Appendix B.

3.5.3. SHEAR REINFORCEMENT

Using the results from section 3.4.2 the shear reinforcement is calculated. To take the torsion moment into account minimum torsion reinforcement is added in the flanges. Minimum stirrup reinforcement is also added to take into account the addition due to torsion in the webs (figure 3.21).

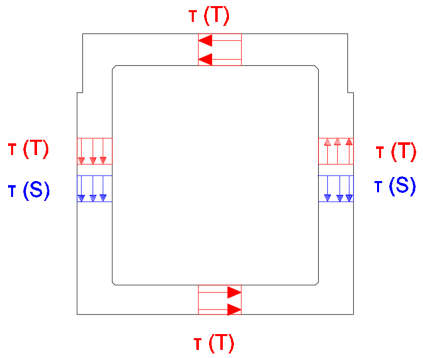

Figure 3.21: Torsion (red) and shear (blue) stress flow in the cross-section

$V_{Rd,c}$ [kN]	960.3
$V_{Ed,shear}$ near support [kN]	1314.43
$V_{Ed,shear}$ at $1/4^{th}$ span [kN]	587.1
$V_{Rd,max}$ [kN]	3353.4

Table 3.20: Important values to check design for shear and torsion

The checks carried out to determine the resistance of the beam against shear are listed below [32]:

1. $V_{Ed} \leq V_{Rd,c}$
2. $V_{Ed} \leq V_{Rd,max}$

Shear reinforcement in webs	4ϕ10 - 200
Torsion reinforcement in top flange	2ϕ10 -450
Torsion reinforcement in bottom flange	2ϕ10 -450

Table 3.21: Shear and torsion reinforcement (X = 0 - 11.25m)

Shear reinforcement in webs	4ϕ10 - 333
Torsion reinforcement in top flange	2ϕ10 -450
Torsion reinforcement in bottom flange	2ϕ10 -450

Table 3.22: Shear and torsion reinforcement (X = 11.25m-22.5m)

The calculation of the stirrups shown in table 3.21 and 3.22 can be found in Appendix C.

3.5.4. SPLIT TENSILE REINFORCEMENT

The introduction of prestress at a constant eccentricity introduces tensile stresses near the supports, to counter this split tensile reinforcement is required. The area of steel used is shown in Appendix D.

3.5.5. FATIGUE VERIFICATION

A beam used in a bridge will be subjected to many cycles of loading due to traffic and this could lead to fatigue failure. For the purpose of fatigue verification Fatigue Load Model 1 was used [46]. Fatigue Load Model 1 has the configuration of Load Model 1 along with additional adjustment factors. The use of Fatigue Load Model 1 without the adjustment factors (table 3.23) would have been excessively conservative [46].

Lane	TS [kN]	$\alpha_{Q,i}$	UDL [kN/m^2]	$\alpha_{q,i}$
Lane 1	300	0.7	9	0.3
Lane 2	200	0.7	2.5	0.3
Lane 3	100	0.7	2.5	0.3
Remaining	-	-	2.5	0.3

Table 3.23: Fatigue Load Model 1

The stress range at top and bottom fibre at mid span cross section were checked. The fatigue load combination as described in EN 1992-1-1 [32] were used to extract the stress ranges. The combination consisted of non-cycling and cycling, where the non-cycling actions represent the most unfavorable frequent combination (SLS) and the cycling actions by use of Fatigue Load Model 1. The checks as per EN1992-1-1 and EN 1992-2 can be found in appendix E.

3.6. STANDARD DESIGN

The cover used for the beam can be found in section 4.1.1 of chapter 4. The bending, shear, torsion, fatigue and split tensile reinforcement were the basic design requirements that the beam was checked for. The outputs were used to calculate the required amounts of prestressing and reinforcing steel. The final cross-section of the beam at mid-span can be seen in figure 3.22 and near the support in figure 3.23. The only difference being the difference in stirrup spacing since shear is higher nearer to the supports (following the theory of simply supported spans). The assumption is made that all the beams have been designed for the most governing scenarios, and have the same design.

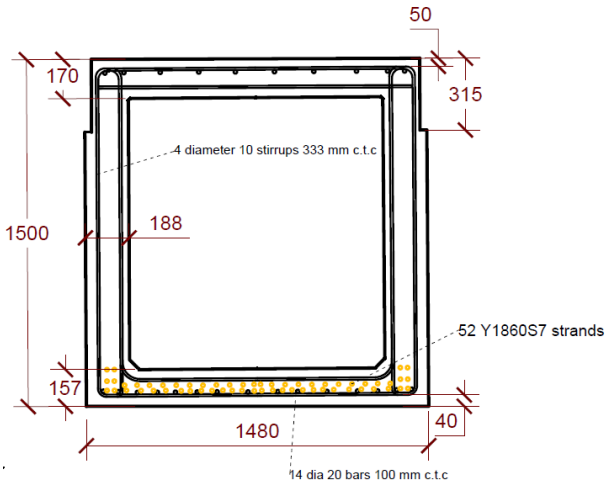

Figure 3.22: Cross-section at mid-span

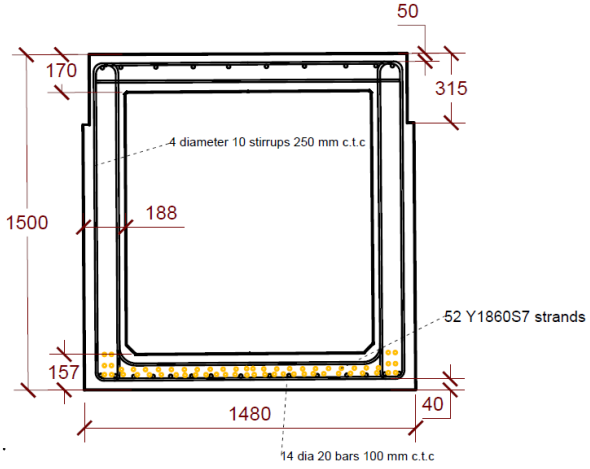

Figure 3.23: Cross-section at support

4

DURABILITY IMPROVEMENT THROUGH COVER INCREASE

The first section of this chapter (section 4.1) discusses the durability of the beam and how it can be improved.

Section 4.2 discusses the use of the DuraCrete model found in literature with the suggested values of model parameters.

Section 4.3 studies different parameters of the DuraCrete model to understand what potential improvements can be made to to some parameters .

Section 4.4 of this chapter discusses the improvements suggested for the DuraCrete model which is a semi-probabilistic model used to design for long-term durability of concrete structures through use of adequate cover. The results from this chapter were obtained using the Monte Carlo method and were used to improve the durability of the beam designed in chapter 3.

4.1. DURABILITY

Once the outputs from the Finite Element analysis have been used to determine the amounts of steel required, a cover value needs to be proposed such that the durability requirements set by the Eurocodes (namely EN 1992-1-1) [32] were met. From literature (chapter 2) it was identified that the main barrier to service life was seen to be corrosion of steel in concrete. The standard form of protection against corrosion is through provision of suitable cover. Once an exposure class corresponding to a certain environment has been chosen, there is a strict set of rules regarding the minimum cement content, maximum water/binder ratio, aggregate size chloride content class specified by EN 206 [33].

4.1.1. COVER

The duration or service life of the structure is planned as 100 years and the the exposure class was selected as XD3/XC3 depending on the surface of the girder. The codes referred to were EN 1992-1-1 [32] and the ROK article 4.4.1.2(5). From figure 4.1, the different surfaces and the associated cover chosen can be seen. The assumption of a lower environment class (XC3) for the inner edges (surfaces 3, 4) of the box-beam is chosen due to the surface being an inner surface of the box-beam not directly exposed to harmful agents.

Prefab Beam						
Surface	1	2	3	4	5	6
Standard environment class	XD3	XD3	XC3	XC3	XD3	XD3
Construction class	S4	S4	S4	S4	S4	S4
Design service life (100 years)	S2	S2	S2	S2	S2	S2
Standard environment class and concrete quality	-S1	-S1	-S1	-S1	-S1	-S1
Element with plate geometry	S0	S0	S0	S0	S0	S0
Quality control applies	-S1	-S1	-S1	-S1	-S1	-S1
Construction class	S4	S4	S4	S4	S4	S4
c_{min}	40	40	25	25	40	40
Reduction water-cement factor [mm]	-5	-5	-5	-5	-5	-5
c_{min} [mm]	35	35	20	20	35	35
Δc_{dev}[mm]	5	5	5	5	5	5
$c_{nom} = c_{min} + \Delta c_{dev}$ [mm]	40	40	25	25	40	40*

Table 4.1: Cover for prefab beam

The concrete covers for the different surfaces of the prefab beam are as follows:

1. XD3, $c_{nom} = 40mm$
2. XD3, $c_{nom} = 40mm$
3. XC3, $c_{nom} = 25mm$
4. XC3, $c_{nom} = 25mm$

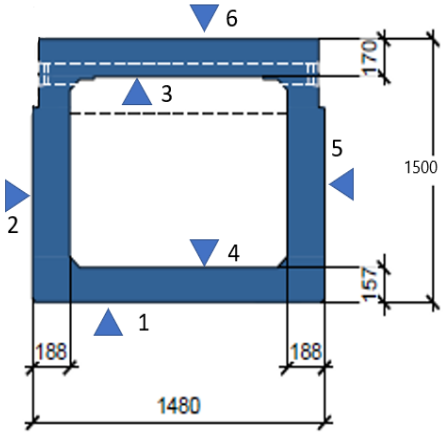

Figure 4.1: Surfaces of prefabricated beam. Source: Consolis Spanbeton [41]

5. XD3, $c_{nom} = 40mm$

6. XD3, $c_{nom} = 50mm$ (extra 5 mm addition due to unformed surface on top and 5mm for surface 6 being non-inspectable after asphalt has been poured)

*For surface 6 (see figure 4.1), an additional 5mm of cover was added due to it being a non-inspect able surface (road being driven on) once asphalt layer is added. Another additional 5 mm was added due to the need for this surface to be rough without a high level of finish (to have better friction with the asphalt). The concrete cover plays in a role in practical matters as it decides the placement of reinforcement as well.
It is clear from EN 1992 [32], that the provision of cover seems to be the most efficient way to prevent corrosion. However, this is limited to 100 years and therefore other service life models are needed in order to try and predict a sufficient cover. However, it was also mentioned in the codes that the addition of extra cover could be a possible way to resist corrosion and improve service life [34].

4.2. DURACRETE MODEL

A literature review of the SLD (service life design) models (see chapter 2) showed that most of the existing models made use of a design service life of 100 years. However, the DuraCrete model (see section 2.4.3) was one such model which allowed for the increment in design service life up to 200 years through an increase in concrete cover. This section will cover the use of the DuraCrete model to obtain cover values and also compare the results with those obtained from the Eurocode [32]. For the comparison of DuraCrete and Eurocodes only cover value for 100 years of service life (against chloride induced corrosion) will be checked, since this is the maximum service life considered by the standards. The model and its parameters were explained in section 2.4, and only the results and comparisons are discussed in this section.

COVER VALUE FOR 100 YEARS OF SERVICE LIFE

For the cover calculation using existing standards (see EN 1992-1-1, section 4 [32] and NEN 206 [33]) an exposure class of XD3 was chosen and a structural class of S4 as described by the EN 1992-1-1 [32]. The cover shown in table 4.3 was calculated taking these conditions into account.
Microsoft Excel was used to calculate cover values (for DuraCrete) and can be found in Appendix K. A w/b (water to binder) ratio of 0.45 (as stated by the standards for XD3 [34]) was used to obtain the diffusion coefficient (D_0) after 28 days, and the time period is first done for 100 years of service life (to facilitate comparison), and then for 200 years. The parameters used in equation 4.1 are shown in table 4.2 and have been obtained from the work done by CUR-Bouw en Infra [10] and is listed in table 4.2.

Parameter	Value
C_s [%]	1.5
C_i [%]	0.1
K_{tot}	1.02
D_0 $[mm^2/day]$	1.21
t [days]	36500
n	0.6
$D(t)$ $[mm^2/day]$	3.07 E-02
C_{crit} [%]	0.6

Table 4.2: Parameter values suggested by DuraCrete [9, 10]

In addition to the calculated cover, a safety margin of 30 mm is also added to bring down the failure probability to 5 % [10]. The final value of cover shown in table 4.3 has this 30 mm added to the value calculated using the DuraCrete formula. When the concentration of chloride ions at the reinforcement level (i.e. concrete cover taken as 'x') exceeds the critical chloride content, failure has occurred, where failure is a chloride content > 0.6 % of mass of cement. [9, 34].

$$C(x,t) = C_s - (C_s - C_i)erf\frac{x}{2\sqrt{K_{tot}D(t)t}} \tag{4.1}$$

Cover as per EN 1992-1-1 [mm]	Cover using DuraCrete model [mm]
50	62

Table 4.3: Cover as per Eurocode [32] and DuraCrete[10, 9] (100 years)

The value of cover using the DuraCrete model (table 4.3) was calculated through an iterative process by changing the cover value until the critical chloride content (0.6 % of cement mass) was reached for a time period 't' = 100 years (figure 4.2). The cover values seen do not have the 30mm safety margin added.

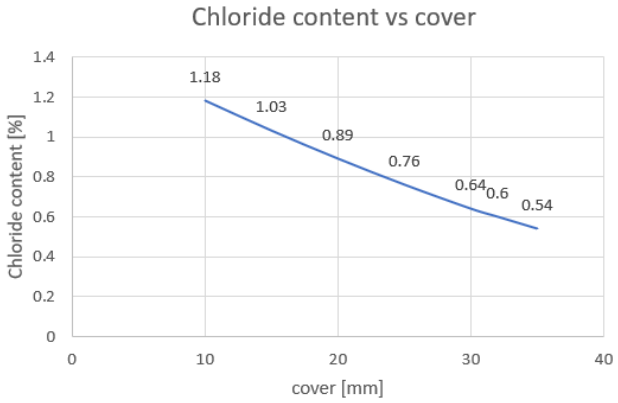

Figure 4.2: Chloride content [%] vs cover [mm] for 100 years

COVER VALUE FOR 200 YEARS OF SERVICE LIFE

Similar to the procedure described for 100 years of service life, the process was repeated for time period of 200 years (keeping all other parameters as shown in table 4.2). The time period of years was converted to days to keep the units consistent throughout the formula (see equation 4.1). When the DuraCrete model was used for calculating cover required for 200 years of service life, the cover value was 66.7 mm (i.e. 6.7 mm more than what was calculated for 100 years). Figure 4.3 gives a visual representation of the cover required as the service life changes. The calculations of this cover value was done using Excel and can be found in Appendix K.

The validity of these parameter values obtained through field testing can be called into question, especially since these parameters are not constant over the service life of the concrete structure. However, in order to use equation 4.1 these parameters need to have a constant value. Hence in the next section, the various parameters, their existing value (as specified in literature [9, 10]), and their uncertainty is discussed.

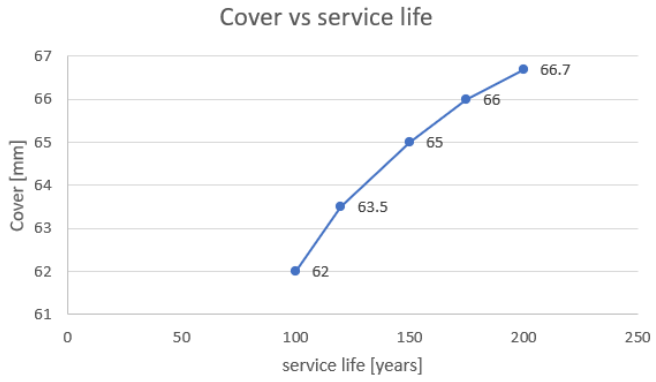

Figure 4.3: Cover[mm] vs service life [years]

4.3. STUDY OF PARAMETERS

The deviation of the DuraCrete model when used to predict chloride ingress on the Krk bridge in Croatia, was a cause for concern regarding the accuracy of the model. This particular bridge (Krk) was in service for 25 years at the time the research was conducted [15]. It needs to be stated that the bridge studied in the research conducted by Oslakovic, I. S et. al. [15] was in an environment with exposure classes XS1 and XS3, and the concrete mixture used had a w/c ratio of 0.36. The binder used was Blast furnace slag cement with 20 % of slag (CEM II/A-S 42,5) [15]. This could be one of the reasons for a deviation seen when using the theoretical values of the DuraCrete model, since there is not much experience using this model for different blends of cement [10]. In order to understand better which parameters required more study, a number of test trails were run using the model keeping all parameters constant while varying only one. This helped to understand which parameter had the most effect on the result (chloride content at the level of reinforcement).

4.3.1. AGEING COEFFICIENT

Equation 2.11 shows the relationship between the time dependant diffusion coefficient (D(t)) and the ageing coefficient (n). The relationship between ageing coefficient (n) with respect to cover, diffusion coefficient, and time were checked to illustrate the sensitivity of this parameter.

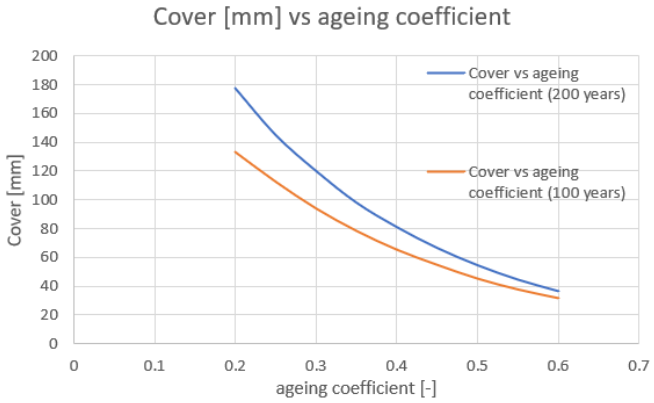

Figure 4.4: Cover vs ageing coefficient

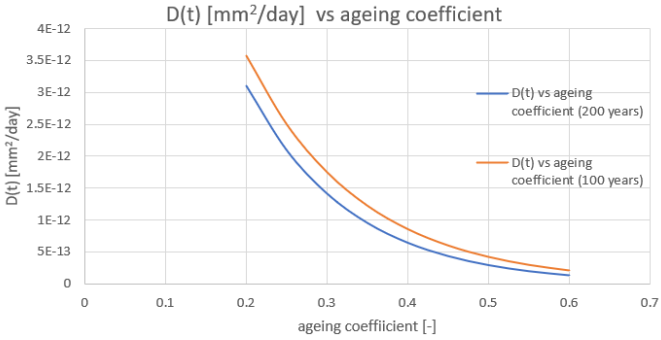

Figure 4.5: Diffusion coefficient (D(t)) vs ageing coefficient

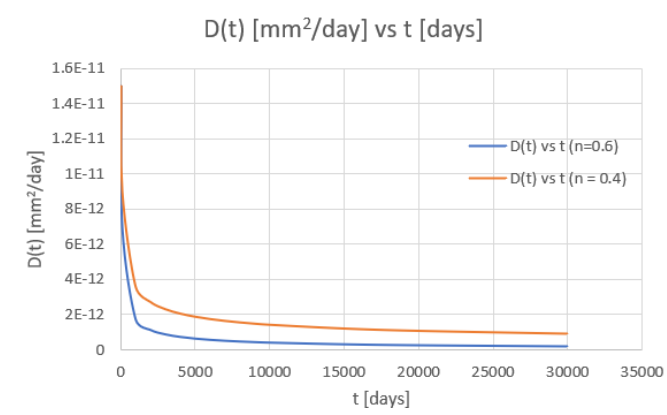

Figure 4.6: Diffusion coefficient (D(t) vs time in days

Figure 4.4 shows how the required cover (mm) changes with different values of ageing coefficient. From literature, the range of the ageing coefficient was seen to fluctuate between 0.2 and 0.6 [14, 9, 15]. An overview of the important n values and the corresponding cover values is shown in table 4.4.
Figure 4.5 shows the change in the time dependant diffusion coefficient with the change in ageing coefficient value for design life of 100 and 200 years, where n is varied from 0.2 to 0.6. The diffusion coefficient is a measure of resistance of the concrete against corrosion, where a lower diffusion coefficient means more resistance to the diffusion of chloride ions through the concrete. Table 4.5 gives an overview of the important points seen in figure 4.5.
Figure 4.6 shows the decrease in diffusion coefficient over time for different ageing coefficient values (n = 0.4 and n = 0.6) over 100 years. From figures 4.4, 4.5, and 4.6, it was concluded that this parameter is sensitive and does indeed affect the results as shown in tables 4.4 and 4.5 and more certainty regarding ageing coefficient to be used is required. It is therefore recommended that more research be conducted to conclude an ageing coefficient (n) value, and owing to a lack of resources to conduct tests and analyse core

samples the suggested value of 0.6 according to DuraCrete is used for the remainder of this report since it is based on measurement data in the Netherlands and is representative of the bridges designed in the country.

Ageing coefficient (n)	Cover for 100 years [mm]	Cover for 200 years [mm]
0.2	133	177.5
0.4	65.6	81
0.6	32	36.7

Table 4.4: Ageing coefficient and effect on Cover value

Ageing coefficient (n)	D(t) for 100 years [mm^2/day]	D(t) for 200 years [mm^2/day]
0.2	3.57E-12	3.11E-12
0.4	8.51E-13	6.45E-13
0.6	2.02E-13	1.34E-13

Table 4.5: Ageing coefficient and effect on time dependant diffusion coefficient (D(t))

4.3.2. SURFACE CHLORIDE CONTENT

The main source of surface chloride content is through the use of deicing salts on the surface of the bridge deck periodically applied in the winter season. This surface chloride content is not constant due to different factors such as wind and rain (runoff) and the surface of the structure onto which the deicing salts are applied. It is therefore concluded that this parameter is a random variable, and affects the results of the DuraCrete model [15].

Therefore, before the DuraCrete model could be used this parameter (C_s) needed a value that was reliable. This parameter was also required to be a constant value to make use of equation 4.1 to predict the chloride content at a particular point in space (x) and time (t).

From the study conducted by Gaal G. C. M. [14], the mean and standard deviation values of surface chloride content were found after collecting 100 cores from 9 bridges in the Netherlands. The collection of cores was done for three age groups of bridges, 1940's, 1960's, and 1980's and use is made of the data collected for the 1960's bridge group owing to the larger number of data samples. The assumption made here is that the data collected (core samples and profiling) from the bridges constructed in the 1960's take into account the change in surface chloride content, since the samples were collected 40 years after the bridge was in use.

4.3.3. REMAINING PARAMETERS IN THE DURACRETE MODEL

The K_{tot} value comprises of k_e and k_c and these being post treatment variables i.e. dependant on the environment of the concrete and the curing duration which are controllable variables if the proper quality and control measures are followed. For precast construction, a higher level of quality and precision can be achieved due to casting in factory conditions rather than on the field. Therefore, the values given in the DuraCrete

report [10] are used to proceed with the calculation of cover for 200 years since these values have been calibrated based on field observations. The study conducted by van der Wegen, G. et. al. [9] showed that there was a linear relationship between the D_{RCM} value (for samples at an age of 28 days) and the w/b (water/binder) ratio. The diffusion coefficient (D_0) was obtained through Rapid Chloride Migration (RCM) testing of a 500 samples consisting 150 different concrete compositions [9]. The obtained D_{RCM} value is used to calculate the time dependant diffusion coefficient $D(t)$ which is then used to calculate chloride concentration (equation 4.1). This calculation of $D(t)$ is seen in appendix K.

MODEL UNCERTAINTY

In order to take into account any deviation from observed values due to the random nature of the parameters involved in equation 4.1 a Model Uncertainty (MU) parameter was used. The study done by Gaal G. C. M. [14], provided the samples obtained from a 35 year old bridge as seen in figure 4.7. The DuraCrete equation to predict chloride concentration is calibrated according to the conditions of the bridge from which the samples were collected. A limitation seen here is that out of the 100 core samples taken from 9 bridges, only 9 chloride profiles were obtained for calibration (seen in figure 4.7). Hence the exact calibration of the DuraCrete model was not possible in terms of ageing coefficient and curing factor (k_e). Another limitation is the site specific nature of the MU parameter since all 9 samples were obtained from a single site.

The data points shown in figure 4.7 were used to determine the model uncertainty, by comparing them with the predicted value obtained using the DuraCrete model calibrated with time of 35 years (12775 days) and the resulting chloride content (%) at similar depths were extracted. The DuraCrete equation used to obtain the predicted values have been calibrated with the assumption of an XD3 exposure class and this is assumed to match the exposure class of the bridge (see figure 4.7) from which the samples were obtained. The calculation of the model uncertainty parameter can be seen in appendix K.

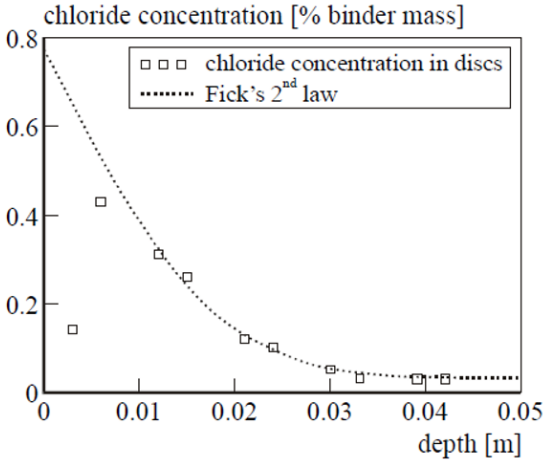

Figure 4.7: The observed chloride profile from analysis. Source: [14]

4.4. USING THE DURACRETE MODEL

Due to the mentioned uncertainties of parameters n and C_s mentioned in section 4.3, a Model Uncertainty (MU) parameter was also modelled as mentioned in the previous section. This MU should take into account some of the uncertainty surrounding the model due to a lack of data. A Monte-Carlo analysis was conducted in order to arrive at a conclusion for the value of cover with a suitable confidence value (or probability of failure). Where, failure is defined as the crossing of the critical chloride threshold at level of reinforcement (x in mm).

A Monte-Carlo simulation consists of building a model of outcomes using the variability (if any) of parameters such as a normal or uniform distribution. It then calculates this over and over for a number of iterations, with each iteration using a random value of the variables (within the specified range or distribution). As the number of iterations increase so does the number of forecasts[18].

The parameter that was recalculated repeatedly was the chloride content at the chosen depth. The surface chloride content (Cs) was seen to have a log-normal distribution from literature [15, 14]. The mean and standard deviation of the distribution is listed in table 4.6 and was adapted from the work done by G. C. M. Gaal [14]. The mean and standard deviation of the MU parameter was done through calibration of the DuraCrete model with observed chloride profiles. The MU parameter was assumed to be normally distributed based on good agreement with a Q-Q (quantile-quantile) plot. This is seen in appendix K. The other variable are deterministic, taking on suggested values according to the DuraCrete report [9] although this decreases the accuracy of the forecasting. Now only the surface chloride content and the MU parameter are modelled with their mean and standard deviation. The parameters used in the model and their distributions can be seen in table 4.7.

Parameter	Mean	Coefficient of variation	Unit
Surface chloride content (C_s)	0.8	1.29	%
Model Uncertainty (MU)	1	0.08	-

Table 4.6: Mean and standard deviation of random variables

Parameter	Distribution
C_s [%]	Log-normal
C_i [%]	Constant value
K_{tot}	Constant value
D_0 [mm^2/day]	Constant value
t [days]	Constant value
n	0.6 (Assumed constant)
$D(t)$ [mm^2/day]	Constant
C_{crit} [%]	Calculated value

Table 4.7: Parameter values and distributions

For this thesis, the Monte-Carlo simulation was first run with 10000 simulations, where as per table 4.7 the various parameters were assigned a mean and standard deviation according to their distribution (if applicable). The chloride content was repeatedly calculated 10000 times as per the DuraCrete model and also multiplied by the MU parameter. The results were counted as pass if the chloride content was less than 0.6 % and a fail if it exceeded this value. The simulations were carried out for different values of cover (mm) until a suitable cover was reached such that the probability of failure fell below 10 %.

Number of trails	Number of passes	Probability of failure [%]
10000	9213	7.87
20000	18502	7.49

Table 4.8: Convergence in probability of failure (cover value 78mm)

The number of passes (or the failure probability) can be seen in table 4.8. It was also noted that convergence was obtained since the probability of failure does not change when increasing the number of trails. Hence the number of iterations chosen for the Monte-Carlo simulation was sufficient.
The cumulative frequency distribution of the obtained chloride content can be seen in figure 4.10 and is seen to be similar to that of a log-normal distribution. When the natural log of the chloride content was plotted a right-skewed distribution was seen as shown in figure 4.9.
The results of the Monte-Carlo analysis revealed that a cover value of approximately 78 mm provided enough cover such that after 200 years, the probability that the chloride concentration (% of mass of cement) would reach or exceed the critical limit (0.6 %) was less than 10 %. Figure shows the decrease in failure probability to 7.6 % for a cover value of 78mm.

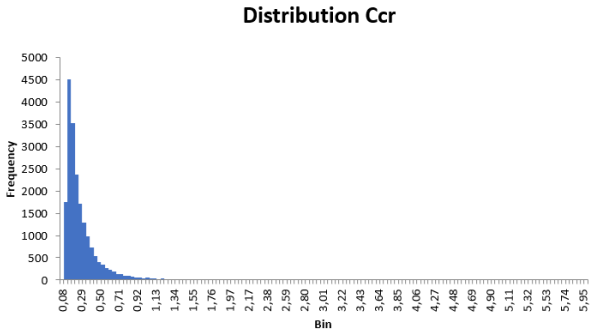

Figure 4.8: The distribution of chloride concentrations for a cover value of 78mm

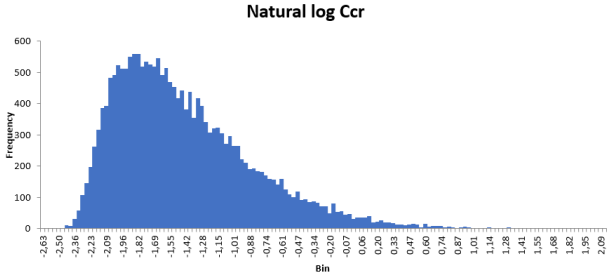

Figure 4.9: The distribution of natural log of chloride concentrations for a cover value of 78mm

4.5. CONCLUSION

The first section (section 4.1) deals with the durability of concrete as discussed in the Eurocodes. The codes specify for each exposure class a fixed value of cement content (minimum), water-binder ratio, chloride content etc. It was concluded that the service life (durability) could be prolonged through an increase in cover value.

The DuraCrete model was seen to be a potential service life design (SLD) model which could be used to design for long service life. The use of the model and the results obtained were seen in section 4.2. The random parameters in the model were discussed in section 4.3 to understand where the uncertainty in the model lay and whether it could be reduced for those parameters. A model uncertainty was used to try and account for the deviations due to the random nature of some variables.

A Monte-Carlo simulation was run and the results were used to obtain a cover value for which the probability of failure was seen to be below 10 %. The assumptions that lead to this result was that the surface chloride content followed a lognormal distribution and the model uncertainty a normal distribution. The choice of the failure probability follows from the DuraCrete report wherein a failure probability of less than 10 % for reinforcing steel was thought to be adequate [9]. Through an iterative process this cover value was found to be 78 mm. This result says that after 200 years the probability that the chloride content will exceed the value of 0.6 at a depth 78 mm into the concrete matrix

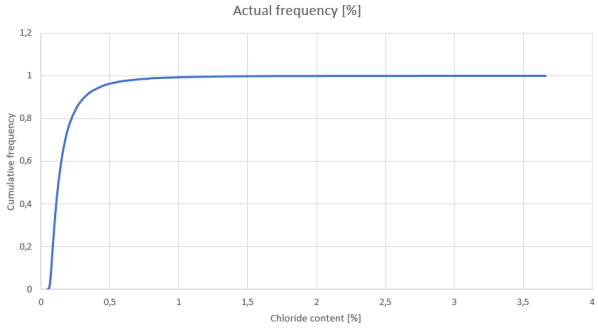

Figure 4.10: The cumulative frequency distribution of chloride content at 78 mm of depth

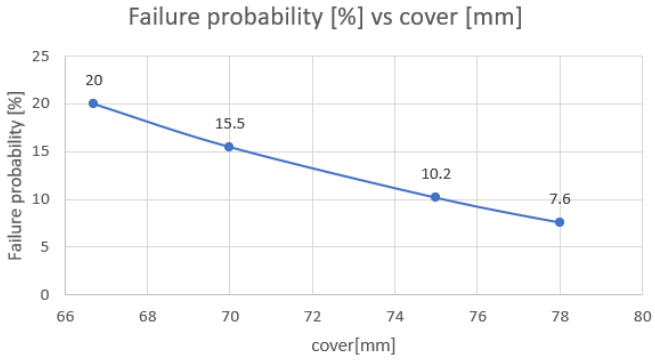

Figure 4.11: Decrease in Failure probability with increasing cover

is 8 %.
The original value of cover (DuraCrete) was 66.7mm and had a failure probability of 20 % when using a Monte Carlo simulation with a cover of 66.7mm. Thus taking into account the variability of the surface chloride content along with a model uncertainty an increase of 11.3 mm in the required cover is seen. The reduction in failure probability from 20 % to 8% is obtained as a consequence. This would lead to a larger increase in the self weight of the structure especially if this cover is added to the flanges and the webs.
To further improve the accuracy of the model, the accuracy of the ageing coefficient can be checked. The collection of core samples from existing structures that were used in the DuraCrete study would allow to check the accuracy of the ageing coefficient and understand whether any changes need to be made to the suggested values. This would reduce the uncertainty regarding the cover chosen for structures with 200 years of service life.

5

BEAM WITH IMPROVED DURABILITY

This chapter will showcase the box-beam designed in chapter 3, with the additional cover to increase service life (durability). The different options available are discussed in section 5.2 and 5.3.

Section 5.5 discusses the adaptability to changing functional requirements for a fictitious scenario where an increase in traffic loads by a factor of two is assumed.

Section 5.6 describes the advantages of the design possibility in terms of capacity, material, and adaptability. Some of the disadvantages seen are also discussed in 5.7.

5.1. INCREASE IN SERVICE LIFE

It was concluded from the last chapter that an increase in cover would be a potential way to increase the durability of the beam, and therefore the design life. From chapter 4, the cover value for concrete to withstand corrosion due to chloride ingress was calculated by making use of the DuraCrete model and a Monte Carlo reliability method. This section will discuss the different possibilities of where this cover increase can be incorporated and the reasons behind the choice of possibilities. Designing for a long service life also means designing for future increase in loads, therefore the overdesign possibilities allowed by cover increase are also explored.

The calculated value of 78mm is cover that could be used such that after 200 years, the probability of the chloride content at that depth exceeding the critical value of 0.6 % is less than 10 %. To be more precise, the probability of exceeding the critical content was 8 %. It needs to be stated that the performance of the prestressing steel during the service life is more important since this decides the structural capacity more than the reinforcing steel does. The prestressing steel being placed in the middle of the flanges give it extra protection as compared to the reinforcing steel which is closer to the surface. By addressing the reinforcing steel safety for 200 years, the prestressing steel is also taken into account. There are different possibilities for the application of this cover increase. Here possibility refers to the increase of cover of a particular part of the beam (webs, flange, or both). All available possibilities are listed as follows:

1. Increase in top flange cover
2. Increase in bottom flange cover
3. Increase in both top and bottom flange covers
4. Increase in web covers
5. Increase in web and bottom flange covers
6. Increase in web and top flange covers
7. Increase in webs, top and bottom flange covers

An increase in cover at the top flange would be most advantageous in terms of achievable bending moment capacity. The addition of cover to the bottom flange would not add much in terms of achievable capacity. From a structural viewpoint, the only advantage seen by the increase in web cover is the possibility of incorporating more prestressing steel due to an increase in overall beam width (increase in web cover on both sides). This increase in prestress would always be limited by the concrete compressive force (N_c) to provide horizontal force equilibrium. The cover at top flange, bottom flange, and the webs must be increased so that 200 years of service life can be ensured for the whole beam. However, the addition of cover everywhere would also increase the self weight of the beam reducing the overall achievable capacity. Three options are explored further, first the top flange was increased. Subsequently, both top and bottom flange cover was increased. Lastly, the web increase was also incorporated.

5.2. DESIGN POSSIBILITY 1 (DP1): INCREASE IN TOP FLANGE COVER

The standard procedure involved in box-beam girder bridges is the use of transverse post-tension through transverse ducts passing through the top flange of the girder. Any transverse post-tension passing through the top flange of the beam would already have approximately 60 mm (or more depending on the size of bar/strands) and therefore is sufficiently protected. The stirrups in the top flange however have only 50mm of cover (see chapter 3) and this steel would require extra cover in order to perform its designated function for 200 years. The result from chapter 4 was that a cover of 78 mm would be sufficient to withstand chloride build up to critical levels, for up to 200 years. This means an additional 38 mm to be added to the dimension of the top flange of the SKK 1500 girder increasing the thickness from 170mm to 208mm. The top flange cover must be increased due to the use of deicing salts on the road surface where only a thin asphalt layer protects the top flange from direct contact with the deicing salts. Henceforth, Design Possibility 1 refers to the beam with an increase in top flange cover. This is seen in figure 5.1.

Resulting UDL on beam due to increase in self self weight (q_{G*}) is calculated in equation 5.1. The UDL is obtained by multiplying the dimensions of cover and width with the density of concrete. The resulting increase in moment (at mid span) is calculated in equation 5.2. The increment in shear force (at support) due to the increase in self weight is calculated in equation 5.3.

$$q_{G*} = 0.038 \times 1.48 \times 25 = 1.406 kN/m \tag{5.1}$$

$$M_{G*} = \frac{q_{G*} \times L^2}{8} = 355.89 kNm \tag{5.2}$$

$$V_{G*} = \frac{q_{G*} \times L}{2} = 31.63 kN \tag{5.3}$$

UDL on beam [kN/m]	Bending moment increase [kNm]	Shear force increase [kN]
1.406	355.89	31.63

Table 5.1: Increase in bending moment due to additional cover (28mm)

The important properties for Design Possibility 1 are shown in the table 5.2 (calculations can be found in appendix M).

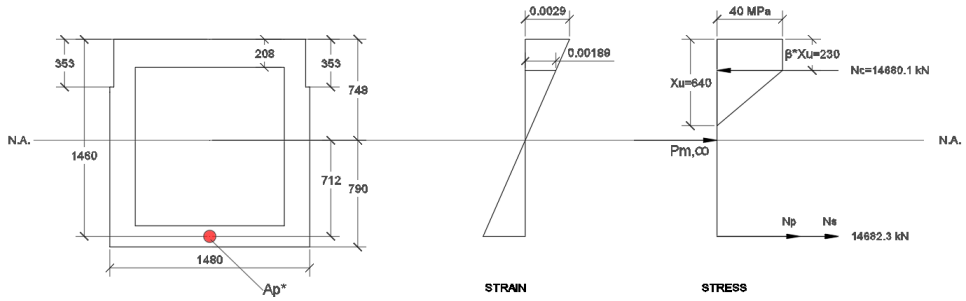

Figure 5.1: Beam with cover increase of top flange (additional 38mm)

Property	Value
Xu [mm]	621.5
Beam height [mm]	1538
Thickness top flange [mm]	208
Thickness bottom flange [mm]	157
Area of section $A_{c,DP1}$ [mm^2]	1068960
Section modulus W_{DP1} [mm^3]	3.687E+8
Area of reinforcement [mm^2]	1500
Area of prestressing steel [mm^2]	9150
Effective depth (reinforcing and prestressing steel) [mm]	1460
Depth from top fiber to neutral axis [mm]	748
Depth from bottom fiber to neutral axis [mm]	790
Force from concrete N_c [kN]	14680.1
Force from steel N + Pm,∞ [kN]	14682.3
M_{Ed} from chapter 3[kNm]	11739.8
$M_{Ed,self}$ increase in self weight [kNm]	355.9
$M_{p,\infty}$ [kNm]	7270.5
M_{Rd} for DP1 [kNm]	11854.5

Table 5.2: Properties for Possibility 1 (Bending moment capacity at ULS)

As seen in table 5.2 the changes made from the standard beam (see chapter 3) apart from cover increase was the increase in the prestressing steel amount by 1200 mm^2 which allowed for the beam to resist a larger bending moment at ULS (11 % more). However since this beam is designed for a service life of 200 years, the extra prestressing steel was added to incorporate an increase in loads over the service life. The bending moment due to SLS load combinations were seen to be 9056.1 kNm per girder when the Eurocode load models and combinations were used (see chapter 3). Equation 5.4 was used to find the maximum SLS moment that could be withstood. Solving this gave a maximum SLS moment of 10792.57 kNm such that no tensile stresses occurred at bottom fibre.

$$\frac{-P_{m,\infty}}{A_{c,DP1}} - \frac{M_{prestress}}{W_{b*}} + \frac{M_{SLS}}{W_{DP1}} \leq 0 \; at \; (t = \infty) \tag{5.4}$$

5.3. DESIGN POSSIBILITY 2 (DP2): INCREASE IN TOP AND BOTTOM FLANGE COVER

The increment of top flange was already discussed in section 5.2. This section will discuss the addition of 38 mm of concrete to the bottom flange (see figure 5.3), why it needs to be done and what changes are seen in the capacity of the beam. The collection of runoff from the deck can flow down the sides of the girder and collect near the bottom flange calling into question the durability of the prestressing steel at this location. The addition of 38 mm of concrete cover makes it such that the stirrups located at the bottom flange have sufficient cover as discussed in chapter 4 and the overall thickness of the bottom flange becomes 195 mm. The addition of cover on top increases the distance to neutral axis from the bottom fibre (Zcb) and the addition of cover to the bottom flange increases the distance from top fibre to neutral axis. The properties for Possibility 2 are shown in table 5.4.

Resulting UDL on beam due to self weight ($q_{G,2*}$) is calculated in equation 5.5. The UDL is obtained by multiplying the dimensions of cover and width with the density of concrete. The resulting increase in moment (at mid span) is calculated in equation 5.6. The increase in shear force (at support) is calculated in equation 5.7

$$q_{G,2*} = 0.076 \times 1.48 \times 25 = 2.81 kN/m \tag{5.5}$$

$$M_{G,2*} = \frac{q_{G,2*} \times L^2}{8} = 711.78 kNm \tag{5.6}$$

$$V_{G,2*} = \frac{q_{G,2*} \times L}{2} = 63.23 kN \tag{5.7}$$

UDL on beam [kN/m]	Bending moment increase [kNm]	Shear force increase [kN]
2.81	711.78	63.23

Table 5.3: Increase in bending moment due to additional cover (66mm)

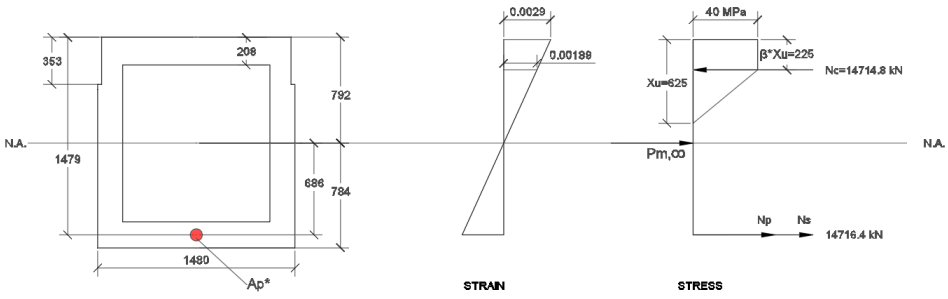

Figure 5.2: Beam with cover increase of top flange and bottom flange (additional 66mm)

Property	Value
Xu [mm]	625
Beam height [mm]	1576
Thickness top flange [mm]	208
Thickness bottom flange [mm]	195
Area of section $A_{c,DP1}$ [mm^2]	1125200
Section modulus W_{DP1} [mm^3]	4.159E+8
Area of reinforcement [mm^2]	1571
Area of prestressing steel [mm^2]	9150
Effective depth (reinforcing and prestressing steel) [mm]	1479
Depth from top fiber to neutral axis [mm]	792
Depth from bottom fiber to neutral axis [mm]	784
Force from concrete N_c [kN]	14714.8
Force from steel N + Pm,∞ [kN]	14716.4
M_{Ed} from chapter 3[kNm]	11739.8
$M_{Ed,self}$ increase in self weight [kNm]	711.8
$M_{p,\infty}$ [kNm]	7005.1
M_{Rd} for DP2 [kNm]	12386.5

Table 5.4: Properties for Possibility 2 (Bending moment capacity at ULS)

The increase in capacity is a little more than that seen in Possibility 1 due to an increase in the internal lever arm (Zct) that increases the bending moment resistance, thus allowing for an extra capacity of 213.32 kNm per girder as compared to Possibility 1. The increase in capacity is only 16 % compared to the initial bending moment resistance at Ultimate Limit State for SKK1500.
All calculations for the increase in bending moment capacity are shown in the spreadsheets in Appendix M

5.4. DESIGN POSSIBILITY 3 (DP3): INCREASE IN TOP AND BOTTOM FLANGE AND WEB COVER

For a beam to have 200 years service life the additional cover will have to be added to all parts of the beam. Therefore this section explores the third and final possibility. Design Possibility 3 consists of the increment of webs, top and bottom flange by 38mm. Resulting UDL on beam due to self weight ($q_{G,3*}$) is calculated in equation 5.8. The UDL is obtained by multiplying the area of cover with the density of concrete. The resulting increase in moment (at mid span) is calculated in equation 5.9. The increase in shear force (at support) is calculated in equation 5.10.

$$q_{G,3*} = (0.353 \times 0.038 \times 2 + 1.223 \times 38 \times 2) \times 25 = 2.99 kN/m \tag{5.8}$$

$$M_{G,3*} = \frac{q_{G,3*} \times L^2}{8} = 757.95 kNm \tag{5.9}$$

$$V_{G,3*} = \frac{q_{G,3*} \times L}{2} = 67.27kN \tag{5.10}$$

UDL on beam [kN/m]	Bending moment increase [kNm]	Shear force increase [kN]
5.89	1469.47	125.5

Table 5.5: Increase in bending moment due to additional cover (DP3)

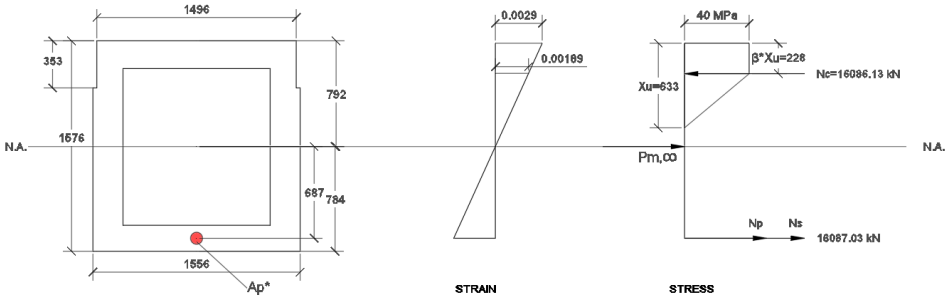

Figure 5.3: Beam with cover increase of webs, top, and bottom flange

Property	Value
Xu [mm]	633
Beam height [mm]	1576
Thickness top flange [mm]	208
Thickness bottom flange [mm]	195
Area of section $A_{c,DP1}$ [mm^2]	1244976
Section modulus W_{DP1} [mm^3]	4.47E+08
Area of reinforcement [mm^2]	2090
Area of prestressing steel [mm^2]	9900
Effective depth (reinforcing and prestressing steel) [mm]	1479
Depth from top fiber to neutral axis [mm]	792
Depth from bottom fiber to neutral axis [mm]	784
Force from concrete N_c [kN]	16086.13
Force from steel N + Pm,∞ [kN]	16087.03
M_{Ed} from chapter 3[kNm]	11739.8
$M_{Ed,self}$ increase in self weight [kNm]	1469.7
$M_{p,\infty}$ [kNm]	7590.25
M_{Rd} for DP2 [kNm]	13508.47

Table 5.6: Properties for Possibility 3 (Bending moment capacity at ULS)

Property	SKK1500	DP1	DP2	DP3
h [mm]	1500	1538	1576	1576
b [mm]	1480	1480	1480	1556
A_c $[mm^2]$	1015000	1068960	1125200	1244976
A_p $[mm^2]$	7800	9150	9150	9900
A_s $[mm^2]$	2340	1500	1571	2090
M_{Rd} [kNm]	10638.24	11854.5	12386.5	13508.47
$M_{selfweight}$ [kNm]	-	355.9	711.8	1469.7

Table 5.7: Comparison between SKK1500 and the different Design Possibilities

Thus Design Possibility 3 is proceeded with in this thesis. All the beams discussed in sections 5.2, 5.3, and 5.4 were designed with the objective to maximise overdesign while still maintaining the horizontal force equilibrium between steel and concrete. An overview of the different properties can be seen in table 5.7. The limitation seen was the Xu/d ratio (EN 1992-1, section 5.1), which did not allow for an increase in Xu (height of compression zone) due to which the prestressing limit was reached. In the following section the performance of only Design Possibility 3 in a fictitious future scenario is discussed. The larger area of concrete allows for larger amount of prestressing to be balanced.

5.5. ADAPTABILITY TO CHANGING LOADS

According to CB'23 (Circular Bouwen 2023) [25] the adaptability of components to be reused must also be investigated. Two types of adaptability were defined, a spatio functional adaptive capacity and technical adaptability. The former covers the adaptability to changing function and space requirements and the latter deals with the disassemblability of the component. The adaptability of the box-beam with cover increase is limited in terms of spatial adaptability, but does offer potential to be functionally adaptable to changing loads, namely traffic loads. The possibility that traffic loads will increase due to either population growth or increase in traffic jams must always be considered. Expansion of roadways is one way to avoid congestion due to traffic, but the extension of bridges might not always be possible owing to space requirements and the complexity of type of bridge. Therefore if expansion is not possible the capacity of the girders might need to be increased to avoid reaching or exceeding the capacity of these girders overdesign could be a potential solution. It is quite difficult to predict the change in traffic since this could be an increase in vehicle weight, number of vehicles, or even the spacing between vehicles. Further, rules and regulations (of the Ministry of Transport) regarding maximum vehicle weight are also factors affecting future traffic scenarios.
For this thesis, the fictitious scenario considered was the increase in traffic loads specified in EN 1991-2 [46]. The exact change in traffic cannot be predicted without carrying out a full probabilistic analysis using traffic data. Hence for this thesis, the scope was reduced to just increasing the coefficients of the tandem systems (TS) load cases in the governing load combinations (ULS and SLS described in chapter 3) by a factor of 2. This approach is quite a conservative one since such a drastic increase in traffic would not be expected within a single life cycle of the beam. This was done on SCIA Engineer 21.0.0030 and the existing model made in chapter 3 was modified for the purpose of this impact

analysis. All the load cases defined (in SCIA) belonging to the tandem systems were multiplied by a factor of 2. Load Model 1 is indicative of the most common traffic scenarios [46], and in this thesis the effect of an increase in the tandem systems is investigated. The outputs for bending and shear are discussed in the following sub-sections.

5.5.1. OUTPUTS FOR BENDING - X2 TANDEM SYSTEMS

BENDING AT ULS

The outputs for bending at Ultimate Limit State and Serviceability Limit State are discussed in this section. Once the output values were extracted from SCIA, the performance of Design Possibility 3 was checked.

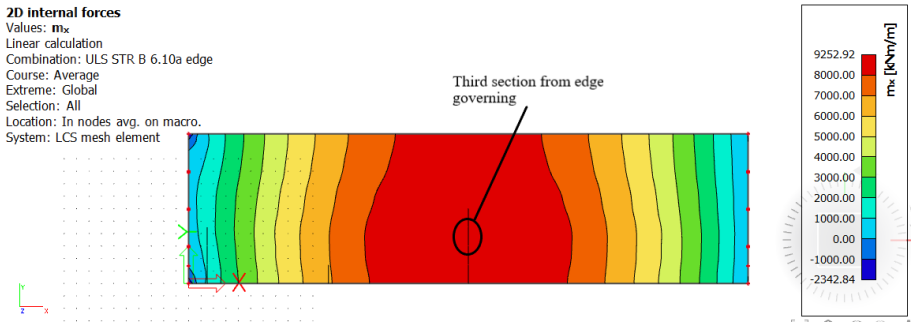

Figure 5.4: Bending output seen when traffic load factors are increase by a factor of 2 - top view

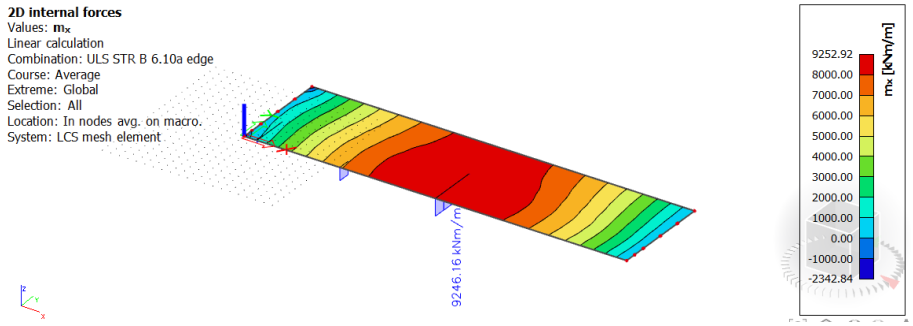

Figure 5.5: Bending output seen when traffic load factors are increase by a factor of 2

Bending output (ULS) in kNm/beam	
Contour plot	9252.92 * 1.48 = 13694.3
Section value	9246.16 * 1.48 = 13684.31

Table 5.8: Bending moment values at ULS for an increase in tandem systems (x2)

The output plots shown in figures 5.4 and 5.5 were used to obtain the final bending moments listed in table 5.8. As noted in table 5.7 all the Design Possibilities would be able

to sufficiently carry this Ultimate Limit State bending load due to the high moment from prestressing to reduce the design moment from live loads.

Bending moment	SKK1500	DP 3
$M_{Ed,x2,SCIA}$ [kNm]	13684.31	13684.31
$M_{p,\infty}$ [kNm]	5832.2	7590.2
M_{Ed} [kNm]	7852.1	7563.8 (incl. self weight increase)
M_{Rd} [kNm]	10638.24	13508.47

Table 5.9: Comparison of standard beam and Design possibility 3

The results in table 5.9 show that the Design Possibility 3 as well as the original beam (SKK1500) can take up bending at ULS for the future scenario considered. The original prestressing steel and reinforcing steel in the standard beam are sufficient at ULS for the future scenario considered. As mentioned before this increment in traffic loads is a conservative approach and is not expected to take place in 200 years.

BENDING AT SLS - X2 TANDEM SYSTEMS

The stress at bottom fibre due to the new SLS load was where the limitation was seen. Using the outputs from table 5.10 the stress at bottom fibre was checked (equation 5.11).

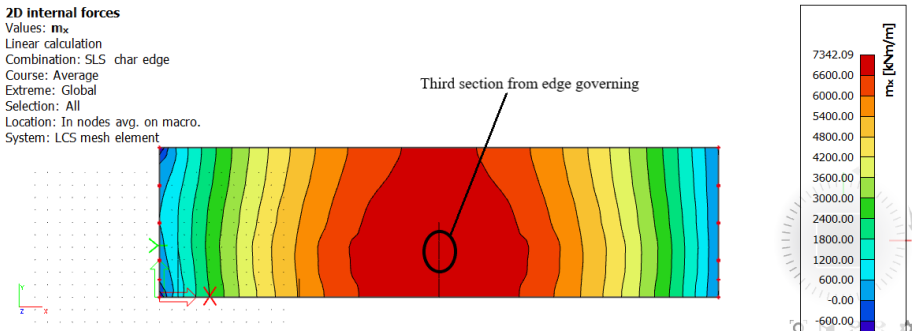

Figure 5.6: Bending output seen when TS load factors are increase by a factor of 2 - top view

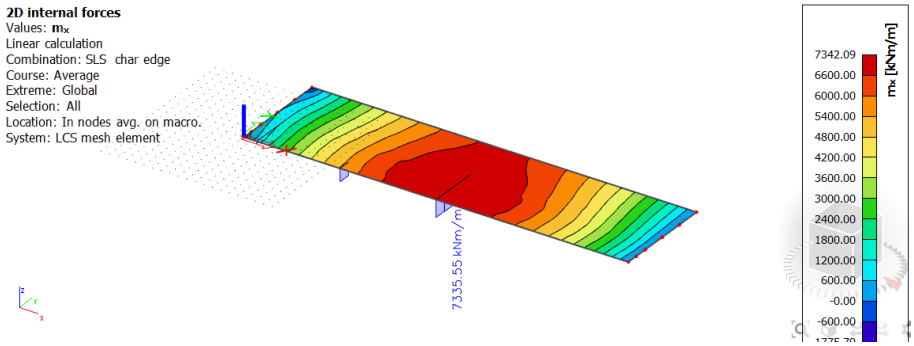

Figure 5.7: Bending output seen when TS load factors are increased by a factor of 2 - isometric view

Bending output (SLS) in kNm/beam	
Contour plot	7342.09 * 1.48 = 10866.29
Section value	7335.55 * 1.48 = 10856.61

Table 5.10: Bending moment values at SLS for an increase in tandem system (x2)

$$\frac{-P_{m,\infty}}{A_{c,DP3}} - \frac{M_{prestress}}{W_{b,DP3}} + \frac{M_{selfweight+SLS}}{W_{b_DP3}} = 1.72MPa < f_{ctm.fl} = 4.4MPa \; at \; (t = \infty) \tag{5.11}$$

The initial choice of prestressing used in SKK1500 (standard beam) is not sufficient especially for a future scenario of x2 increase in traffic. Therefore the prestressing was increased in Design Possibility 3, where the increase in cover allows for an increase in prestressing. However, for an increase by a factor of 2 for the tandem systems of Load Model 1 the bending moment at SLS is still quite high (10856.6 kNm per girder) as seen in table 5.10. The stress at bottom fibre for Design Possibility is checked to understand whether the current design is sufficient. The values to be substituted into equation 5.11 can be found in table 5.6. Although the stress is below $f_{ctm,fl}$ and in theory concrete should not crack, this condition can be safely assumed if no tension were allowed to occur. Therefore, a further increase in prestressing steel is required to prevent cracking (stress less than 0 $N/mm2$) while in use (SLS). From the point of view of prestressing steel, an increase of strands from 58 to 71 is required, i.e. from 8700 to 10650 mm^2 for no cracking in SLS to occur. The limiting factor seen here was the amount of concrete that is able to contribute to the concrete compressive force to maintain horizontal equilibrium with the tensile force in the steel. This can be overcome by increasing the height of the concrete section or using higher strength concrete but is not explored further since this thesis explores the design recommendation of sufficient cover to prevent ingress up to 200 years and the benefits of this cover increase.

5.5.2. OUTPUTS FOR SHEAR - X2 TANDEM SYSTEMS

The increase in shear force at the section where shear force is maximum is discussed in this sub-section. Figures 5.8 and 5.9 show the output plots obtained from SCIA Engineer 21.0.0030.

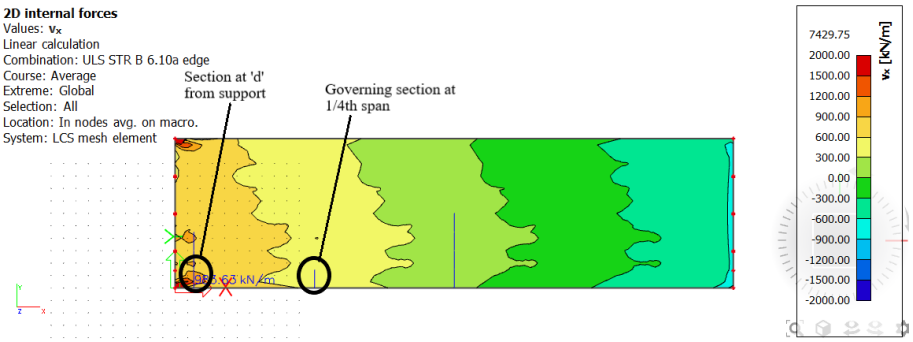

Figure 5.8: Shear output seen when TS load factors are increase by a factor of 2 - top view

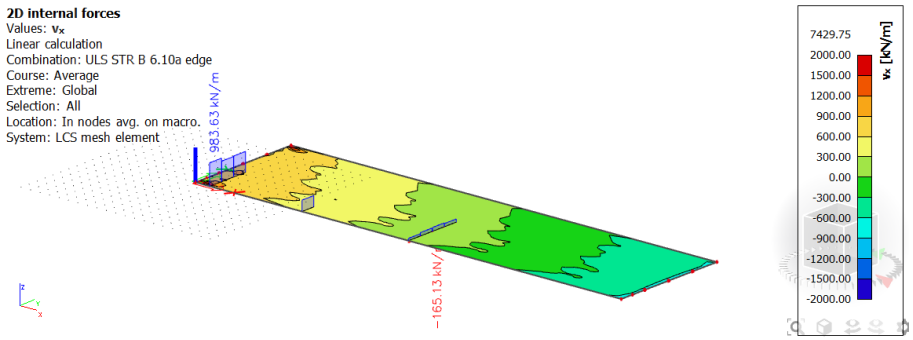

Figure 5.9: Shear output seen when TS factors are increase by a factor of 2

Shear output (ULS) in kN	
Contour plot	1200 * 1.48 = 1776
Section value	983.63 * 1.48 = 1455.77

Table 5.11: Shear force values at ULS for future scenario of x2 traffic

-	Current scenario - DP 3	Fictitious scenario (x2 tandem) - DP 3
V_{Ed} [kN]	1314.43	1455.77
A_{sw}/s [mm^2/m]	963.03	1061.65
z = 0.9*d [mm]	1331.1	1331.1
fyd [MPa]	435	435
θ [◦]	22	22

Table 5.12: Comparison of required reinforcement for both beams- current vs future scenario

Both steel requirements per meter can be satisfied through a choice of 4 ϕ 10 bars placed at 333mm centre-to-centre per meter. The initial choice of stirrups is suitable to take the increase in shear force, and no extra stirrups are required to take the shear force coming from the increase in load factors of the tandem systems.

5.5.3. FATIGUE VERIFICATION - 200 YEARS

A probabilistic study taking into account the traffic loads, axle weights, spacing between vehicles would be required in order to say something regarding the fatigue performance of the beam [36]. However, the increment of tandem system by a factor of two is assumed to be the fictitious future scenario within this thesis. The fatigue verification according to FLM1 was performed similar to chapter 3, section 3.5.5. Following the same procedure, the stress arising due to self weight would increase if Design Possibility 3 was used and the stress arising from prestress would also increase owing to the increased number of strands (52 to 66).
This leads to a change in the maximum and minimum stresses arising from the loading on the bridge, however it still falls below the allowable stress range described by the S-N curves for prestressing steel [32]. For the fatigue verification of the beam for 100 years 50 million cycles were considered with the assumption of traffic category 2 (Roads and motorways with medium flow rates of lorries) [46]. If 200 years were to be considered for the same traffic category the number of cycles increase to 1E+08. However, the use of FLM1 which is quite conservative [46], and still gives a higher allowable stress range due to which even 1E+08 cycles does not pose any problems.
Considering the traffic category 1 (Roads and motorways with two or more lanes per direction with high flow rate of lorries) increases the number of cycles to 4E+08. Further, if the assumption was to consider two slow lanes, one in each direction the number of cycles would increase upto 8E+08 cycles for 200 years. Keeping such a scenario in mind the fatigue verification was checked and the calculation can be seen in appendix E.

5.6. ADVANTAGES

The advantages of Design Possibility 3 are discussed in this section. As mentioned in literature [25] the adaptability to changing functional requirements was one factor that affected the reusability of the box-beam girder. As shown in section 5.4, overdesign allows for an increase in bending moment capacity through increase of prestress (made possible through cover increase). For the future traffic scenario considered, the beam can take up bending in Ultimate Limit State, while it still behaves well in Serviceability Limit State where the stress at the bottom fibre was still less that 4.4 MPa ($fctm,fl$).

Therefore for an increase in load factors of the tandem systems (in LM1) by 2, Design Possibility 3 would be able to perform adequately.

Property	SKK1500	Design Possibility 3
Area (A_c) [mm^2]	1015000	1244976
Prestressing steel [mm^2]	7800	9900
Reinforcing steel (longitudinal) [mm^2]	2430	2090
Bending Moment capacity (ULS) [kNm]	10638.24	13508.5

Table 5.13: Material used for both beams

The increase in self weight can be balanced by an increase in prestress, and the increase in concrete section (through cover increase) allows for a balance to be maintained (horizontal equilibrium between steel and concrete). Therefore through the usage of extra concrete and prestressing steel as seen in table 5.13 a more adaptable (to changing loads) and durable beam can be achieved.

5.7. DISADVANTAGES

The disadvantages seen when using Design Possibility 3 are discussed in this section.

- increase in self weight due to additional cover of 76mm (38 on top and 38 on bottom) as well as 38mm to both webs
- this increase in cover adds to design moment (M_{Ed}) by 1469.7 kNm thereby reducing some of the extra capacity achieved from increase in prestress
- more material being used in the form of concrete and prestressing steel

More labor cost is also a disadvantage to consider but may not be as important as the increased material usage. Increase of prestress will require an increase in split tensile reinforcement at the massive part of the box-beam.

5.8. CONCLUSION

Ultimately, Design Possibility 3 is chosen as the beam to proceed with. All the beams have adequate bending moment resistance at Ultimate Limit State. Design Possibility 3 also performs quite well at Serviceability Limit State as well. The increment of prestressing to 66 strands allows to keep stresses at the bottom fibre below $f_{ctm,fl}$. With an increment in prestressing steel by 27 % and an increase in concrete volume by 10.34 mm^3, Design Possibility 3 can be achieved.
The increment of self weight does lead to a decrease in overall capacity but is compensated by an increase in prestress. The beam uses extra prestressing but can withstand chloride ingress upto 200 years. An added advantage is that it could also take up the loads arising from a future fictitious scenario where the tandem systems of Load Model 1 was increased.
A full probabilistic traffic study might be able to show a more accurate prediction after which the overdesign can be done efficiently. For the future scenario considered the

shear capacity of Design possibility 3 serves adequately and no increment in reinforcement was required at the critical cross-section near the support.

6

CIRCULARITY INDEX AND DISASSEMBLABILITY

Section 6.1 discusses the need for measurement of circular aspects of assets and components. Section 6.2 will address if the indicators found in literature (for assets) could be adapted for single components (box-beam girder), and attempt to evaluate a circularity score for the box-beam. This is done in section 6.2.

Section 6.3 will discuss the key aspects that affect the disassemblability of a box-beam girder from a bridge. Section 6.4 will discuss a method which attempts to score the demountability of the box-beam based on the key aspects discussed in section 6.3.

6.5 mentions the extra material used for Design Possibility 3. 6.6 discuss the various advantages seen in the form of increased durability, the potential for multiple life-cycles, and increased adaptability in terms of increase in loads.

6.1. NEED FOR MEASUREMENT

As discussed in the literature review chapter (section 2.3), there are many important indicators that can help measure circularity of assets and components. It is important to understand why this needs to be done. An index that allows for the measurement of circularity could prove to be beneficial when trying to compare similar quoted prices by contractors for a project. One could argue that an LCA (Life Cycle Analysis) could be enough to conclude whether a certain design is circular enough, but as seen from the literature, the LCA is limited by its methodology since it is based on linear cycles and was used mainly for the measurement of cradle-to-grave designs. Multiple life cycles cannot be measured by the LCA method [19]. Hence a circularity indicator that could give a score based on relevant parameters could help compare design alternatives in terms of circularity. It should be noted that within the scope of this thesis, only reusability was looked into whereas circularity depends on many variables of which reusability is only a small part of. Hence inspiration was taken from the relevant literature [17], in two forms. The first was to see whether the aim of this thesis (increasing the service life to 200 years and re-usability) agreed well with existing literature and second, whether the composite indicator could be adapted for the beam designed in this thesis and used to validate the conclusions. The second part is required in order to validate whether the durability study and the corresponding results when applied to a box-beam improved the circularity (reusability) score or not. Here, circularity is not just reusability, thus two things will be checked, (i) whether more robustness (200 years) contributes to the reusability, (ii) whether the increase in robustness contributes positively to circularity (and if not reusability then where?).

6.2. RELEVANT INDICATORS

As seen from literature [17, 5, 9, 7], there are a few logical and obvious reasons for the choice of some indicators (and sub-indicators). However, the circularity score for box-beam bridges was only done in the work done by Coenen T.B.J. [27] but the demountability of box-beams is still an area where research is scarce. In this chapter the indicator developed by Coenen T. B. J. [27] was adapted to measure the circularity of a precast box-beam girder along with a scoring of the demountability of the box-beam.

These indicators chosen to evaluate the Bridge Circularity Index (BCI) were discussed in chapter 2, but within this chapter are adapted for a beam (when required) since the indicators from literature [17] was for circularity on an asset level. Although reusability is the primary interest, literature [6, 17] has shown that the characteristics that make up the indicators are quite inter-related. For example, within this thesis the cover was increased to enhance the durability of the beam, but this beam is quite unique in its characteristics i.e. straight, 45 meters in length, with a height of 1500 mm (figure 3.3b for SKK1500). Enhancing the cover to improve durability makes it even more unique such that it can only be reused for certain bridges that fit this profile. Therefore even though the durability of the beam is increased (increases circularity score), its uniqueness goes up (decreases circularity score) making it harder to reuse.

The various indicators along with the relevant sub-indicators used within this thesis are described below. The choice is made to keep the indicator scoring system consistent

with existing literature (therefore from 0 to 1). The possibility of adapting existing indicators from literature was also checked and can be seen in the appendix L.

6.2.1. DESIGN INPUT

For the beam designed within this thesis, one can argue that the Design Input indicator might not be too useful since this beam design makes use of all virgin raw materials. It is important to keep in mind however, that this argument holds true only for the first life cycle, and when one moves to the second life cycle, the beam is 100 percent reused without the need for raw materials, hence reducing the need for additional material.
An important point to understand is that just a high circularity score (or Design Input score) can be misleading because this particular score can be high either by using recycled and reused materials or by designing with a high robustness in mind. Therefore the context of the bridge is important - 'What is it designed for?' rather than how long its technical life is. This thesis was done with a particular bridge in mind, discussed in chapter 3. On evaluating both beams as per the method outlined by Coenen [27], the beam designed for 200 years has a score of 0.7 and the beam for 100 years has a score of 0.55, the calculation is shown in Appendix L.

6.2.2. RESOURCE AVAILABILITY

The resource availability for the beam was calculated using the method proposed by Coenen T. J. [17] for which the formulas were explained in chapter 2. The final score obtained for the Resource Availability indicator (0.18) made use of the mass of all elements of the beam (concrete, prestressing steel, reinforcing steel) and the respective scarcity scores. The calculation of this is seen in Appendix L.

6.2.3. REUSABILITY

Since the primary goal of the thesis was to evaluate reusability this indicator is studied in detail, and along with the necessary sub-indicators score the reusability of the component. The use of expert opinions were necessary as a starting point for the work done by Coenen [17] and the same is used here as well. The point of difference here is that some things might change since this is the study of reusability on a component level. The effect of change of cover is what this thesis attempts to validate (evaluate) and hence use is made of the existing indicator but modified to fit the purpose of this thesis.
The opinion of the author is that disassembly is the most important sub-indicator when evaluating reusability. The other study of this thesis however was a durability study (chapter 4) to see if increasing the life also increased the possibility of reuse. As a middle ground, this thesis will make suggestions on how demounatability (or disassemblability) can be realised and show the difference this sub-indicator has on the circularity score. When trying to measure this indicator (Reusability), literature calls upon three sub-indicators [27], (i) disassemblability, (ii) transportability, and (iii) uniqueness.

DISASSEMBLABILITY

In order to assess the disassemblability, one needs to remember that the point of interest is disassembling the beam from the bridge (asset), this concept follows the literature [17] and no adaption (for beam) is required. The required information is a list of all

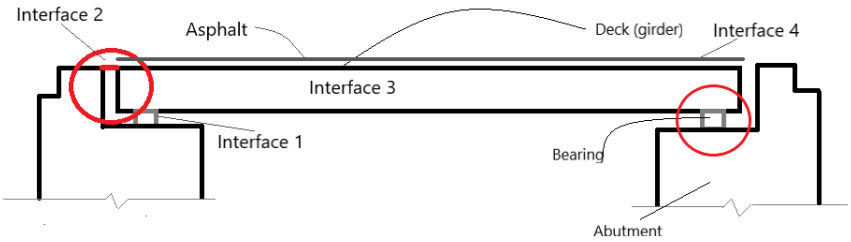

Figure 6.1: Sketch showing the interface between beam and other components

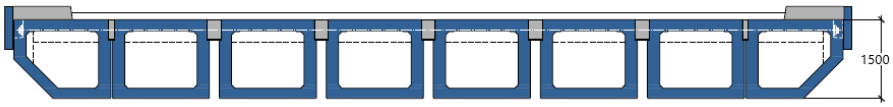

Figure 6.2: Beam-to-beam interface in the transverse direction

connections of the beam to the bridge. If standard practice is followed there will be four main points of concern where demountability is concerned for the beam. The removal of the kerbs and parapets was not a scope of this thesis, although the NTA 8081:2021 [23] makes mention of how parapets and railing can be removed. The kerbs however might have to be integrated with the edge beams in future designs. For a simply supported span (45 meters), a simple scheme is shown in figure 6.1. Here the beam has connection with the abutment, the bearings, and with the adjacent box-beams through reinforcement or transverse post-tension (figure 6.2).

Table 6.1 gives an overview of the different interfaces that the beam has with the asset. The work done by Coenen [17] [27], makes use of a scoring system with values between 0 and 1 where 0 represents non-agreement (non-circular) and 1 represents good agreement (circular) and this system is adopted within this thesis (for this indicator) as well.

Most of the important details that are required come from the design of the bridge. One limitation within this thesis is that this is not a complete design of a bridge, rather a component (box-beam) that is part of the bridge. Nevertheless, the connection details that are already demountable (beam to bearing) are not looked into. However, certain suggestions will be made in order to improve the circularity score in order to promote future research regarding similar topics. For the use of the Bridge Circularity Indicator

Interface	Disassembly
Beam-beam	No
Beam-bearing	Yes
Beam-abutment	Yes (provided IFD is applied)
Beam-asphalt	Yes (provided asphalt will not be reused)

Table 6.1: Beam interfaces and disassembly

developed by Coenen B. T. [17], the demountability sub-indicator score was taken from the supporting documents provided for the evaluation of a box-beam bridge [27].

TRANSPORTABILITY

The transportability of the girder was explained in chapter 2, section 2.3.4. Using the sub-indicator formulas seen in sub-section 2.3.4, one can score the transportability of the component (beam in this case), which will be used to ultimately score demountability. The new owner (client deciding to reuse the girder) needs to be assured from a financial viewpoint that reusing the girder is more economical than casting a new beam. Another limitation seen here is the possibilities of reuse, depending on the bridge characteristics of the new site (where this girder will be reused). This beam is designed for a straight bridge with no skew, hence limiting the potential reuse to new bridges that are straight and have no skew as well.
The transport of girders via canals and waterways seems to be the most ideal way to transport with respect to weight (in tonnes) of the girder. However, the availability of this mode of transport is not always guaranteed. The combination of having a waterway and a roadway available for transport of the girder could warrant the highest transportability score (1), this was suggested by Coenen [17] as well. This is perfectly logical owing to the fact that it is uncommon to have all three modes of transport available at a single location. Another assumption applied in this thesis is the exclusion of rail travel for this particular girder, as it seems quite impractical (or even impossible) to transport said girder via railway. This leaves two possibilities for transport of this particular girder. Keep in mind this is just an indicator for the reuse of the prefab girder, and may need to be adjusted for other components. An indicator for components is not done in this thesis, but is simple enough to adapt using reasoning.

Scenario	Road (1 lane)	Road (2-3 lane)	Transportability
1	✓	✓	1
2	✓	-	1
3	-	✓	0.75
4	-	-	0

Table 6.2: Available modes of transport

Since this thesis was for the circularity (and reusability) for the most common bridge found in the Netherlands, the water and rail mode of transport are omitted since the bridge spans a governmental road. The only two options of transport could be 1 lane road or 2-3 lane road for the transport of the girder. Table 6.2 gives an overview of the different possibilities regarding available modes of transport.
An explanation of the scores is warranted here and to understand this figure 2.9 needs to be referred to. Since the available modes are only 1-lane and 2-3 lane roads, a score of 1 is given to 1-lane roads (instead of 0.8) and for the second available option a score of 0.75 (0.6/0.8). A new valuation is given to the available modes as seen in table 6.2. The location is not looked into since this is almost impossible to predict.
The two scores above (1 and 0.75) refer to the transportability scores for the available

modes of transport, which will be used to transport the girder. The total transportability (T) then becomes (equation L.9) 0.755. The calculation of this sub-indicator can be found in the appendix L.

UNIQUENESS

The argument for this sub-indicator is logical, the more unique a girder is, the more difficult to reuse elsewhere. The limitations from literature was that no component had been standardized yet [17]. The formula presented in literature requires the mass of all standardised components (for asset uniqueness). Since this thesis focuses on beams, another alternative method to calculate or at least classify uniqueness will be put forward. One idea is to think of standardisation based on rough dimensions of the girder with respect to span (similar to the brochures published by Consolis Spanbeton). Fixing a span-to-depth ratio could also be one way to standardize certain components (girders in this thesis). Once classified, a score can be given and this will be used further to score the reusability (ultimately). Another important point to keep in mind is that no bridge (that exists) at the moment is really demountable (box-beam bridges), and hence this girder (designed in this thesis) realistically has no place to go unless demountability of future bridges is made a reality. Only then will this concept of reusability move forward and become a reality.

6.2.4. ADAPTABILITY

This sub-indicator was also discussed in detail in the chapter 2, however the method applied to calculate the Adaptability was on an asset level and trying to adapt it would require a change in the score of the weights which would deviate from the existing indicator and the result would no longer be valid. However looking at the indicator and its respective sub-indicators, it can be logically reasoned that the way in which the scores are finally achieved would be the same for both the standard beam (chapter 3) and for Design 2 (top and bottom cover increase as described in chapter 5).
Therefore, even though a difference will be seen it would not show in the Resource Availability, Reusability, or Adaptability indicators.

6.2.5. IMPACT OF COVER INCREASE

It was seen from literature, that the increase of cover is valued less as compared to other adaptability and flexibility requirements. However, it can be argued that durability is a requirement for reuse to be possible. The author agrees that the 3 main sub-indicators (section 6.2.3) are more relevant from the reusability point of view, but fail to be the only criteria to judge the reusability. If a component is not durable, the disassemblability, transportability, and uniqueness would not matter since said component would not be able to adequately performs its function at the new location. The scope of this thesis is to try and improve the service life (durability) and try and measure the impact of this improved durability on the reusability of the box-beam. What has been discovered when using the existing method to 'measure' circularity [17] was that durability was not 'seen' to impact the reusability indicator. Rather, the impact was seen in the Design Input indicator. One major drawback seen here is that when comparing a standard beam (designed according to the Eurocodes) and the beam for 200 year service life (with respect

of chloride ingress), only the Design Input score seems to separate them. This is because the robustness was chosen to be included within the Design Input indicator. One possible conclusion that is seen here is that durability and reusability aren't as connected as initially thought to be, it is definitely a precondition but not the most important one.

6.3. DISASSEMBLABILITY

Another important sub-indicator seen was disassemblability (sub-indicator under Reusability in chapter 2) sub-indicator, where a lot of potential for improvement is seen. This section will talk about the limitations of the current construction procedures with regards to the disassemblability aspect of the beam. Qualitative suggestion will be made since the scope of the thesis was about durability and reuse. In order to assess this particular sub-indicator, the interfaces as mentioned in section 6.2.3 will need to be referenced. There is not much literature concerning the separation of the box-beams from the bridge, and its subsequent reuse. Therefore this thesis aims to provide some information regarding the demountability of box-beams from the bridge via a scoring method [6, 5]. The following sections will provide information regarding the different interfaces (sub-section 6.3.1) found in a box-beam bridge and finally a demountability scoring is done in a global manner (section 6.4).

6.3.1. INTERFACES

More information regarding the interfaces between the beam and the surrounding components are needed in order to better understand demounatability/disassemblability. As seen from section 6.2.3, there are four interfaces where the beam is connected to the bridge. The different interfaces will be discussed here in detail along with potential suggestions that could improve the disassembly in the future. As the number of interfaces increase so does the difficulty of realising a demountable component. Once this is done, key aspects for the demountability of the beam can be identified and is done in section 6.4.

BEAM-BEARING INTERFACE

This interface is a a simple one where the beam is placed on top of the bearing without any other complicated connections (other than simple grout). Bearings are the components that connect the superstructure with the substructure. They rest on the abutments/piers with the beams resting on top. Normally for a precast bridge, elastomeric bearings are used owing to their lower price and the need for a higher number of bearings (at least two per beam at each support). If heavier loads are expected pot or spherical bearings can be used. The different types of bearings will not be discussed here, since it is the connection/interface that is of interest. The main function of the bearing is to allow movement of the beam due to shrinkage or thermal expansion (or contraction) and therefore not fixed in place. There are certain bridges where the bearings are fixed providing no degrees of freedom but that is not the case in this thesis. Standard practice allows for the removal of bearings for their replacement periodically (20-25 years) as mentioned in the ROK 1.4 RTD1007-1:2013 [47]. Therefore this interface is one that is removed at least once during the lifetime of the bridge. Traditional methods of replacing bearings involve the use of a jacks to lift/prop up the superstructure by a small

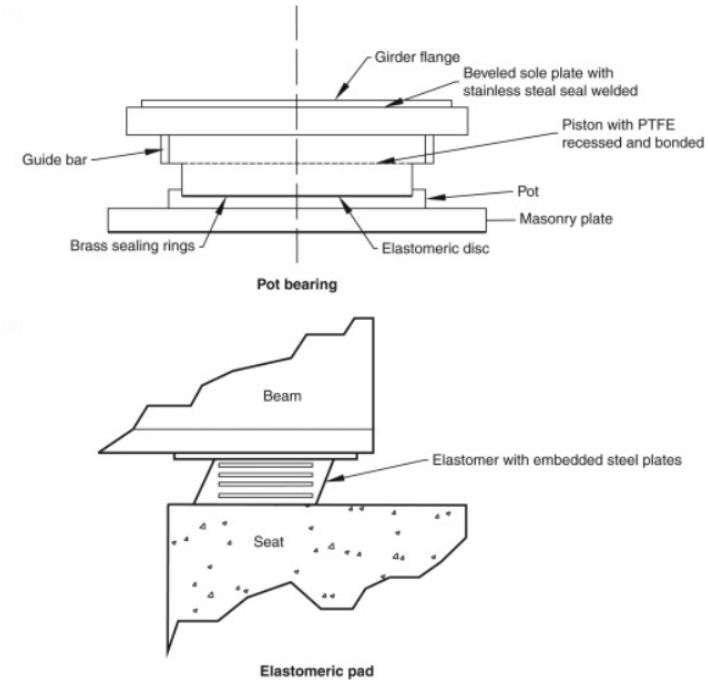

Figure 6.3: Different options for bearings for the box-beam in this thesis [48]

distance as well as support the superstructure while workers saw/chip out the grout and remove the bolts attaching the bearings (old) to the superstructure and substructure respectively. The seat/abutment must have enough space in order to set up the jacks.

BEAM-BEAM INTERFACE

The beams are interconnected via transverse post-tension through the top layer and a cast insitu layer between as well (figure 6.4). This transverse post-tension is inserted through ducts in the top flange of the box-beam(s), grouted (for durability reasons as well as bond) and then post-tensioned once the grout hardens. This interface is a little more complicated owing to the use of cast in place concrete between the longitudinal joints (of lower strength class) between the box-beams. The figures 6.4 and 6.5 hope to provide a little more clarity regarding the various interfaces present between two adjacent box-beams.

BEAM-ABUTMENT INTERFACE

This particular interface cannot really be called an interface, rather a connection between the 'hammerhead' part of the beam and the abutment. More information regarding the different types of joints are described in RTD 1001 ROK 1.4 Appendix A [47], but one condition all the joints must satisfy is a water tight seal between the abutment and the girders to prevent build up of water in the space between the abutment and the girder (figure 6.6). This is marked red in figure 6.6.

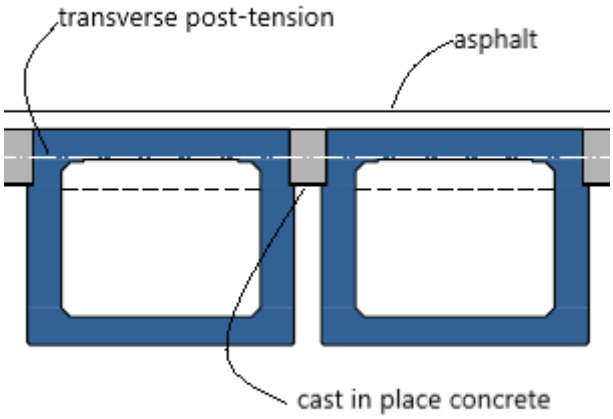

Figure 6.4: Connection in transverse direction for box-beams [41]

Figure 6.5: Duct passing through top flange [49]

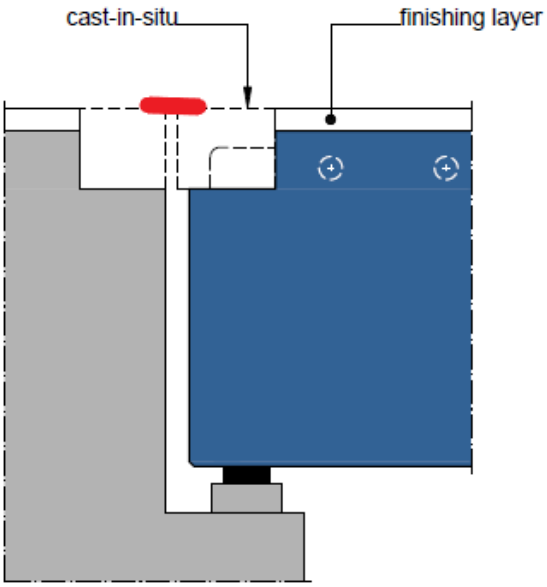

Figure 6.6: Beam to abutment interface/connection [41]

BEAM-ASPHALT INTERFACE

If one follows standard practice, the final finishing layer would be 140mm of asphalt poured directly on top of the box-beams. Once this has hardened, the bridge is ready for use. Asphalt reapplication does take place periodically but this is not a point of interest. There will come a point in time when the bridge is no longer needed in that particular location, and the beam is to be dismantled (or disassembled) from the bridge. When this time does arrive, there is no real way to separate the asphalt from the beam and preserve the asphalt layer as a whole.

6.4. DEMOUNTABILITY SCORING

This scoring is based on a global overview of the connections found in a box-beam bridge. The author is aware that to study the demountability of a bridge would require a detailed study of the design of a bridge. However, to understand the which part of the bridge requires more focus a demountability scoring system is developed. In order to do this some key aspects need to be introduced, these are (i) number of interfaces, (ii) interface simplicity , (iii) ease of accessibility, (iv) durability.

6.4.1. ACCESSIBILITY

It stands to reason that for a connection to be demountable it had to be accessible, no matter the simplicity (or complexity) of the connection. Inspiration is taken from the work done by Van Vliet M.[6] and the scores for various accessibility conditions are seen

in table 6.3

Accessibility	
Accessible without any operation	4
Accessible with non-damaging operation	3
Accessible through damage without affecting function	2
Accessible through reparable damage	1
Not accessible	0

Table 6.3: Accessibility options and scores

6.4.2. NUMBER OF INTERFACES

Once accessibility is assured, it can be argued that the next priority must be the number of interfaces. This would influence the time and effort required to disassemble/disconnect the beam from the bridge. The various scoring options for this particular characteristic is shown in table 6.4. Interface here refers to the point where the beam is in contact with another component of the bridge. If standard practice is followed there will be four main points where demountability of the beam is concerned.

Number of interfaces	
One to two interfaces	4
Three interfaces	3
Four interfaces	2
Five interfaces	1
Greater than five	0

Table 6.4: Number of interfaces and scores

6.4.3. SIMPLICITY OF INTERFACES

The next feature that defined the beams demountability was the simplicity if the interface. For the features and their scores inspiration from work done by van Iperen L. [50] and van Vliet M. [6] was taken, with a slight change in some features to better represent those found for a box-beam girder. Table 6.5 shows the features chosen that best represent the types of connections found in the bridge. Dry connections refer tho those connections that use mechanical fasteners without any adhesives. Connections with added elements make use of bolts, nuts and screws. Direct integral connections refer to those connections that make use of nails or pins to connect interfaces. Use of grout or mortar to connect interfaces falls into the category of wet connections without reinforcement and wet connection here refers to cast insitu concrete with reinforcement. Most of the connections found in a prefabricated bridge make use of wet connections [47] and due to this score quite low with regards to simplicity.

Simplicity of interface	
Dry connection	4
Connection with added elements	3
Direct integral connections	2
Wet connections without reinforcement	1
Wet connection	0

Table 6.5: Simplicity of interfaces and scores

6.4.4. DURABILITY

The durability was seen as the least important factor, since it can be argued that durability only makes sense if the component can be disassembled first and only then can reuse follow. For reuse to be possible it needs to be durable, thus allowing for use in the next life cycle. Therefore it can be said that more durability increases the possibility for more life cycles. The different choices of design life (in years) and the respective scores can be found in table 6.6.

Durability	
Very high design life ≥ 150 years	4
High design life ≥ 100 years	3
Intermediate design life > 75 years	2
Low design life ≥ 50 year	1
Design life < 50 years	0

Table 6.6: Durability of the beam and scores

NOTE

Some of these key aspects, namely accessibility and simplicity of interfaces cannot have just one score since these key features are described by the number of interfaces. In these cases the average score of accessibility (for each interface) and simplicity (for each interface) is used as the final score of the aspect i.e. internally weighing them where each interface accessibility (or interface simplicity) has a weight of 1. This is elaborated in Appendix I.

6.4.5. WEIGHTING

The weight of these key aspects will need to be done to know how much these key aspects actually contribute to demountability. In order to weigh these aspects the method proposed by Song and Kang [51] which adapts the widely used Analytical Hierarchy Process(AHP) [52] such that its limitations were reduced and is simple to use. The application of the method to arrive at the final weights seen in table can be found in appendix J.

Key aspect	Weight
Accessibility	0.31
Number of interfaces	0.28
Simplicity of interfaces	0.26
Durability	0.15

Table 6.7: Weighting of key aspects

6.5. COST OF REUSE

It is ultimately the economic feasibility that decides the feasibility of reuse. To help the goal of reuse of elements a government mandate should introduced through the form of legislation where the new norm becomes reuse and recycling wherever possible. This could end up costing a lot more than just casting an entirely new bridge, but this might be the price to pay to preserve our environment.

6.5.1. EXTRA MATERIAL REQUIRED

The excess material required for Design 3 is elaborated here. When comparing the standard box-beam (chapter 3) to that in chapter 5, the main differences are the amounts of concrete, prestressing steel and the overcapacity that is achieved (shown in table 6.8. Other than material an extra capacity of 1451 kNm per girder can be achieved without

Extra material	
Concrete [m^3]	5.75
Prestressing steel [mm^2]	2100

Table 6.8: Extra material required for Design option 2

much else changing except for the split tensile reinforcement.

6.6. ADVANTAGES

The advantages of the durability study (and its application) (see chapter 3 and 5) would be the multiple service lives of the box beam. From literature it was seen that the use-life cycle of components is usually much shorter than the technical life [5]. The advantage of having increased durability can only be realised once disassemblability is made possible. One can argue however that with this increased durability comes a higher potential to recycle the components within the concrete i.e. prestressing and reinforcing steel. From the point of view of numbers, the Design 2 beam has the potential of 200 years of service meaning it has twice the utility of a standard beam in terms of durability against corrosion. The beam for the future has a higher demountability score than that of a standard beam owing to its improved durability. The scoring method puts forward certain key aspects regarding the demountability of box-beam girders specifically.

6.7. CONCLUSION

This chapter in the first section dealt with the adaptation of an existing indicator which described bridge/viaduct circularity on an asset level through a Bridge Circularity Indicator (BCI). It was seen that a complete adaptation was not possible since the weights attached to different indicators dealt with the whole bridge (as an asset). These weights could not be directly adapted to a component since expert opinions were used to determine them and how they related to the asset as a whole. This was one of the limitations seen in existing indicators, the personal bias arising out of expert opinions make adaptation to different projects (and components) difficult.

Direct application of existing indicators depends on what the indicator is, since some indicators (for an asset) require component circularity to be measured first (Disassemblability and Transportability). Material level circularity indicators are used to calculate how much fraction of the used material comes from various sources (Design Input). This applies only to mass (of component or asset) depending on what the MCI is calculated for. Resource Availability depends on mass and scarcity and can be measured for a component or an asset (by including total mass or mass of component). Hence almost 3 out of the 4 indicators could be directly applied in terms of formula to be applied.

Adaptability, however, could not be directly adapted due to what it tries to evaluate. This comes down to how the indicator was made, and the weighing behind the options were done specifically on a global level to be applied to a bridge/viaduct. Adapting this was not possible owing to the inability to use the statements (Yes/No) and the corresponding weights (expert opinions). Due to Adaptability not being measurable, the overall circularity score could not be obtained.

To improve the future scope in terms of research, a scoring system to judge the demountability of a box-beam and its connections within a bridge was devised to better understand how the box-beam was integrated into the bridge system. However, this was just a preliminary step, and a bridge would need to be studied in detail to judge the demountability.

This was done through identification of key factors and a scoring system based on weighing the different aspects to get an overall score for the demountability if the box-beam. It was seen from the results that the type/simplicity of the connections is where the demountability and hence the reusability of the beam suffers.

It was seen that an increase of cover does increase the overall circularity score, but not the reusability score when using existing indicators. Lack of literature concerning adjacent box-beam girders further prompted a small study into the disassemblability of the beam to further improve future flexibility and adaptability of box-beam girders. This also provides insight into the method to determine future areas of improvement concerning circularity. First, it should be determined which areas contribute most to the circularity (or its sub-categories like reuse). In this thesis it was seen that the score was brought down by the technical barrier of wet connections and increasing the durability although advantageous, the effect of which was diminished by the technical complexity of the connection/interface.

7

Conclusion and Future recommendations

This chapter presents first a summary of the work done. Subsequently the conclusions of this thesis in the form of answers to the sub research questions followed by the main research question. The research questions were put forward in chapter 1.

Lastly, the future recommendation to further improve this thesis are discussed in the next section.

7.1. SUMMARY OF THE WORK

The objective of this thesis was to investigate the extension of the service life of box-beam bridge beams from the design phase. Subsequently, its effect on the circular performance of the beam was studied to suggest improvements and future areas of research. The circular aspects considered were adaptability and future demountability of the box beam. The first step within this thesis was to design a box beam making use of the Eurocodes. The maximum service life described within the Eurocodes was 100 years, and this thesis explores the possibility of extending this further to 200 years with regards to chloride ingress. An overall design for 200 years would require aspects such as fatigue life, future change in traffic loads etc. to be taken into account which was not part of the scope of this thesis. Literature review on the service life of concrete structures, deterioration mechanisms, and service life models led to two main conclusions. First, the service life could be improved through an increase in concrete cover. Second, the DuraCrete model could be used to find the extra amount of cover required. Due to the uncertainty of the random variables in the model, the distribution of the surface chloride content and a model uncertainty parameter were used to run a Monte Carlo simulation. This cover was then applied to the standard beam and its adaptability to an increase in loads was checked. Load Model 1 which describes the most common traffic scenarios on a bridge consists of uniformly distributed loads and tandem system loads. The load factors of the tandem systems were increased by a factor of 2 to simulate this fictitious future scenario that might occur in 200 years. The result was that although the beam with an extra cover had an increased self-weight, the extra concrete section allowed for an increase in prestressing steel from 52 to 66 strands. The extra material required was only 5.75 cubic meters of concrete and 2100 mm2 of prestressing steel. This increase allowed for the beam to resist the new bending moments and shear forces at ULS and SLS for 200 years. To study the circularity of the beam, the reusability of the beam and its barriers were studied. The increase in life span allows for the beam to be in use longer, thereby keeping it at its highest value. The increase in lifespan loses its effect if the bridge is no longer required in a particular area and cannot be demounted. Therefore, to keep it at its highest value level the barriers to demountability were also investigated. Through this key aspects affecting demountability were identified, and weighed against each other to obtain a score for the beam on a global level. The aspect with the lowest score was the monolithic connections, especially the connections of the box beams in the transverse direction. This is one area where future research is needed for the eventual reuse of the box beam to become a reality.

7.2. CONCLUSION

Sub research question I - Where and how do the current durability practices deviate from those involved in circular practices regarding a box-beam girder?

If the circular design strategy of value retention (through life extension) and subsequent value creation (multiple life cycle, designing future proof) is the basis of circularity, it needs to be incorporated from the design phase itself, rather than as a measure once maintenance is required. The Eurocodes make no mention of these terms and how to incorporate them.

This thesis dealt with an increment of service life from the design phase onward, by making the beam more durable for 200 years with regards to chloride ingress as a first step. It was seen from EC2 [32] that durability was assured in the form of cover value being assigned to a certain exposure class, following a deemed-to-satisfy approach. This cover value assigned was determined through lab testing and is not always indicative of actual field conditions. This is another limitation that might overestimate the durability as well. Durability also means the concrete having sufficient mechanical properties over its lifetime but in the codes used for design, no consideration about the change or reduction in mechanical properties of concrete was discussed. Especially if the intention is to reuse for multiple life cycles, properties such as compressive strength, tensile strength, prestress in the steel, etc. may change over time and may not be enough to resist the loads and taxes in the future. Additionally, the durability of concrete as specified in the Eurocodes deals with uncracked concrete, and while this may be enough if no cracking during Serviceability Limit State is allowed, the removal and reuse of this girder may induce some cracking in the beam, which can affect the durability in the next life cycle and there is no mention of durability of cracked concrete in the Eurocodes. The last deviation seen was the limitation of reference period of 100 years. The effect that a 200 year reference period might have on the other aspects of design are difficult to predict.

Sub research question II - What are the main factor(s) that affect the service life of concrete and what design recommendations can be made to increase the service life?

MAIN FACTOR AFFECTING SERVICE LIFE

From literature, (chapter 2), it was identified that one of the most common forms of deterioration faced by concrete structures is corrosion of reinforcing and prestressing steel. Within this thesis the durability was studied to improve the performance of the beam against chloride ingress for 200 years. Other factors such as fatigue verification and traffic load increase would need to be looked into for a more comprehensive design for 200 years. However, the penetration of chlorides were deemed to be most governing, since this led to loss of steel cross-section and could lead to structural collapse. Penetration of other agents could also cause a decrease in durability, however corrosion induced by ingress of chlorides was reasoned to be the most aggressive. From the review of the codes (EN 1992, chapter 4), which discusses the durability of concrete structures, only the penetration of these agents and the nature of the environment were considered for durability.

DESIGN RECOMMENDATION THROUGH COVER INCREASE

Due to strict requirements specified by the Eurocodes. the design option of cover increase was chosen to improve durability. This was seen to be more beneficial since it also allowed for an increase in prestressing strands, as well as extra section of concrete to balance the steel force arising from prestress. The limitation seen was that this also added to the self weight of the girder. The results of the Monte Carlo simulations revealed that a cover value of 78 mm provided sufficient cover against ingress of chlorides. Subsequently the probability of the limit state being exceeded was less than 10 %.

Sub research question III - How do these design recommendations affect the adaptability and demountability of the beam?

ADAPTABILITY

The design recommendation being an increase in cover allows for room to overdesign wherein an increase in capacity is seen (chapter 5) by using more prestressing steel. Design Possibility 3 (DP3) becomes the beam to withstand chloride ingress for 200 years. For use for 200 years, a fictitious future scenario of increased traffic load was considered to judge the performance of the beam. The fictitious scenario considered was an increase in the tandem systems of Load Model 1. The increase in cover allows for an increase in prestressing thereby improving the performance of the beam for this fictitious future scenario considered. In such a situation the beam has sufficient over-design such that it could still be applicable for use (SLS) with stresses at the bottom fibre below $f_{ctm,fl}$. The shear force increase seen could be handled through the initial choice of stirrups. However until and unless the exact change in load (close to exact) is known through a probabilistic study (for example) it is impossible to know how much to over design. In this way it was seen that the beam has the potential to adapt to changing loads, although a higher initial cost will be suffered when using the box-beam during the first life-cycle. However it needs to be stated that this is not a given for every box-beam bridge, and it could be specific to the design of the bridge and what loads it might carry. This improved capacity could make the beam a likely candidate for reuse in lower capacity scenarios in the second or third life cycle.

CIRCULARITY AND DEMOUNTABILITY

Once the principle of life span extension was achieved against chloride ingress, the next goal was to maintain the high value of the beam. The service life and the technical life of assets are not always the same. Once the bridge is no longer required at a particular location, demolition would lead to waste accumulation, and using construction and demolition waste as road sub grade would be a form of down-cycling. The future scope must therefore be to reuse the beam. The scoring system within this thesis looks at the beam within the bridge on a global level classifying different key aspects, where it was concluded that the simplicity of the interface plays a large role in the eventual reuse of a component. Reuse would ensure that the beam contributes to construction at a high value.

7.3. MAIN RESEARCH QUESTION

How can prefabricated box beam girders be designed for the future (design service life of 200 years) considering the government's circular plans for the economy?

The Dutch government aims for a waste-free economy by the year 2050, and have come up with certain circular design strategies and principles, the direct application of which maybe not be enough to see results immediately. Circular design principles used by Rijkswaterstaat need to be implemented from a design stage rather than as an end of life practice. The principle explored within this thesis is reuse by keeping the beam at its highest level of value. To do this the circular design principle of life extension was implemented from the design stage rather than at end of life stage.

Designing for the future meant taking into account the most common deterioration mechanism of corrosion, such that the reinforcing and prestressing steel were protected for longer periods of time (200 years was chosen). Once corrosion has begun and propagated there is very little that can be done in the form of maintenance to repair the beam. Prevention of corrosion through cover increase of the webs, top and bottom flange of the girder. The increase in service life sees an increase in the reuse potential, although as seen from literature and the scoring method developed for this girder, more importance needs to be given to demountability.

The design principle of life extension being implemented from the design stage does help to achieve the function of value retention since the beam can now be in service longer. The second principle namely value creation facilitated through multiple life cycles and designing future proof was the next step. The approach towards circularity should go hand in hand with technical advancement. Circular design principles can be developed but their impact will always be foreshadowed by technical barriers (or standard practice) as seen in the demountability scoring system in this thesis. An increased durability can be realised through cover increase (value retention is achieved) but the next step of value creation (facilitate multiple life cycles) cannot be realised until the technical barriers to reuse can be addressed. Hence, both design principles are important and value retention is a prerequisite, although its contribution to overall circularity is not very significant.

The last point to be discussed is that circularity will always be a developing concept, and what is done with the beam after 200 years must also be taken into account. The reuse of a component will only contribute to short-term circularity (longevity), which is good, but when designing circularly the long term circularity must also be taken into account from the early design stage. This is a limitation of this thesis, in that the scope was more focused on the detach-ability and not the practicality of eventual reuse and the eventual recycling that should be done.

7.4. RECOMMENDATIONS

The following recommendations are made in order to take this topic further, such that the circularity of box-beam girders is improved further.

1. The possibility of standardizing of unbonded transverse post-tension such that the beam-beam interface (see chapter 6) is improved further improving the demountability score. This would require a design feasibility study where a potential solution might be the constant monitoring of the stress levels in the strands to ensure that adequate prestressing is always maintained. The unbonded nature of the strands could allow for replacement when a drop in stress is detected.

2. The probabilistic study of the traffic loads to determine what the future increase in traffic might look like, and which load factors need to change to properly account for traffic change. The different types of vehicles or change in traffic laws which would allow heavier vehicles/special vehicles are quite difficult to predict due to which a full probabilistic analysis that could take this into account would give a clearer picture on the factors that would need to change.

3. The increment in the number of cycles call into question the fatigue resistance of concrete since 200 years will mean at least twice the number of cycles considered by the prevailing standards. Fatigue Load Model 1 (FLM1) is most often used to verify the fatigue resistance of concrete owing to its simplicity of application, and future research could topics could be to see whether FLM1 could still be applied for 200 years.

4. The possibility of corrosion occurring due to simultaneous actions of carbonation and chloride ingress would ensure a safer beam especially when the design service life is planned for 200 years. Carbonation is a phenomenon that brings about a change in pH of concrete and this might possibly reduce the chloride binding capacity of concrete leading to higher content of chloride or influence the rate of corrosion due to chloride ingress

5. Further improvement of the DuraCrete model by properly accounting for the variability in the aging coefficient. Collection of core samples from the same bridges will highlight whether the chosen 'n' values take into account ageing of concrete in the right manner. This can be done through further back calculation to check whether the diffusion coefficients (through RCM) of the newly collected samples and that predicted by using the time dependant diffusion equation match. The probability of failure to be associated with design for long service lives can also be improved by reducing the uncertainty surrounding this parameter.

BIBLIOGRAPHY

[1] K. Anastasiades et al. “Translating the circular economy to bridge construction: Lessons learnt from a critical literature review”. In: *Renewable and Sustainable Energy Reviews* 117 (2020), p. 109522. ISSN: 1364-0321. DOI: https://doi.org/10.1016/j.rser.2019.109522. URL: https://www.sciencedirect.com/science/article/pii/S1364032119307300.

[2] Government of the Netherlands. *Circular Dutch Economy by 2050*. URL: https://www.government.nl/topics/circular-economy/circular-dutch-economy-by-2050.

[3] Government of Netherlands. *A Circular Economy in the Netherlands by 2050*. URL: https://www.government.nl/topics/circular-economy/documents/policy-notes/2016/09/14/a-circular-economy-in-the-netherlands-by-2050.

[4] E Schut, M Crielaard, and M Mesman. “Circular economy in the Dutch construction sector: A perspective for the market and government”. In: (2016).

[5] Elma Durmisevic. “Transformable building structures: design for dissassembly as a way to introduce sustainable engineering to building design & construction”. In: (2006).

[6] M Van Vliet. “Disassembling the steps towards Building Circularity”. In: *Eindhoven Univ. Technol. Eindhoven* (2018).

[7] J Verberne. “Building circularity indicators: an approach for measuring circularity of a building”. In: *Eindhoven Univ. Technol* (2016).

[8] O. Schepers ; Witteveen+Bos R. Dijcker. *Circular design in the MIRT process : action perspectives for policymakers, advisors, designers and managers*. URL: https://puc.overheid.nl/rijkswaterstaat/doc/PUC_158440_31/.

[9] Gert van der Wegen, Rob B Polder, and Klaas van Breugel. “Guideline for service life design of structural concrete–a performance based approach with regard to chloride induced corrosion”. In: *Heron* 57.3 (2012), pp. 153–168.

[10] CUR Durability Guideline. “Durability of Structural Concrete with regard to Chloride-Initiated Reinforcement Corrosion”. In: *CUR Construction and Infrastructure* (2009), pp. 1–65.

[11] Olugbenga O. Akinade et al. “Design for Deconstruction (DfD): Critical success factors for diverting end-of-life waste from landfills”. In: *Waste Management* 60 (2017). Special Thematic Issue: Urban Mining and Circular Economy, pp. 3–13. ISSN: 0956-053X. DOI: https://doi.org/10.1016/j.wasman.2016.08.017. URL: https://www.sciencedirect.com/science/article/pii/S0956053X16304767.

[12] Bradley Guy, Scott Shell, and Homsey Esherick. “Design for deconstruction and materials reuse”. In: *Proceedings of the CIB Task Group* 39.4 (2006), pp. 189–209.

[13] *EN 1990 Eurocode: Basis of structural design*. EN. Brussels: CEN, 2002.

[14] Gerardus Cornelis Maria Gaal. “Prediction of deterioration of concrete bridges”. In: (2004).

[15] Irina Stipanovic Oslakovic, Dubravka Bjegovic, and Dunja Mikulic. “Evaluation of service life design models on concrete structures exposed to marine environment”. In: *Materials and structures* 43.10 (2010), pp. 1397–1412.

[16] S Berlo. “Assessing the circularity of infrastructure assets: a methodology to inspect and assess 1 on 1 reuse of concrete components”. MA thesis. University of Twente, 2019.

[17] Tom Coenen. “Circular bridges and viaducts”. In: *Reproduction* (2019).

[18] IBM Cloud Education. *Monte Carlo simulation*. URL: https://www.ibm.com/in-en/cloud/learn/monte-carlo-simulation.

[19] Lucia Rigamonti and Eliana Mancini. “Life cycle assessment and circularity indicators”. In: *The International Journal of Life Cycle Assessment* (2021), pp. 1–6.

[20] Geoffrey Lonca et al. “Does material circularity rhyme with environmental efficiency? Case studies on used tires”. In: *Journal of Cleaner Production* 183 (2018), pp. 424–435.

[21] Benjamin Sanchez and Carl Haas. “A novel selective disassembly sequence planning method for adaptive reuse of buildings”. In: *Journal of Cleaner Production* 183 (2018), pp. 998–1010.

[22] Hoda Abuzied et al. “A review of advances in design for disassembly with active disassembly applications”. In: *Engineering Science and Technology, an International Journal* 23.3 (2020), pp. 618–624.

[23] *NTA 8085:2021 IFD construction of fixed bridges and viaducts*. NEN. Netherlands: NEN, 2021.

[24] Mark Alexander and Hans Beushausen. “Durability, service life prediction, and modelling for reinforced concrete structures–review and critique”. In: *Cement and Concrete Research* 122 (2019), pp. 17–29.

[25] *Guide Measuring circularity, Working agreements for circular construction Version 2.0*. CB’23. Netherlands: CB’23, 2020.

[26] Ellen MacArthur Foundation. “Circularity indicators: An approach to measuring circularity—Methodology”. In: *Isle of Wight* (2015).

[27] Tom BJ Coenen et al. “Development of a bridge circularity assessment framework to promote resource efficiency in infrastructure projects”. In: *Journal of Industrial Ecology* 25.2 (2021), pp. 288–304.

[28] Jaap Willem Boersma. *Development of a Concept Demountable Footing to Foundation (F2F) dowel connection for the application of Multiple Life cycles*. 2021.

[29] Pieter Robert Beurskens. “The development of an evaluation method to support circular building design”. English. PhD thesis. Netherlands: University of Twente, Sept. 2021. ISBN: 978-90-365-5204-2. DOI: 10.3990/1.9789036552042.

[30] Shamsad Ahmad. “Reinforcement corrosion in concrete structures, its monitoring and service life prediction—-a review”. In: *Cement and concrete composites* 25.4-5 (2003), pp. 459–471.

[31] RB Holland, KE Kurtis, and LF Kahn. “Effect of different concrete materials on the corrosion of the embedded reinforcing steel”. In: *Corrosion of Steel in Concrete Structures* (2016), pp. 131–147.

[32] *EN 1992-1-1 Eurocode 2: Design of concrete structures - Part 1-1: General ruels and rules for buildings*. EN. Brussels: CEN, 2005.

[33] *NEN-EN 206+NEN 8005: Concrete - Specification, performance, production and conformity + Dutch supplement to NEN-EN 206+A1*. Marnixstraat 17, B-1000 Brussel: CEN, 2017.

[34] C Gehlen et al. “fib Bulletin 76: Benchmarking of Deemed-to-Satisfy Provisions in Standards–Durability of Reinforced Concrete Structures Exposed to Chlorides”. In: (2015).

[35] Bernard Enright and Eugene J O’Brien. “Monte Carlo simulation of extreme traffic loading on short and medium span bridges”. In: *Structure and Infrastructure Engineering* 9.12 (2013), pp. 1267–1282.

[36] Cathal Leahy, Eugene OBrien, and Alan O’Connor. “The effect of traffic growth on characteristic bridge load effects”. In: *Transportation Research Procedia* 14 (2016), pp. 3990–3999.

[37] JL Smith, Yash Paul Virmani, et al. *Materials and methods for corrosion control of reinforced and prestressed concrete structures in new construction*. Tech. rep. United States. Federal Highway Administration, 2000.

[38] AJM Siemes and C Edvardsen. “Duracrete: Service life design for concrete structures”. In: *Durability of Building Materials and Components 8. Service Life and Asset Management. Proceedings of the 8th International Conference on Durability of Building Materials and Components, 8dbmc, Volume 2: Durability of Building Assemblies and Methods of Service Life Prediction*. NRC Research Press. 1999, p. 1343.

[39] Martina Šomodıková, Alfred Strauss, and Ivan Zambon. “fib models for modeling of chloride ion ingress and concrete carbonation: Levels of assessment of input parameters”. In: *Structural Concrete* 21.4 (2020), pp. 1377–1384.

[40] K van Breugel, RB Polder, and MR de Rooij. “Long-term performance of marine structures in the Netherlands-validation of predictive models for chloride ingress”. In: (2017).

[41] Consolis Spanbeton. *Box girder solutions*. URL: https://www.spanbeton.nl/content/files/Files/Kennisportaal/Kokerbalk/ENG__WEBSITE__SKK.pdf.

[42] *Orthotropic properties of plates*. URL: https://kc.scia.net/FAQ/Content/FAQ/Modelling/Orthotropic%20behavior%20of%20plates/Orthotropic%20behavior%20of%20plates.htm.

[43] Guido Hogendoorn. *Transverse load-spread of a voided bridge deck: Comparison between a grillage model and an orthotropic plate model*. 2021.

[44] *NEN-EN 1990+A1+A1/C2:2019/NB:2019 Nationale bijlage bij NEN-EN 1990+A1:2006+A1:2006/C2:2019*. NEN. Netherlands: NEN, 2019.

[45] *EN 1991-1-1 Eurocode 1: Actions on structures - Part 1-1: General actions-Densities, self weight, imposed loads for buildings*. EN. Brussels: CEN, 2002.

[46] *EN 1991-2 Eurocode 1: Actions on structures - Part 2: Traffic loads on bridges*. EN. Brussels: CEN, 2003.

[47] *ROK 1.4 Bijlage A RTD1007-1:2013*. Rijkswaterstaat. Netherlands: Rijkswaterstaat, 2013.

[48] Mark Hurt and Steven D. Schrock. "Chapter 2 - Bridge Elements and Materials". In: *Highway Bridge Maintenance Planning and Scheduling*. Ed. by Mark Hurt and Steven D. Schrock. Butterworth-Heinemann, 2016, pp. 31–98. ISBN: 978-0-12-802069-2. DOI: https://doi.org/10.1016/B978-0-12-802069-2.00002-7. URL: https://www.sciencedirect.com/science/article/pii/B9780128020692000027.

[49] Haitsma Beton BV. *A9 bridge over the Gaasp*. URL: https://www.haitsma.nl/projecten/amsterdam-a9-brug-over-de-gaasp/.

[50] L van Iperen. "Flexible floor systems: The effectiveness of flexibility measures in improving the circularity of building components". In: *Delft Univ. Technol. Delft* (2021).

[51] Bangweon Song and Seokjoong Kang. "A Method of Assigning Weights Using a Ranking and Nonhierarchy Comparison." In: *Advances in Decision Sciences* (2016).

[52] Kamal M Al-Subhi Al-Harbi. "Application of the AHP in project management". In: *International journal of project management* 19.1 (2001), pp. 19–27.

[53] Yong Bai and Wei-Liang Jin. "Chapter 33 - Random Variables and Uncertainty Analysis". In: *Marine Structural Design (Second Edition)*. Ed. by Yong Bai and Wei-Liang Jin. Second Edition. Oxford: Butterworth-Heinemann, 2016, pp. 615–625. ISBN: 978-0-08-099997-5. DOI: https://doi.org/10.1016/B978-0-08-099997-5.00033-2. URL: https://www.sciencedirect.com/science/article/pii/B9780080999975000332.

A

PRESTRESS CALCULATION

This appendix shows the steps for the calculation of the required prestressing of the box-beam girder.

A

A.1. CALCULATION OF REQUIRED PRESTRESS

The outputs from the analysis were used to determine the maximum SLS bending moment.
Various SLS load combinations were generated as per EN 1990 [32], namely characteristic, quasi-permanent, and frequent. The relevant load and ψ factors can be found in EN1990 Annex A2 table A2.6, and the load factors for unfavorable actions were taken to be on the conservative side.
The outputs from the analysis were used to determine the maximum SLS bending moment. To finalize the final prestress, it was calculated at t = 0 and at t = ∞.

$$\frac{-P_o}{A_c} + \frac{M_{prestress}}{W_t} - \frac{M_{self\,weight}}{W_t} \leq 0 \; at \; (t = 0, top fiber) \tag{A.1}$$

$$\frac{-P_{m,\infty}}{A_c} - \frac{M_{prestress}}{W_b} + \frac{M_{self\,weight+SLS}}{W_b} \leq 0 \; at \; (t = \infty) \tag{A.2}$$

In equation A.1 the initial prestress force is calculated by keeping the stress at top fiber less than or equal to 0 and in equation A.2, the principle is the same, the only difference being that maximum moment coming from SLS combinations is added and therefore stress at bottom fiber is checked. $P_{m,\infty}$ is taken as $0.8 \times P_{m,0}$ meaning an assumption of 20 % prestress losses. On solving equations A.1 and A.2 for $P_{m,0}$ we get:

$$10700.66kN \leq P_{m,0} \leq 25222.38kN \tag{A.3}$$

The choice is made to use Y1860S7 strands for prestressing where each strand has an area of approximately 150 mm^2. As per EN 1992, clause 5.10.3, the stress in the strand immediately after tensioning ($\sigma_{pm,0}$) should be equal to $min(0.75 * f_{pk}, 0.85 * f_{p0.1k})$ = 1395 MPa.
Knowing the stress and force in the steel the area A_p of steel required can be calculated as shown below:

$$A_p = \frac{P_{m,0}}{\sigma_{pm,0}} = 7670.7mm^2 \tag{A.4}$$

Total number of strands required:

$$n_{strands} = \frac{10700.66}{150} \simeq 61 \; strands \tag{A.5}$$

The actual area of steel used then becomes $52 \times 150 = 7800mm^2$ Applied prestressing force becomes 10881.75 kN.
Assuming a 20 % loss in prestress no cracking can still be seen during the Serviceability Limit State.

B

BENDING MOMENT AT ULS VERIFICATION

This appendix deals with the verification of bending moment at ULS. The Excel spreadsheet that was used is shown here. The procedure follows that followed in the course Prestressed Concrete (CIE4160).

The graph referred to in step 4 of the calculation refers to figure B.1. The spreadsheets on the following pages show the calculation done in order to determine the bending moment capacity at Ultimate Limit State.

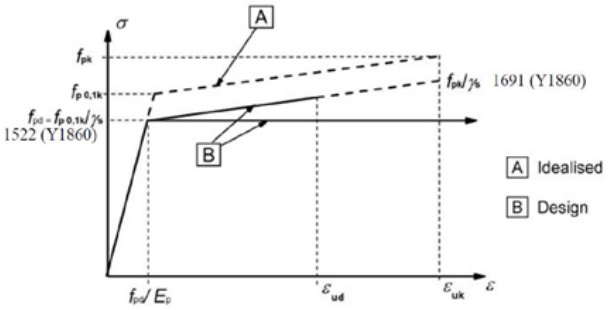

Figure B.1: Important prestress points

Concrete properties		
Area of concrete [mm^2]	Ac	1015000
Eccentricity of prestressing and reinforcing steel [mm]	ep = es	670
(relative to neutral axis)		
Effective depth [mm]	dp = ds	1422
Concrete C60/75		
Distance from centroid to top fibre [mm]	Zt	752
Distance from centroid to bottom fibre [mm]	Zcb	748
Concrete modulus of elasticity [Mpa]	Ec	39100
Design compressive strength	fcd	40
Thickness bottom flange [mm]	tb	157
Height of box-beam [mm]	h	1500
Thickness top flange [mm]	tf	170
Prestressing steel properties (Y1860 S7 - seven strands)		
Total area [mm^2]	Ap	7800
Prestressing steel modulus of elasticity [Mpa]	Ep	195000
Working prestress [Mpa] - assuming 20% losses	σ_{pm0}	1116
Stress in steel at failure [Mpa] (assumed)	f_{pd}	1522
Reinforcing steel properties (B500)		
Reinforcing steel modulus of elasticity [Mpa]	Es	200000
Total area of steel [mm2]	As	2430
Step 1 - Estimation of concrete compression zone (Xu) [mm]	Xu	616.00
Nc - P_{m0} = As*fyd + Ap*(f_{pd}-σ_{pm0})		
Force to balance from tensile zone [N]	As*fyd + Ap*fpd	1.3E+07
Nc = α*b*fcd*Xu (assuming rectangular cross-section)		
Surface factor for C60/75 (α)	α	0.67
Width of box-beam [mm]	b	1420
Step 2 - Check height of compression zone (EN 1992 cl 5.5)		
Ratio of redistributed moment to elastic bending moment	δ	1
No redistribution is assumed		
Xu/d < 1-7f/(ε_{cu}*10^6+7f)	0.43 < 0.44	
Step 3 - Strains in reinforcing and prestressing steel (for Xu)		
ε_s =	εcu(ds/Xu - 1)	0.00379
Δεp	εcu(dp/Xu - 1)	0.00379
εp =	Δεp + σ_{pm0}/E_p	9.52E-03

B

Step 4 - Actual prestress and force in steel		
Asuumed steel stress at failure [Mpa]	f_{pd}	1522
Steel strain (prestressing steel)	$\varepsilon p = \Delta\varepsilon p + \sigma_{pc\infty}/E_p$	9.52E-03
Using graph, actual stress at failure (linear interpolation) [Mpa]		1532.61
Force in reinforcing steel [kN]	Ns = As * fyd	1057.05
Increase of force in prestressing steel [kN]	ΔNp = Ap * (fpd,actual - σpc∞)	3249.58
Total steel force [kN]	N = Ns+ΔNp	4306.63
Working prestress force [kN]	Pm,∞ = Ap * σpc∞	8704.8
Total force to be balanced by concrete	**N+Pm,∞**	13011.43
Step 5 - Stress and strains in concrete section (upto Xu)		
Total concrete compressive force [kN]	**Nc**	13012.163
Flange force [kN]	b * fcd * tf	10192.1103
Remaining height with constant stress [kN]	(0.348*Xu -tf)*2*tw*fcd	1131.88909
Force from triangular stress distribution [kN]	0.5*fcd*0.6528Xu*2*tw	1688.16354

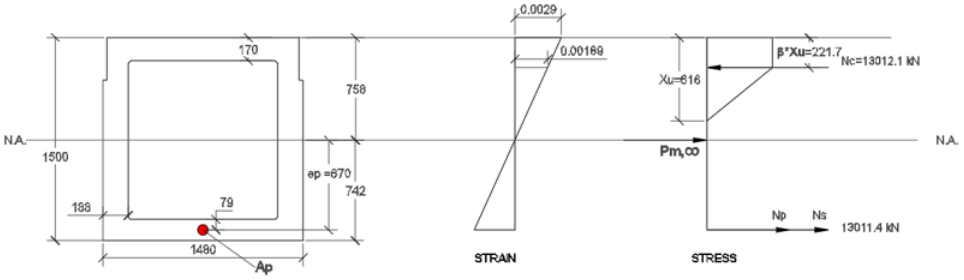

MRd calculated by taking moment equilibrium about centroid [kNm]		10638.2413
Considering box beam as rectangle [kNm] (+)	α*b*Xu*fcd*(Zt-β*Xu)	1.243E+10
Part to subtract (hollow part of box-beam) - 2 parts- [kNm] (-)	A*lever arm (A) + B*lever arm (B)	4677352721
Constant width stress part- A [kN]	0.348*Xu*fcd*(b-2*tw)	1959.29088
Triangular area stress part - B [kN]	0.5*(Xu-0.348Xu)*(b-2*tw)*σflange	8868.03456
lever arm A (about centroid) [mm]	Zt-0.348*Xu + (0.348Xu-tf)/2	559.816
lever arm B (about centroid) [mm]	Zt - 0.348Xu - (Xu-0.348*Xu)/3	403.754667
Tensile force from steel [kN] * eccentricity [mm] (+)	{σ,pu (actual) - σpc∞}*ep + fyd*As*ep	2885444910
MEd (SCIA)		11739.8
M_{Ed} (SCIA) -Mp,∞[kNm]		5907.584
Mp,∞		5832.216
UC = M_{Ed}/M_{Rd}		0.56

< 1

C

SHEAR REINFORCEMENT CALCULATION

This appendix will show the calculation of the required shear reinforcement in the webs of the box beams.

The steps followed to reach the reinforcement for stirrup design at the critical cross-section near the support are described:

1. For members with vertical shear reinforcement, $V_{Rd,max}$ is calculated

2. It is checked that V_{Ed} is less than $V_{Rd,max}$

3. The design shear force is used to find the required area of stirrups along with the spacing (A_{sw}/s)

4. Minimum torsion reinforcement is calculated for the top and bottom flanges

		Massive	Hollow	Hollow	
Stirrups for webs		1,5	2,01	11,25	
V_{ed}		1314,43	1314,43	587,1	[kN]
$V_{Rd,max}$	αcw*bw*0.9d*fcd*v1/(cotθ+tanθ)	13199,7	13199,6	3353,4	[kN]
$V_{Ed} < V_{Rd,max}$		Yes	Yes	Yes	
Asw/s	V_{Ed}/(0.9d*fywd*cotθ)	0,95393	0,95393	0,42608	[mm²/mm]
T_{Ed}		194,9	194,9	62,97	[kNm]
$T_{Rd,max}$	2*v*αcw*fcd*Ak*te*sinθ*cosθ	5002,97	2188,21	2188,21	[kNm]
$V_{Ed}/V_{Rd,max} + T_{Ed}/T_{Rd,max} <1$		0,13854	0,18865	0,20385	
		Yes	**Yes**	**Yes**	
$V_{Ed,i} = (T_{Ed}*zi)/2*Ak$					
As/s_w=	$\rho_{w,min}$*bw*sinα	1,83372	0,46586	0,46586	
As/s_w=	$V_{Ed,i}$ /(fywd*zi*cotθ)	0,19	0,19	0,14	[mm²/mm]
As/s_w total for both webs		1,83372	**1,41979**	**0,89194**	[mm²/mm]
Stirrups for flanges					
As/s_w (top flange)			**0,21**	**0,21**	[mm²/mm]
As/s_w (top flange, min)	$\rho_{w,min}$*bw*sinα		0,21	0,21	[mm²/mm]
VEd,flange,bottom	$V_{Ed,i} = (T_{Ed}*zi)/2*Ak$				
As/s_w (bottom flange)			**0,194**	**0,194**	[mm²/mm]
As/s_w (bottom flange, mi	$\rho_{w,min}$*bw*sinα		0,194	0,194	[mm²/mm]
Longitudinal reinforcement required					
∑Asl =	(TEd * cotθ* uk)/(2*Ak*fyd)	1985,15	1688,07	545,395	[mm²]
∑Asl, flange(top/bottom)	∑Asl*z1/uk	491,766	414,872	134,04	[mm²]
∑Asl, webs (left/right)=	∑Asl*z2/uk	500,647	429,161	138,657	[mm²]

αcw		1,06	1,1	1,1	
b		1480	1480	1480	[mm]
h		1500	1500	1500	[mm]
bw,webs		1480	376	376	[mm]
bw,flanges		1500	327	327	[mm]
thickness top flange			170	170	[mm]
thickness bottom flange			157	157	[mm]
thickness left web			188	188	[mm]
thickness right web			188	188	[mm]
te,flange		372,5	157	157	[mm]
te,webs		372,5	188	188	[mm^2]
	A	2220000	2220000	2220000	[mm]
	u	5960	5960	5960	
	A/u	372,5	372,5	372,5	
te,web,left				188	[mm]
te,web,right				188	[mm]
te,top flange				170	[mm]
te,bottom flange				157	[mm]
Ak		1248751	1726758	1726758	[mm^2]
uk		4470,8	5257	5257	[mm]
	z1	1107,52	1292	1292	[mm]
	z2	1127,52	1336,5	1336,5	[mm]
fck		60	60	60	[Mpa]
fcd		40	40	40	[Mpa]
fyk		500	500	500	[Mpa]
fyd		435	435	435	[Mpa]
fywd		435	435	435	[Mpa]
v = 0,6*(1-fck/250)		0,456	0,456	0,456	
θ		22°	22°	22°	
α		90°	90°	90°	
ρw,min = 0,08*√(fck)/fyk		0,00124	0,00124	0,00124	

D

STRUT AND TIE MODELS

This appendix shows the strut and tie models used to calculate the split tensile reinforcement at the supports.

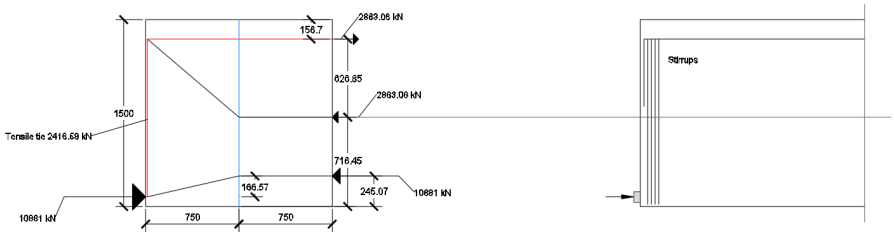

Figure D.1: Strut and tie model for the vertical orientation of the beam

The amount of steel required can be calculated by assuming a steel stress of 250 MPa in the reinforcement and dividing the force in the tie (see figure D.1) with this stress. This gives a required steel value of 9666 mm^2.

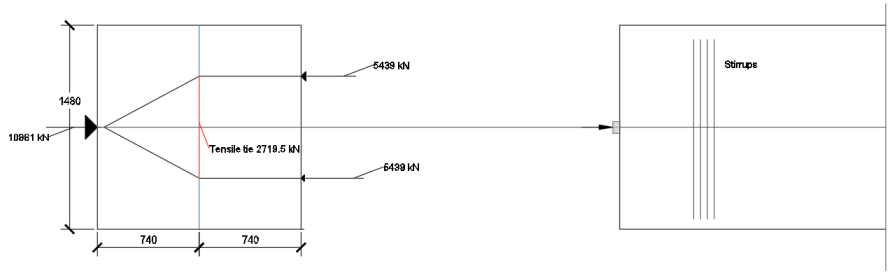

Figure D.2: Strut and tie model for the horizontal orientation of the beam

By similarly assuming a steel stress of 250 MPa, and dividing the force in the tie (see figure D.2) by this value, the area of steel required is 10878 mm^2.
The assumption of steel stress of 250 MPa is a conservative one since if B500 grade steel were to be used the design yield force would be 435 MPa.

E

FATIGUE VERIFICATION

E.1. FATIGUE VERIFICATION 100 YEARS

Assuming traffic category 2 [46] and 1 slow lane, the fatigue verification is shown.

Material after 28 days			
fck [Mpa]	60		
fcd [Mpa]	44,44	γc	1,35
fcd,fat [Mpa]	33,78	k1	1
Ec,fat [Mpa]	19302	βcc(t0)	1

If the stresses at the bottom are ≤ fctm, cross section is uncracked

Mfat= 1390,28 [kNm] Number of cycles 5,00E+07

Stress check			Bottom fibre		Top fibre
			(L/2)		(L/2)
	X=		**22,5**		**22,5**
	σ,Pm,∞		-23,38		6,30
	σ,c,self		18,22		-18,31
	σ,c,dead		0,27		-0,27
	σ,c,min		-4,89		-12,28
	σ,c,fat		3,53		-3,55
	σ,c,max		-1,37		-15,82
R=	σcmin/σ,cmax=				0,78

Eq 6,106 EN1992-2
{1-(Log(N)*(1-R)^0,5/14)}*fcd,fat -24,983638 Mpa
6,106 rearranged to find σ,c,max (permissab σ,c,max<-24,9 satisfied

Prestressing steel Concrete is uncracked because the stress at bottom fibre is: -1,37

Δσp= (σcmax/Ecfat)*Ep= -13,796742

Using EC2 6,8:	Δσseu ≤ ΔσRsk(n)	
	σ,smax - σ,smin ≤ Δσs/γm	γm=1,1
	Where Δσs (106)=	185 Mpa
	k2 = 9 (EC2 table 6,4N)	
	13,8 ≤ 108,89	

E.2. FATIGUE VERIFICATION 200 YEARS

Assuming traffic category 1 [46] and 2 slow lanes, the fatigue verification is shown.

Material after 28 days			
fck [Mpa]	60		
fcd [Mpa]	44,44	γc	1,35
fcd,fat [Mpa]	33,78	k1	1
Ec,fat [Mpa]	19302	βcc(t0)	1

If the stresses at the bottom are ≤ fctm, cross section is uncracked

Mfat= 1390,28 [kNm] Number of cycles 8,00E+08 Assume 2 slow lanes; Assume traffic category 1

Stress check			Bottom fibre		Top fibre
			(L/2)		(L/2)
	X=		**22,5**		**22,5**
	σ,Pm,∞		-30,15		8,48
	σ,c,self		21,95		-22,06
	σ,c,dead		0,27		-0,27
	σ,c,min		-7,94		-13,85
	σ,c,fat		3,53		-3,55
	σ,c,max		-4,41		-17,40
R=	σcmin/σ,cmax=				0,80

Eq 6,106 EN1992-2
{1-(Log(N)*(1-R)^0,5/14)}*fcd,fat -24,08 Mpa
Eq 6,106 rearranged to find σ,c,max (permissable) σ,c,max<-24,08 satisfied

Prestressing steel Concrete is uncracked because the stress at bottom fibre is: -4,41

Δσp= (σcmax/Ecfat)*Ep= 44,52

Using EC2 6,8:	Δσseu ≤ ΔσRsk(n)	
	σ,smax - σ,smin ≤ Δσs/γm	γm=1,1
	Where Δσs (10^6)=	185 Mpa
	k2 = 9 (EC2 table 6,4N)	
	44,52 ≤	80,02 (Allowable Δσ)

F

LOAD COMBINATIONS

The load combinations for the ULS and SLS combinations are explained in this appendix.

For this thesis, only those loads which are governing need to be used to make the load combinations.

F.1. LOAD FACTORS AND COMBINATION FACTORS

The load factors (γ) for permanent loads (G), prestressing (P), and variable loads (Q) differ with different combinations. The load factors found in NEN-EN 1990+A1+A1/C2/NB:2019 (Table NB16 A2.4(B)) were used to determine the coefficients for the load combinations. Similarly the combination factors (ψ) can also be found in NEN-EN 1990+A1+A1/C2/NB:2019 (Table NB19).

Belasting	Symbool		ψ_0	ψ_1	ψ_2
Verkeersbelastingen (zie NEN-EN 1991-2+C1:2015, tabel 4.4)	gr1a (LM1 + voetgangers- of fietspad-belastingen)	TS	0,8	0,8	0,4
		UDL		0,8	
		Horizontale belasting		0,8	
		Voetgangers- + fietspad-belastingen		0,8 [d]	
	gr1b (enkele as)		0	0,8 [b]	0
	gr2 (horizontale krachten dominant)		0,8	0,8 [c]	0
	gr3 (voetgangersbelastingen)		0	0,8 [b]	0
	gr4 (LM4 – belasting door een menigte)		0	0,8 [b]	0
	gr5 (LM3 – speciale voertuigen)	TS	0	0,8 [b]	0
		UDL		0,8 [b]	
		Horizontale belastingen		0,8 [b]	
		Speciaal voertuig		1,0 [b]	
Windkrachten	F_{Wk}	blijvende ontwerpsituatie	0,3	0,6 [b]	0
		Uitvoering	0,8	0	0
	F_W*		1,0	0	–
Thermische belastingen	T_k		0,3	0,8 [b]	0,3 [a]
Sneeuwbelastingen	$Q_{Sn,k}$	blijvende ontwerpsituatie	0	0	0
		Uitvoering	0,6	0	0
Belastingen tijdens de bouw	Q_c		1,0	0	1,0

[a] In de uiterste grenstoestand mag voor ψ_2 voor thermische belasting de waarde 0 zijn aangehouden.

[b] Voor aanrijding op of onder de brug en aanvaring is $\psi_1 = 0$.

[c] Voor scheurvomingsberekeningen van beton zijn de verschillende waarden van ψ_1 gelijk aan de waarden behorend bij gr1a (zie voor de waarden van ψ Tabel NB.19).

[d] Voor scheurvormingsberekeningen van beton moet $\psi_1 = 0$,4 zijn aangehouden.

OPMERKING Groepen verkeersbelastingen hoeven niet met elkaar te zijn gecombineerd.

Figure F.1: Combination factors for slow traffic. Source: [44]

After multiplication of the relevant combination factors with load factors the coefficients for the loads are obtained as seen in figure F.3 and F.4.

Belasting	Belastingscombinaties												
	gr1a	gr1b	gr2	gr3	gr4	gr5	W [b]		T [b]		S	A1 [a,b]	
TS	1	0	0,8	0	0	0,8	0,8	0,64	0,8	0,64	0	0,8	0,64
UDL	1	0	0,8	0	0	0,8	0,8	0,64	0,8	0,64	0	0,8	0,64
Enkele as	0	1	0	0	0	0	0	0	0	0	0	0	0
Horizontale belasting	0,8	0	1	0	0	0,8	0,64	0,8	0,64	0,8	0	0,64	0,8
Voetpaden	0,4	0	0,4	1	1	0	0,32	0,32	0,32	0,32	0	0,32	0,32
Mensenmenigte	0	0	0	0	1	0	0	0	0	0	0	0	0
Bijzondere voertuigen	0	0	0	0	0	1	0	0	0	0	0	0	0
Wind [c] F_{wk}	0,3	0	0,3	0	0	0,3	1	1	0,3	0,3	0	0	0
F^*_w	1	0	1	0	0	1	0	0	0	0	0	0	0
Temperatuur	0,3	0	0,3	0	0,3	0,3	0,3	0,3	1	1	0	0	0
Sneeuw	0	0	0	0	0	0	0	0	0,	0	1	0	0
Impact op of onder de brug	0	0	0	0	0	0	0	0	0	0	0	1	1
Aardbevingsbelasting	0	0	0	0	0	0	0	0	0	0	0	0	0

[a] A1 = aanrijding op of onder de brug en aanvaring.

[b] Bij deze combinaties is in eerste kolom gr1a × Ψ_0 en de tweede kolom gr2 × Ψ_0 .Voor de definitie van de groep verkeersbelasting gr1a en gr2 zie NEN-EN 1991-2+C1.

[c] Waar verkeersbelasting op (delen van) de brug aanwezig is, mag zijn gerekend met F^*_w in plaats van F_{wk}.

Figure F.2: Combination factors for STR load combinations. Source: [44]

	EQU (Set A)		STR/GEO (Set B) 6.10a		STR/GEO (Set B) 6.10b	
Load	gr1a	gr2	gr1a	gr2	gr1a	gr2
Permanent G	1.05	1.05	1.35	1.35	1.25	1.25
Prestressing	1	1	1	1	1	1
LM1 TS	1.35	1.2	1.08	0.864	1.35	1.08
LM1-UDL	1.35	1.2	1.08	0.864	1.35	1.08
Horizontal forces	1.2	1.35	0.864	1.08	1.08	1.35
Temperature loads	0.45	0.45	0.45	0.45	0.45	0.45

Figure F.3: ULS load coefficients

	Eq. 6.14b		Eq. 6.15b		Eq. 6.16b	
Load	gr1a	gr2	gr1a	gr2	gr1a	gr2
Permanent G	1	1	1	1	1	1
Prestressing	1	1	1	1	1	1
LM1 TS	1	0.8	0.8	0.4	0.4	0.4
LM1-UDL	1	0.8	0.8	0.4	0.4	0.4
Horizontal forces	0.8	1	0.4	0.8	0.4	0.4
Temperature loads	0.3	0.3	0.3	0.3	0.3	0.3

Figure F.4: SLS load coefficients

G

VERIFICATION BY HAND CALCULATION

Hand calculation to check bending at midspan

This part of the document contains the simple hand check that was done to verify that the outputs from obtained from SCIA Engineer 21.0 The output coming from bending and shear are checked at the critical cross-sections. For the check, only self-weight, dead loads, and Load Model 1 are checked to get an idea of whether the values are comparable.

The tandem systems should give the maximum moment as seen in figure 1 when placed at the midspan. The corresponding moment arising from the tandem system is converted into an equivalent UDL (kN/m) load. Using the effective width, the load acting per girder is found, although this gives just an approximation and not an accurate value. The value seen at ULS for bending as per SCIA was 7932.29 * 1.48 = 11739.8 kNm per girder (ULS STR/GEO 6.10 a edge). It is expected that the results from the hand calculation will be much greater (since it is an approximation). The lane arrangement chosen to verify the model is seen in figure 2.

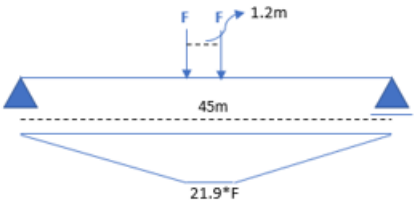

Figure 1- Maximum bending moment at mid-span due to tandem system loads

$$M_{max} = \frac{q_{eq} * L^2}{8} = \frac{q_{eq} * 45^2}{8}$$

$$21.9 * F = \frac{q_{eq} * 45^2}{8}$$

$$q_{eq} = \frac{8 * 21.9 * F}{45^2} = 0.0865 * F$$

Lane arrangement chosen (edge)

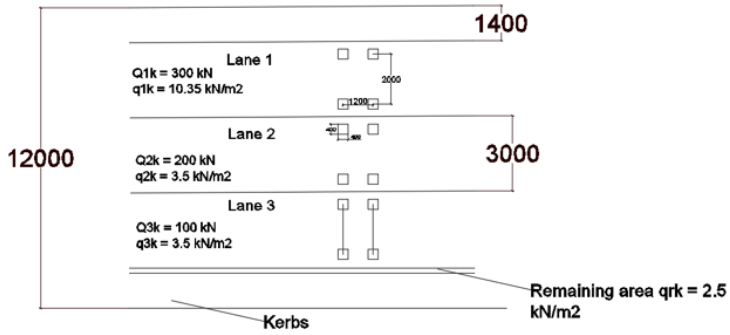

Figure 2- Lane arrangement (edge)

- Lane 1 has a UDL of 10.35 kN/m2 and TS loads of 300 kN (green) each
- Lane 2 has a UDL of 3.5 kN/m2 and TS loads of 200 kN (blue) each
- Lane 3 has a UDL of 3.5 kN/m2 and TS loads of 100 kN (black) each

By considering the height from the centroidal axis of the beam to the top fiber of the asphalt layer equal to about 1 m and for a 45° load distribution the effective can be found

Effective width for 1 Tandem system (beff,1)

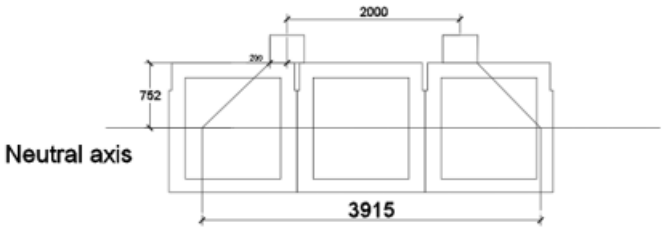

Effective width for 2 Tandem system (beff,2)

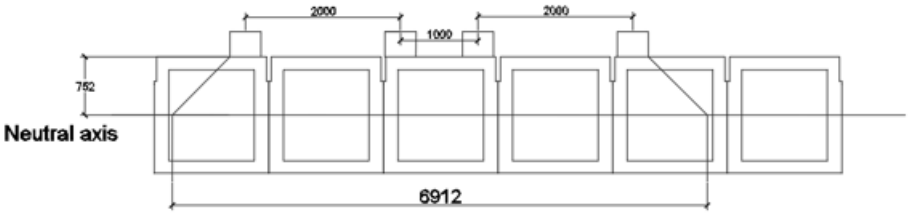

Effective width for 3 Tandem system (beff,3)

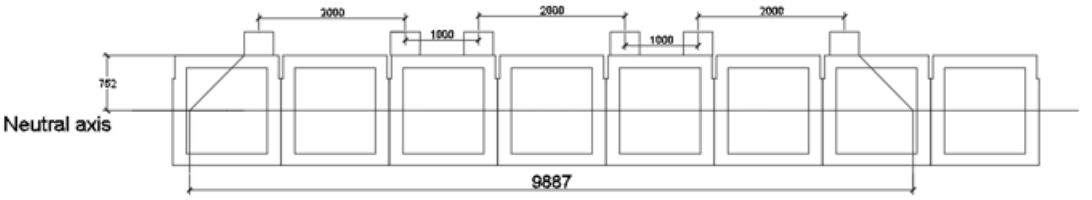

The arrangement of the TS loads (LM1) can be split into corresponding TS loads of 100 kN each.

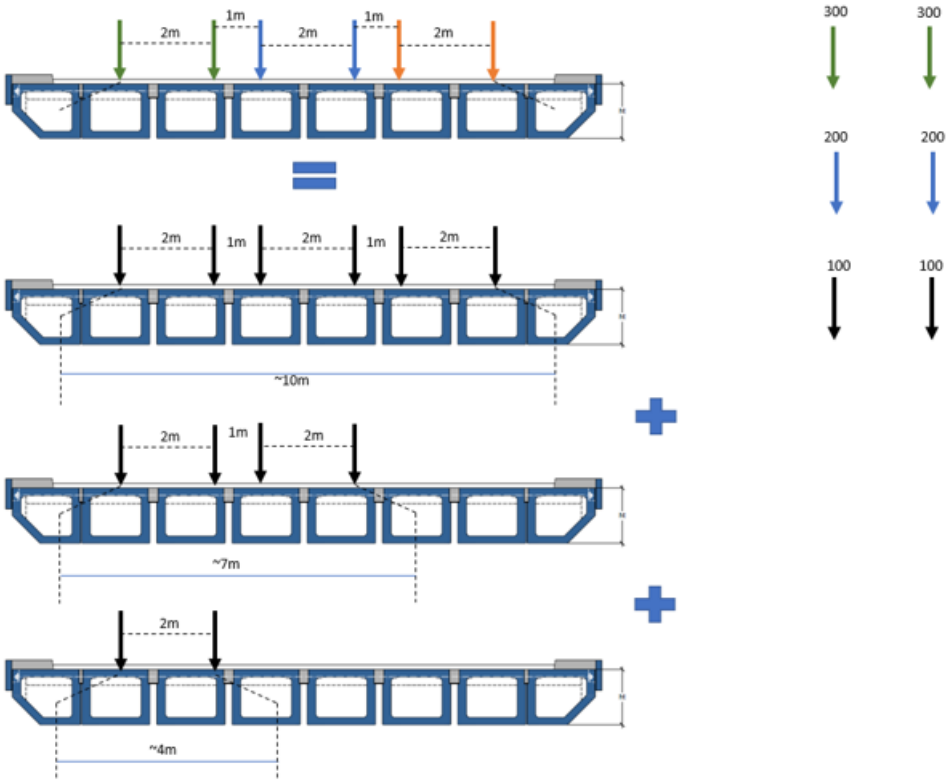

Figure 3- Splitting of the tandem loads on the deck

(1) The TS can be converted into corresponding UDL loads acting on each girder

$$\frac{0.0865 * Qik * 1.5\ (width\ of\ girder)}{b_{eff}}$$

$$\frac{0.0865 * 300 * 1.5}{10} + \frac{0.0865 * 200 * 1.5}{7} + \frac{0.0865 * 100 * 1.5}{4}$$

$$= 10.84 \frac{kN}{m} per\ girder$$

G

(2) Similarily the loads arising from the UDL per lane can be converted into corresponding loads per girder. The same 45° load distribution was considered for the calculation of the effective width of the UDL's acting on the deck.

$$\frac{qik * width\ (m) * 1.5\ (width\ of\ girder)}{b_{eff,UDL}}$$

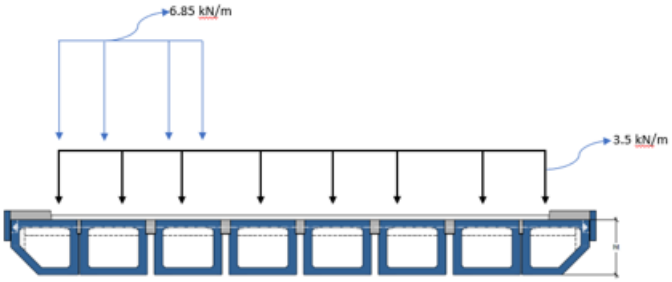

$$\frac{3.5 * 9.2 * 1.5}{10.704} + \frac{6.85 * 3 * 1.5}{4.504} = 11.35 \frac{kN}{m} per\ girder$$

(3) Asphalt on the deck was similarly converted into a UDL for the girder

Density of asphalt = 23 kN/m^3

Thickness of asphalt layer = 140 mm = 0.14m

Area load (asphalt) = 23 * 0.14 = 3.22 kN/m^2

Corresponding line load (multiply with width of girder) = 3.22 * 1.48 = 4.76 kN/m

(4) Self weight of SKK 1500 = 28.1 kN/m (taken from Spanbeton catalogue)

Hand calculations done to identify the load per girder:

1) Due to TS loads – 10.84 kN/m per girder

2) Due to UDL - 11.35 kN/m per girder

3) Due to asphalt – 4.76 kN/m

4) Self weight (SKK1500)- 28.1 kN/m

$$M_g(self\ weight) = \frac{(28.1) * 45^2}{8} = 7112.81\ kNm$$

$$M_{LL} = \frac{(10.84 + 11.35) * 45^2}{8} = 5616.8\ kNm$$

$$M_{asphalt} = \frac{(4.76) * 45^2}{8} = 1204.87\ kNm$$

$$\boldsymbol{M_{Total} = 13934.47\ kNm}$$

$$M_{ULS,Scia} = 11739.8\ kNm$$

This was an approximation method used and hence gives a much larger value that would be obtained using a finite element software. The values are comparable and hence this serves as a check for bending output obtained.

Check for shear

The shear output at ULS (SCIA) gave a value of 1314.68 kN near the supports.

Using the loads per girder for self-weight, asphalt, TS, and the UDL's from Load Model 1

The equation to calculate shear for a simply supported beam can be used

$$Vtotal = \frac{qL}{2} = \frac{q_{LL} + q_G + q_{asphalt}}{2} = 1238.63\ kN$$

Once again, the values are comparable. Hence the shear value obtained through SCIA is validated.

H

ORTHOTROPY

This chapter will show the calculations of the orthotropy parameters needed such that the plate imitates the behavior of the box beams. The calculations were carried out using Excel.

Strength class (prefab girder)	C60/75		
Strength class (longitudinal joints)	C30/37		
E1[N/mm2] (for C60/75)	39100	G1 [N/mm2]	16291.7
E2[N/mm2] (for C30/37)	32837	G2 [N/mm2]	13682.1
v (Poisson ratio)	0.2		
$\gamma_{concrete}$ [kN/m3]	25		

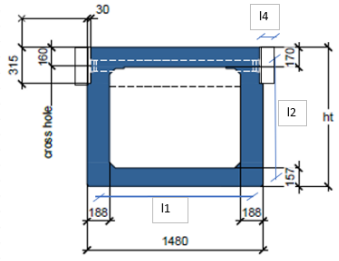

SKK1500 dimensions

Height [mm]		1500
Width [mm]		1480
Thickness top flange [mm]	t1	170
Thickness bottom flange [mm]	t3	157
Thickness webs [mm]	t2	188
Longitudinal joint Height [mm]	t4	315
center-to-center between flanges [mm]	l2	1336.5
center to-center between beams [mm]	b	1500
Longitudinal joint width [mm]	l4	104
center-to-center distance between webs [mm]	l1	1292

Longitudinal bending stiffness

	Area [mm2]	Z[mm] - from bottom fibre	I_x [mm4]
SKK1500	1.02E+06	748	2.95E+11
Extra (C30/37)	6.30E+03	1.34E+03	5.42E+08
Composite	1.02E+06	760	3.03E+11

D11 =	$E1*I_x/b$	7898.2 MNm

Transverse bending stiffness

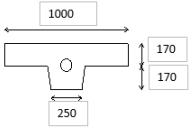

Data top flange		
Width [mm]	bflens =	1000
Width rib, onderzijde [mm]	brib =	250
Height rib [mm]	trib =	170
Campher rib [mm]		25
	zbf [mm]	218.8888889
	EI1 [Nmm2]	60585250880
	EI2 [Nmm2]	10825278133
	EI3 [Nmm2]	6304700679
	EI4 [Nmm2]	85529097281

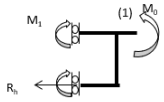

Unity moment M0 [kNm]	1000
α = (2*EI1*l1)/6*(EI2*l1)	1.929803287
β = 2+(3EI2*l1)/(EI3*l2)	6.979541955
M1	781.8076601
M2 = Mo/(2*α-α/β+1)	218.1923399
M3	31.26169902
φ0	9.55211E-06
φ1	8.33615E-06
φ2	3.20317E-06

D22 =	**(M0 x bw) / (2 x φ0) =**	**78.5**	**[MNm]**
D12 =	**v*D22**	**15.7**	**[MNm]**

Torsional stiffness

Creduction=	0.6	Calculations are made with a 40% reduction in the torsional stiffness due to cracking

Box profile

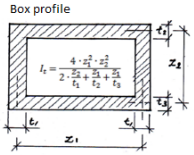

	4*Ak2 / (l1/t1 + 2 x (l2/t2) + l3/t3) =	3.96932E+11	Torsional moment of box-beam
	Ak [mm2] =	1726758	
1/3*t4^3*l4=	(cast-insitu part on both sides of box beam)	2167074000	Additional torsional moment of cast-insitu pa
	$I_{T,total}$ [mm4]	3.99099E+11	

where z1 = l1, z2 = l2

Kxy=	G1*I_T,total/b	4.33466E+12	4334.660959 MNm
Kyx=	G2*t^3/6	71274247734	71.27424773 MNm

D33 =	**$C_{reduction}$*(Kxy + Kyx) / 4**	**660.9 [MN/m]**

Shear bending stiffness

G1	E1 / (2 (1 + v))=	16291.7
G2	E2 / (2 (1 + v))=	13682.1

D44 =	**(5/6*G1*t2*2*ht)/bctc**	**5104.7 [MN/m]**
D55 =	**5/6*G2*hjoint**	**3591.5 [MN/m]**

Membrane parameters

d11= (E1 * hfict) / (1 – v2)		27731.1 [MN/m]
hfict=	A_{tot}/b_{ctc}	680.9 [mm]
d22 = (E2 * h2) / (1 – v2)		10774.6 [MN/m]
d12 = v*d22		2154.9 [MN/m]
d33		7434.1 [MN/m]
G12= √(E1 * E2) / (2 (1 + v)) [N/mm2]		14930.0 [Mpa]
$h_{gem} = h_{fct} + h_{long.jt.}$ [mm]		497.9 [mm]

I

DEMOUNTABILITY SCORE

The demountability scores for the box-beam are shown in this appendix.

As mentioned in chapter 6, subsection 6.4.4, some key aspects were not directly derived from tables 6.3, and 6.5. In order to arrive at a single score value for these key aspects, the average of the four values were taken, i.e. the weight of each interface accessibility was taken as 1.
As seen in chapter 6, there were four interfaces identified, and each interface has its own accessibility value.

		Weight	Score
Interface 1	Beam-bearing	1	3
Interface 2	Beam-abutment	1	2
Interface 3	Beam-beam	1	1
Interface 4	Beam-asphalt	1	1
Overall accessibility score			**1.75**

Figure I.1: Accessibility score

	Weight	Simplicity
Interface 1	1	1
Interface 2	1	3
Interface 3	1	0
Interface 4	1	1
Overall simplicity score		**1.25**

Figure I.2: Overall simplicity score

Key aspects	Final scores of key aspects	Weights	Contribution to demountability
Acessibility	1.75	0.31	0.5425
Number of interfaces	2	0.28	0.56
Simplicity of interfaces	1.25	0.26	0.325
Durability	4	0.15	0.6
	Demountability		**2.0275**

Figure I.3: Demountability score

J

WEIGHTING OF KEY ASPECTS

This appendix will elaborate on how the weights of the key aspects to determine the demountability score.

J.1. PAIRWISE SCORING

In order to arrive at the weights, the pairwise scoring method adapted by Song and Kang [51] were applied. This involves prioritizing the key aspects, which was done through reasoning in this thesis. Once prioritized, a pairwise comparison is carried out wherein the attribute with the higher priority gets a score of 10 and the following attribute (in the priority list) gets a score lower relative score. The pairwise comparison is done is this manner for each attribute and the attribute with the next highest priority. Following this a range between the attribute with the highest priority and the attribute with the lowest priority is set up, such that all the other attributes fall within this range. Once all the relative pairwise comparisons are done, the scores are converted into a new score with a relative importance referenced to the highest score of 10 (attribute with highest priority). All the intermediate scores within the range are obtained by converting the relative importance value to fit within the range.

Rank	1	2	3	4
Characteristic	Accessibility (A)	Number of connections/interfaces (N)	Simplicity/type of connections (T)	Durability (D)
Result				
A:N	10	9		
N:T		10	9	
T:D			10	5
Score ratio	10	9	8.1	4.05
Score bound	10			5
Conversion	**10**	**9.16**	**8.4**	**5**
Weight	0.31	0.28	0.26	0.15

Figure J.1: Weight determination for demountability score

K

DuraCrete calculations

This appendix consists of two sections. The first section will discuss the calculation of the diffusion coefficient and the value of cover (for 100 and 200 years) using the DuraCrete model. The second section deals with the calculation of the model uncertainty parameter (MU) used within this thesis.

K.1. CALCULATION OF TIME DEPENDANT DIFFUSION COEFFICIENT (D(T) AND COVER

Equation K.1 gives the formulation of the time dependant diffusion coefficient. The D_0 value is obtained from the study conducted by van der Wegen, G. et. al. [9].

$$D(t) = D_0(\frac{t_0}{t})^n \tag{K.1}$$

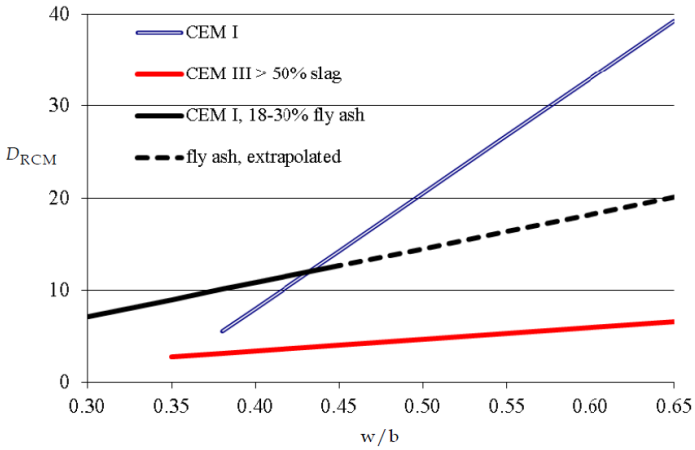

Figure K.1: Relationship between D_{RCM} and w/b ratio

From figure K.1 the D_o (diffusion coefficient at 28 days) is obtained and this is input into equation K.1 to calculate the time dependant diffusion coefficient. To keep the units consistent the values obtained from figure K.1 were converted from m^2/s to mm^2/day. Table K.1 gives an overview of the diffusion coefficients for 100 and 200 years, where years are converted to days. The critical chloride content is 0.6 % of mass of binder [9].

Time [days]	D_0 $[mm^2/day]$	D(t) $[mm^2/day]$
36500	1.21	1.64E-02
73000	1.21	1.08E-02

Table K.1: D_o and $D(t)$ values for 100 and 200 years

The equation used to calculate the chloride ion concentration at a particular depth (x in mm) is described in equation K.2 [9].

$$C(x,t) = C_s - (C_s - C_i)erf\frac{x}{2\sqrt{K_{tot}D(t)t}} \tag{K.2}$$

By using the DuraCrete model as described in literature [9, 10] the values of cover found for 100 and 200 years are 32 and 36.7 mm respectively. The calculations were carried out using Excel and are shown in figures K.2 and K.3.

Chloride content (x,t) [%]	Ccr	0.60274
Surface chloride content [%]	Cs	1.5
Initial chloride content [%]	Ci	0.1
Cover value [mm]	x (cover)	32
ke*kc	Ktot	1.02
Envionmental variable	ke	0.68
Coefficient for post treatment	kc	1.5
Diffusion coefficient (after 28 days)	Do	1.21E+00
Reference time [days]	te	28
Time [days]	t	36500
Ageing coefficient	n (ageing)	0.6
Time dependant diffusion coefficient	D(t)	1.64E-02

Figure K.2: Cover required to reach Ccrit (%) after 100 years

Chloride content (x,t) [%]	Ccr	0.60381
Surface chloride content [%]	Cs	1.5
Initial chloride content [%]	Ci	0.1
Cover value [mm]	x (cover)	36.7
ke*kc	Ktot	1.02
Envionmental variable	ke	0.68
Coefficient for post treatment	kc	1.5
Diffusion coefficient (after 28 days)	Do	1.21E+00
Reference time [days]	te	28
Time [days]	t	73000
Ageing coefficient	n (ageing)	0.6
Time dependant diffusion coefficient	D(t)	1.08E-02

Figure K.3: Cover required to reach Ccrit(%) after 200 years

Time [years]	100	200
Cover as per equation K.2[mm]	32	36.7
Safety margin [mm]	30	30
Total cover [mm]	62	66.7

Table K.2: Cover calculated using the DuraCrete model

K.2. MODEL UNCERTAINTY

In order to take into account deviations in the model due to uncertainty of model parameters a model uncertainty (MU) was used. This MU parameter should account for these deviations and reduce the uncertainty of the results obtained using the model. The principle behind assessing a model uncertainty is to compare them with more refined models or in service experiences [53]. In this case the number of data samples obtained from in service bridges was limited to 9 samples which reduces the accuracy of the MU but is proceeded with nonetheless.

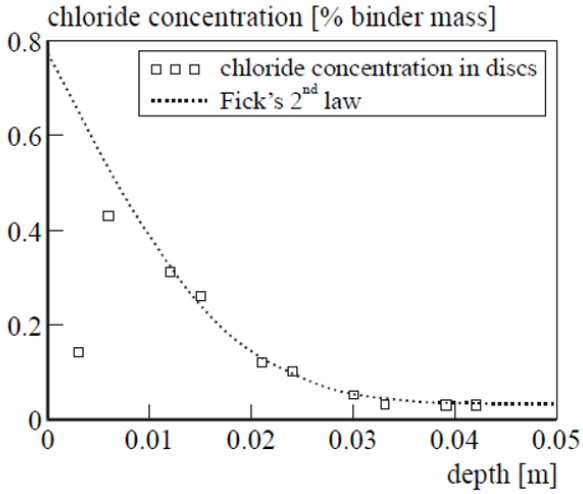

Figure K.4: Chloride profile values from a 35 year old bridge [14]

Figure K.4 was used to obtain the observed chloride concentration values at the corresponding depths.

x [mm]	Ccl, predicted [%]	Ccl,obs [%	MU
0	1.34	0.13	0.097015
7	1.23	0.41	0.333333
12	1.04	0.31	0.298077
15	0.93	0.25	0.268817
20	0.77	0.11	0.142857
23	0.68	0.1	0.147059
30	0.5	0.05	0.1
32	0.46	0.04	0.086957
40	0.32	0.04	0.125
42	0.29	0.04	0.137931

Figure K.5: Calculation of the MU parameter using values obtained from figure K.4

Mean	Standard deviation
0.15	0.086

Table K.3: Mean and standard deviation of the MU parameter

In order to use the model uncertainty parameter in the Monte-Carlo simulations it was assumed the the parameter followed a normal distribution. Another assumption made was that it was unbiased and had a standard deviation shown in table K.3.

L

ADAPTING INDICATOR FROM LITERATURE

This appendix shows the adaptation of the existing bridge circularity indicator as developed by Coenen. T. [17] wherever possible.

L.1. DESIGN INPUT

The design input (DI) indicator was discussed in detail in the literature review. Shown here is the attempt to try and adapt it to a box-beam. Since this indicator is an adaptation of the MCI (Material Circularity Indicator) developed by the Ellen MacArthur Foundation and their partners [26], it deals with the material composition of the asset. In this case adapting to a beam simply involved calculating the materials used to manufacture the beam.

L.1.1. MATERIAL INPUT

$$LF = 1 - (k * F_{Rec} + F_{Reu}) - F_{ren,v} \tag{L.1}$$

This indicator (LF) does not apply since a new girder to be produced using all virgin

Frec	0
Freu	0
Fren,v	0
k	0.8
Linear fraction (LF)	1

Figure L.1: Linear fraction of a box-beam

Material	Density [kg/m3]	Weight [kg]	Remark
Prefab girder	2549.29	138133.27	Weight from hollow (41m) and weight from massive (4m)
Prestressing steel	1172 g/m (taken from pr EN10138-3)	2742.48	52 strands over 45 meters (1172 g/m for one strand)
Reinforcing steel	7850	54.86	4300 mm2 for longitudinal reinforcement , 2257.1 for torsion (longitudinal)
Total [kg]		140930.61	

Figure L.2: Material Input calculated for a box-beam

recyclability		1.019849
mass of concrete [kg]	138133.27	
mass of steel reinforcement [kg]	54.86	
mass of prestressing steel [kg]	2742.48	
recyclability of concrete (1-5)	1	
recyclability of steel (1-5)	2	

Figure L.3: Recyclability of a box-beam

materials will not have any fraction of reused or recycled materials (see figure L.1).

$$MI = \frac{(LF + (1 - recyclable))}{2} \tag{L.2}$$

The MI was calculated to be 0.49 for a box beam girder
An assumption was made here that the concrete has a recyclability score of 1 (lowest) and steel a score of 2, where the recyclable score ranges from 1-5.

L.1.2. ROBUSTNESS

$$CR = \frac{a}{Robustness} \tag{L.3}$$

The Robustness calculation is not clearly mention and therefore the least possible value was assumed, using equation L.3 where a = 0.9 (suggested value). The robustness is doubled when calculating for the box-beam for 200 years, this is done assuming that resistance against corrosion is a form of robustness (against environmental load).

$$DI = 1 - MI \times CR = 1 - 0.49 \times 0.9 = 0.56\ (SKK1500) \tag{L.4}$$

$$DI = 1 - MI \times CR = 1 - 0.49 \times 0.45 = 0.78\ (Design\ 3) \tag{L.5}$$

L.2. RESOURCE AVAILABILITY

This indicator is also based on the weight of the different components that comprise the asset, and makes use of the scarcity of the product (material). Hence this indicator could also be adapted as shown in figure.

$$S_{total} = SF \times \frac{\sum_{i=1}^{n} SOP_i \times M_i \times 10}{M_{total}} \tag{L.6}$$

Material	Scarcity	Weight [kg]	Weight*Scarcity
Prefab girder	2.04E-03	138133.27	2.82E+02
Prestressing steel	2.94E-02	2742.48	8.06E+01
Reinforcing steel	2.94E-02	54.86	1.61E+00

Figure L.4: Calculation of RA inputs

The RA is calculated using inputs from table L.4 with the scaling factor (SF) of 7 as suggested by literature[17]. The final value of RA was calculated to be 0.18 for a box-beam girder.

L.3. REUSABILITY

$$RU_i = \sum [1-k] \times -U_i \times T_i + k \times D \times T \tag{L.7}$$

Where,

k = weight of disassemblability to uniqueness = 0.7

Ui = uniqueness of each component

Ti = transportability of each component

D = overall disassemblability (value from [17] used)

T = Overall transportability score (calculated in subsection L.3.2)

All the RU_i values of the different components (steel, prestressing, and concrete) are needed to find the overall reusability as shown in equation L.8 .

$$Reusability = \sum (RU_i \times M_i) / \sum M_i = 0.33 \tag{L.8}$$

L.3.1. DISASSEMBLABILITY

This value had no specific steps and therefore was not adapted, rather the value used in the calculation of a box-beam bride was used [**coenen**].

L.3.2. TRANSPORTABILITY

$$T = \frac{\sum (M_j \times T_j)}{\sum M_j} \tag{L.9}$$

Where,

$$M_j = mass\ of\ component\ j$$

$$T_j = transportability\ of\ component\ j$$

Transportation infrastructure	Valuation	Available	
Water, rail, 1-lane road	1	No	
Water, 1-lane road	0.9	No	
Rail, 1-lane road	0.9	No	
1-lane road	0.8	Yes	1
Water, rail, 2,3-lane road	0.8	No	
Water, 2,3-lane road	0.7	No	
Rail, 2,3-lane road	0.7	No	
2,3-lane road	0.6	Yes	0.75
Water, rail	0.4	No	
Water	0.3	No	
Rail	0.2	No	

Figure L.5: Transportability options considered for the box-beam

L.3.3. UNIQUENESS

No method of standardization exists due to which this indicator is not used [17].

L.4. ADAPTABILITY

This indicator as mentioned in literature was not adaptable since Yes/No statements applicable for the asset were used to evaluate it (chapter 2). These Yes/No statements had weights assigned to them, determined through expert opinions which could not be applied to a beam.

In order to calculate the overall circularity score the different indicators needed to be weighted based on the context of the bridge. This step would not be applicable for a beam since a separate beam context would be needed. This would be the case for any component that needs to be scored. Therefore an overall circularity score could not be calculated for a beam using the existing indicator.

M

DESIGN POSSIBILITY 1, 2 AND 3

The design possibilities discussed in chapter 5can be found in this appendix. The first section shown the ULS bending resistance achieved for Design Possibility 1. The second section shows the same for Design Possibility 2 followed by Design Possibility 3.

M.1. DESIGN POSSIBILITY 1

The design is an iterative process, where the height of the compressive zone needed to be changed until horizontal force equilibrium was achieved. Excel was used to make this iterative process easier. The final iteration in which the chosen height of the concrete compressive zone is seen.

Concrete properties		
Area of concrete [mm^2]	Ac	1068960
Eccentricity of prestressing and reinforcing steel [mm]	ep = es	712
(relative to neutral axis)		
Effective depth [mm]	dp = ds	1460
Concrete C60/75		
Distance from centroid to top fibre [mm]	Zt	748
Distance from centroid to bottom fibre [mm]	Zcb	790
Concrete modulus of elasticity [Mpa]	Ec	39100
Design compressive strength	fcd	40
Thickness bottom flange [mm]	tb	157
Height of box-beam [mm]	h	1538
Thickness top flange [mm]	tf	208
Prestressing steel properties (Y1860 S7 - seven strands)		
Total area [mm^2]	Ap	9150
Prestressing steel modulus of elasticity [Mpa]	Ep	195000
Working prestress [Mpa] - assuming 20% losses	σ_{pcp}	1116
Stress in steel at failure [Mpa]	f_{pd}	1522
Reinforcing steel properties (B500)		
Reinforcing steel modulus of elasticity [Mpa]	Es	200000
Total area [mm2]	As	1500
Step 1 - Estimation of concrete compression zone (Xu) [mm]	Xu	621.5
Nc - P_{mcp} = As*fyd + Ap*(f_{pd}-σ_{pcp})		
Force to balance from tensile zone [N]	As*fyd + Ap*fpd	1.5E+07
Nc = α*b*fcd*Xu (assuming rectangular cross-section)		
Surface factor for C60/75 (α)	α	0.67
Width of box-beam [mm]	b	1420
Step 2 - Check height of compression zone (EN 1992 cl 5.5)		
Ratio of redistributed moment to elastic bending moment	δ	1
No redistribution is assumed		
Xu/d < 1-7f/(ε_{cu}*10^6+7f)	0.43 < 0.44	
Step 3 - Strains in reinforcing and prestressing steel (for Xu)		
ε_s =	εcu(ds/Xu - 1)	0.00391
Δεp	εcu(dp/Xu - 1)	0.00391
εp =	Δεp + σ_{pcp}/E_P	9.64E-03

Step 4 - Actual prestress and force in steel		
Asuumed steel stress at failure [Mpa]	f_{pd}	1522
Steel strain (prestressing steel)	$\varepsilon p = \Delta\varepsilon p + \sigma_{pc\infty}/E_p$	9.64E-03
Using graph, actual stress at failure (linear interpolation) [Mpa]		1533.35
Force in reinforcing steel [kN]	Ns = As * fyd	652.5
Increase of force in prestressing steel [kN]	ΔNp = Ap * (fpd,actual - σpc∞)	3818.73
Total steel force [kN]	N = Ns+ΔNp	4471.23
Working prestress force [kN]	Pm,∞ = Ap * σpc∞	10211.4
Total force to be balanced by concrete	**N+Pm,∞**	#########
Step 5 - Stress and strains in concrete section (upto Xu)		
Total concrete compressive force [kN]	**Nc**	14680.1
Flange force [kN]	b * fcd * tf	11894.2
Remaining height with constant stress [kN]	(0.348*Xu -tf)*2*tw*fcd	1454.49
Force from triangular stress distribution [kN]	0.5*fcd*0.6528Xu*2*tw	1331.4

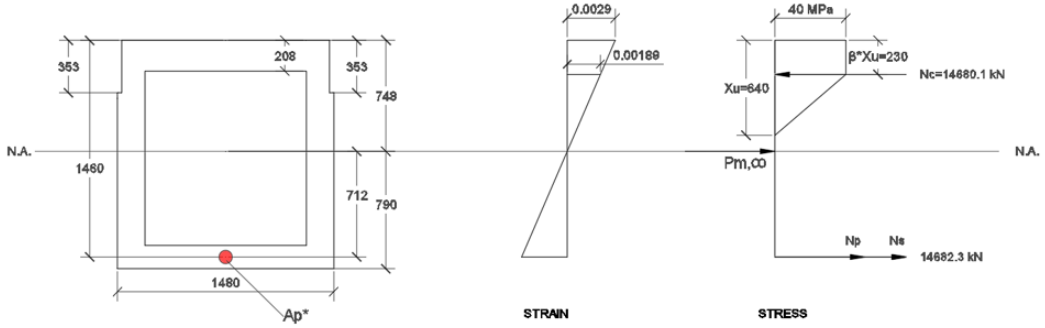

MRd calculated by taking moment equilibrium about centroid [kNm]		11838.4	
Considering box beam as rectangle [kNm] (+)	α*b*Xu*fcd*(Zt-β*Xu)	12399.7	
Part to subtract (hollow part of box-beam) - 2 parts- [kNm] (-)	A*lever arm (A) + B*lever arm (B)	3744.85	
Constant width stress part- A [kN]	0.348*Xu*fcd*(b-2*tw)	365.733	
Triangular area stress part - B [kN]	0.5*(Xu-0.348Xu)*(b-2*tw)*σflange	8947.21	
lever arm A (about centroid) [mm]	Zt-0.348*Xu + (0.348Xu-tf)/2	535.859	
lever arm B (about centroid) [mm]	Zt - 0.348Xu - (Xu-0.348*Xu)/3	396.645	
Tensile force from steel [kN] * eccentricity [mm] (+)	{σ,pu (actual) - σpc∞}*ep + fyd*As*ep	3183.51	
M_{Ed} (SCIA,ULS) [kN]		11739.8	
M_{Ed} (SCIA,x2) [kN]		13684.3	
Mp,∞ [kNm]		7270.52	
UC = (M_{ed} -Mp,∞)/M_{Rd}		0.38	<1
UC_{x2} =(Med,x2 -Mp,∞)/MRd		0.57	<1

M.2. DESIGN POSSIBILITY 2

The same conditions mentioned in the previous section hold for the calculation shown in this section.

Concrete properties		
Area of concrete [mm^2]	Ac	1125200
Eccentricity of prestressing and reinforcing steel [mm]	ep = es	686
(relative to neutral axis)		
Effective depth [mm]	dp = ds	1479
Concrete C60/75		
Distance from centroid to top fibre [mm]	Zt	792
Distance from centroid to bottom fibre [mm]	Zcb	784
Concrete modulus of elasticity [Mpa]	Ec	39100
Design compressive strength	fcd	40
Thickness bottom flange [mm]	tb	195
Height of box-beam [mm]	h	1576
Thickness top flange [mm]	tf	208
Prestressing steel properties (Y1860 S7 - seven strands)		
Total area [mm^2]	Ap	9150
Prestressing steel modulus of elasticity [Mpa]	Ep	195000
Working prestress [Mpa] - assuming 20% losses	σ_{pcp}	1116
Stress in steel at failure [Mpa]	f_{pd}	1522
Reinforcing steel properties (B500)		
Reinforcing steel modulus of elasticity [Mpa]	Es	200000
Total area [mm2]	As	1571
Step 1 - Estimation of concrete compression zone (Xu) [mm]	Xu	625.00
Nc - P_{rncp} = As*fyd + Ap*(f_{pd}-σ_{pcp})		
Force to balance from tensile zone [N]	As*fyd + Ap*fpd	1.5E+07
Nc = α*b*fcd*Xu (assuming rectangular cross-section)		
Surface factor for C60/75 (α)	α	0.67
Width of box-beam [mm]	b	1420
Step 2 - Check height of compression zone (EN 1992 cl 5.5)		
Ratio of redistributed moment to elastic bending moment	δ	1
No redistribution is assumed		
Xu/d < 1-7f/(ε_{cu}*10^6+7f)	0.43 < 0.44	
Step 3 - Strains in reinforcing and prestressing steel (for Xu)		
ε_s =	εcu(ds/Xu - 1)	0.00396
Δεp	εcu(dp/Xu - 1)	0.00396
εp =	Δεp + σ_{pcp}/E_P	9.69E-03

Step 4 - Actual prestress and force in steel		
Asuumed steel stress at failure [Mpa]	f_{pd}	1522
Steel strain (prestressing steel)	$\varepsilon p = \Delta\varepsilon p + \sigma_{p\infty}/E_p$	9.69E-03
Using graph, actual stress at failure (linear interpolation) [Mpa]		
Force in reinforcing steel [kN]	Ns = As * fyd	683.385
Increase of force in prestressing steel [kN]	ΔNp = Ap * (fpd,actual - σpꝏ)	3821.57
Total steel force [kN]	N = Ns+ΔNp	4504.96
Working prestress force [kN]	Pm,ꝏ = Ap * σpꝏ	10211.4
Total force to be balanced by concrete	**N+Pm,ꝏ**	14714.16
Step 5 - Stress and strains in concrete section (upto Xu)		
Total concrete compressive force [kN]	**Nc**	14714.161
force from fcd width [kN]	b * fcd * tf	11909.418
Force from trap in LJ [kN]	(0.348*Xu -tf)*2*tw*fcd	1446.0542
force from webs (remaining) [kN]	0.5*fcd*0.6528Xu*2*tw	1358.6889

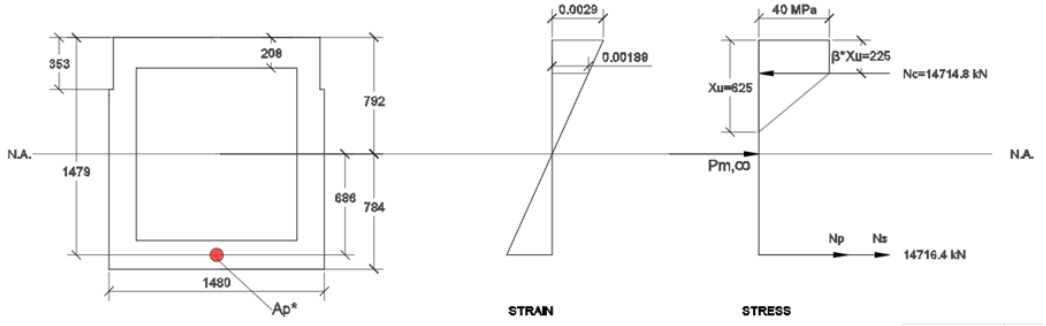

MRd calculated by taking moment equilibrium about centroid [kNm]		12386.541	
Considering box beam as rectangle [kNm] (+)	α*b*Xu*fcd*(Zt-β*Xu)	13486.095	
Part to subtract (hollow part of box-beam) - 2 parts- [kNm] (-)	A*lever arm (A) + B*lever arm (B)	4189.9542	
Constant width stress part- A [kN]	0.348*Xu*fcd*(b-2*tw)	419.52	
Triangular area stress part - B [kN]	0.5*(Xu-0.348Xu)*(b-2*tw)*σflange	8997.6	
lever arm A (about centroid) [mm]	Zt-0.348*Xu + (0.348Xu-tf)/2	579.25	
lever arm B (about centroid) [mm]	Zt - 0.348Xu - (Xu-0.348*Xu)/3	438.66667	
Tensile force from steel [kN] * eccentricity [mm] (+)	{σ,pu (actual) - σpꝏ}*ep + fyd*As*ep	3090.4	
M_{Ed} (SCIA,ULS) [kN]		11739.8	
M_{Ed} (SCIA,x2) [kN]		13684.3	
Mp,ꝏ [kNm]		7005.02	
UC = (M_{ed} -Mp,ꝏ)/M_{Rd}		0.44	<1
UC_{x2} =(Med,x2 -Mp,ꝏ)/MRd		0.60	<1

M.3. DESIGN POSSIBILITY 3

The same conditions mentioned in the previous section hold for the calculation shown in this section.

Concrete properties		
Area of concrete [mm^2]	Ac	1244976
Eccentricity of prestressing and reinforcing steel [mm]	ep = es	687
(relative to neutral axis)		
Effective depth [mm]	dp = ds	1479
Concrete C60/75		
Distance from centroid to top fibre [mm]	Zt	792
Distance from centroid to bottom fibre [mm]	Zcb	784
Concrete modulus of elasticity [Mpa]	Ec	39100
Design compressive strength	fcd	40
Thickness bottom flange [mm]	tb	195
Height of box-beam [mm]	h	1576
Thickness top flange [mm]	tf	208
Web thickness [mm]	tw	452
Prestressing steel properties (Y1860 S7 - seven strands)		
Total area [mm^2]	Ap	9900
Prestressing steel modulus of elasticity [Mpa]	Ep	195000
Working prestress [Mpa] - assuming 20% losses	σ_{pcp}	1116
Stress in steel at failure [Mpa]	f_{pd}	1522
Reinforcing steel properties (B500)		
Reinforcing steel modulus of elasticity [Mpa]	Es	200000
Total area [mm2]	As	2090
Step 1 - Estimation of concrete compression zone (Xu) [mm]	Xu	633.00
Nc - P_{max} = As*fyd + Ap*(f_{pd}-σ_{pcp})		
Force to balance from tensile zone [N]	As*fyd + Ap*fpd	1.6E+07
Nc = α*b*fcd*Xu (assuming rectangular cross-section)		
Surface factor for C60/75 (α)	α	0.67
Width of box-beam [mm]	b	1496
Step 2 - Check height of compression zone (EN 1992 cl 5.5)		
Ratio of redistributed moment to elastic bending moment	δ	1
No redistribution is assumed		
Xu/d < 1-7f/(ε_{cu}*10^6+7f)	0.43 < 0.44	
Step 3 - Strains in reinforcing and prestressing steel (for Xu)		
ε_s =	εcu(ds/Xu - 1)	0.00388
Δεp	εcu(dp/Xu - 1)	0.00388
εp =	Δεp + σ_{pcp}/E_p	9.60E-03

Step 4 - Actual prestress and force in steel		
Asuumed steel stress at failure [Mpa]	f_{pd}	1522
Steel strain (prestressing steel)	$\varepsilon p = \Delta\varepsilon p + \sigma_{p\infty}/E_p$	9.60E-03
Using graph, actual stress at failure (linear interpolation) [Mpa]		
Force in reinforcing steel [kN]	Ns = As * fyd	909.15
Increase of force in prestressing steel [kN]	ΔNp = Ap * (fpd,actual - σpꝏ)	4129.48
Total steel force [kN]	N = Ns+ΔNp	5038.63
Working prestress force [kN]	Pm,ꝏ = Ap * σpꝏ	11048.4
Total force to be balanced by concrete	**N+Pm,ꝏ**	16087.03
Step 5 - Stress and strains in concrete section (upto Xu)		
Total concrete compressive force [kN]	**Nc**	16086.132
force from fcd width [kN]	b * fcd * tf	12607.846
Force from trap in LJ [kN]	(0.348*Xu -tf)*2*tw*fcd	1769.3533
force from webs (remaining) [kN]	0.5*fcd*0.6528Xu*2*tw	1708.9336

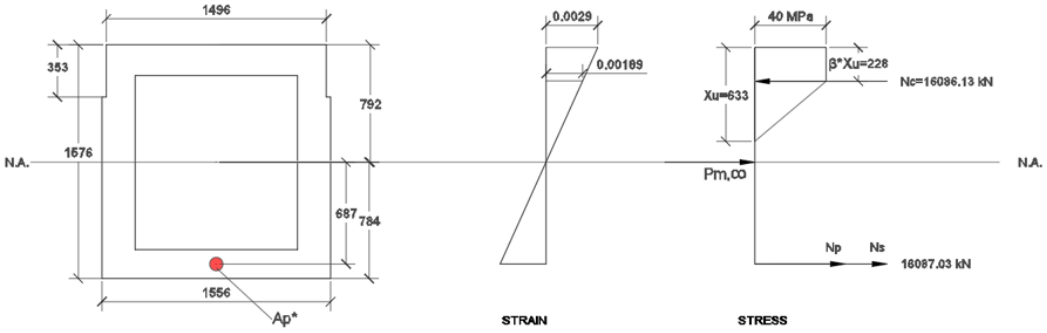

MRd calculated by taking moment equilibrium about centroid [kNm]		13508.474
Considering box beam as rectangle [kNm] (+)	α*b*Xu*fcd*(Zt-β*Xu)	14316.656
Part to subtract (hollow part of box-beam) - 2 parts- [kNm] (-)	A*lever arm (A) + B*lever arm (B)	4269.7198
Constant width stress part- A [kN]	0.348*Xu*fcd*(b-2*tw)	542.46144
Triangular area stress part - B [kN]	0.5*(Xu-0.348Xu)*(b-2*tw)*σflange	9112.7693
lever arm A (about centroid) [mm]	Zt-0.348*Xu + (0.348Xu-tf)/2	577.858
lever arm B (about centroid) [mm]	Zt - 0.348Xu - (Xu-0.348*Xu)/3	434.144
Tensile force from steel [kN] * eccentricity [mm] (+)	{σ,pu (actual) - σpꝏ}*ep + fyd*As*ep	3461.5374
M_{Ed} (SCIA,ULS) [kN]		11739.8
M_{Ed} (SCIA,x2) [kN]		13684.3
Mp,ꝏ [kNm]		7590.25
UC = (M_{ed} -Mp,ꝏ)/M_{Rd}		0.42 <1
UC_{x2} =(Med,x2 -Mp,ꝏ)/MRd		0.56 <1